APPLICATION OF ICE NUCLEATION PROTEINS TO IMPROVE PROCESS EFFICIENCY OF FREEZING TECHNOLOGIES WITH ALTERED ICE MORPHOLOGY

By

JUE JIN

A dissertation submitted to the

School of Graduate Studies

Rutgers, the State University of New Jersey

In partial fulfillment of the requirements

For the degree of

Doctor of Philosophy

Graduate Program in Food Science

Written under the direction of

Dr. Tung-Ching Lee

And approved by

_____

_____

_____

_____

_____

New Brunswick, New Jersey

January, 2018

ABSTRACT OF THE DISSERTATION

Application of Ice Nucleation Proteins to Improve Process Efficiency of Freezing Technologies with Altered Ice Morphology

By JUE JIN

Dissertation Director:
Dr. Tung-Ching Lee

This research aimed at applying ice nucleation proteins (INPs) in freezing technologies to improve the efficiency of both freeze concentration and freeze drying processes, with further understanding of the related mechanism of ice morphology using a novel imaging technique (X-ray Computed Tomography).

The application of INPs to freeze concentration process showed significant improvement of process efficiency in a desalination model. With the addition of INPs, an estimation of approximately 50% of the energy cost could be saved to obtain fresh drinking water (<500 ppm). Moreover, the related mechanism of ice morphology was investigated by optical microscope and three dimensional X-ray computed tomography. Their use indicated that INPs promoted the development of a lamellar structured ice matrix with larger hydraulic diameters, which facilitated brine drainage and contained less brine entrapment as compared to control samples. These results

suggested great potential for applying INPs to develop an energy-saving freeze concentration method via the alteration of ice morphology.

Our results also showed that INPs could significantly improve freeze drying process efficiency with increased primary drying rate in different food systems. Those improvements further led to reduced total drying time, which suggested an estimated total energy saving of 28.5% with INPs. Our ice morphology results indicated the ability of INPs to alter ice morphology with lamellar ice structure and larger crystal size, which were very likely to facilitate the water vapor flow and improve the sublimation rate. These results revealed great potential of using INPs to improve the efficiency of freeze drying process for a wide range of food and other applications.

Thus, our study reveals the great potential of applying INPs to improve process efficiency of freezing technologies including freeze concentration and freeze drying processes, which can lead to wide applications of INPs to produce food products with higher quality at lower cost. Our study also provides new insights into the three dimensional internal structures of frozen matrices and their relationship with process efficiency, which emphasizes the importance of controlling freezing process and the related ice morphology. Our data of ice morphology change is the first study available in the literature to reveal that INPs could not only affect the nucleation temperature but also significantly change the macroscopic ice structure. This finding of INPs altering ice morphology can have significant impact on basic scientific research and practical applications in food, nutraceutical and pharmaceutical industries.

ACKNOWLEDGEMENT

I acknowledge with sincere gratitude my major advisor, Dr. Tung-Ching Lee, for his guidance and support throughout my Ph.D. study at Rutgers University. Without his contribution and encouragement, I would never be able to complete this project. He has been my mentor on every aspect of my life through these years. His intelligence and enthusiasm about science inspired my initial interest in research, and will always encourage me in the pursuit of scientific research in my future career.

My gratitude extends to my committee member, Dr. Qingrong Huang, for his insightful discussions and generously providing the access to the instruments in his laboratory. His great contributions facilitated the completion of my research study. He always provided valuable suggestions on my academic life and career development when I felt confused about my future. I would also like to thank Dr. Paul Takhistov for his willingness to be on my committee. His valuable comments and advice make this study more comprehensive. Many thanks also go to my committee member and the co-author of my papers, Dr. Edward Yurkow, for his help and support during my research. Dr. Yurkow generously provided the access to the imaging equipment at the Molecular Imaging Center. He also helped me analyze the imaging data and gave many valuable advices during the preparation of my manuscript submissions. Without his contribution, the papers based on this project would not have been possible.

I also would like to thank Derek Adler at Molecular Imaging Center for his technical support in setting up the X-ray Computed Tomography instrument and

teaching me how to use the equipment, as well as processing the imaging data. I also want to thank all my labmates, Ke Shi, Zhengkun Zhou, Xiaoyuan Wang, Shiqi Lin, Pei Wang, for all their help and support. My gratitude also extends to Staffs at Food Science Department, Karen Ratzan, Deborah Koch, Yakov Uchitel, Dave Petrenka and William Sumal, for all their assistance and help during my graduate study.

My deepest appreciation also goes to my speech therapist, Gina Vekselman, for her assistance in improving my speech fluency. Her encouragement helped me overcome the fear and anxiety from my speech disfluency. My appreciation also extends to the student clinicians, Cheryl Lupica, Lauren Ostrovsky and Jessica Aviles at the Center of Communication Disorder at Kean University. They always patiently and carefully listened to my questions and concerns and identified the most appropriate approaches and treatment for my speech. Without their hardwork, my speech would never progress this much. Additionally, I would like to thank Dr. Siobhan Gibbons at CAPS, who patiently listened to my confusions during my graduate study and help me walk through my toughest time.

Last but most, I am indebted to my mom for her unconditional love and endless support. Thanks her for always standing firmly behind me through tough times. My gratitude towards my mom is way beyond description. My thanks also extend to my dearest grandparents for their constant encouragement and understanding although I’m so far away from them. I also would like to thank all my friends for keeping me company and turning my graduate study hopeful and joyful.

PREFACE

This dissertation is written in manuscript style, which includes two manuscripts (Chapter IV and V). These two manuscripts summarize the major research results of applying ice nucleation proteins (INPs) in two freezing technologies, including freeze concentration and freeze drying processes. The process efficiency of both freezing technologies is improved through the mechanism of ice morphology alteration by INPs.

The research results in Chapter IV have been published under the title of "A Novel Approach to Improve the Efficiency of Block Freeze Concentration Using Ice Nucleation Proteins with Altered Ice Morphology" in the *Journal of Agricultural and Food Chemistry* (2017, 65(11), 2373-2382) co-authored with Dr. Edward Yurkow, Derek Adler, and Dr. Tung-Ching Lee* on March 22, 2017.

The research results in Chapter V have been published under the title of "Improved Freeze Drying Efficiency by Ice Nucleation Proteins with Ice Morphology Modification" in the *Food Research International* (Volume 160, April 2018, Pages from 90 to 97) co-authored with Dr. Edward Yurkow, Derek Adler, and Dr. Tung-Ching Lee*.

The additional research works that related to this study are cited in appendix as the useful information for reference. The additional results include the effect of growth conditions on the activity of INPs and related surface hydrophobicity (Appendix A), safety evaluation of INPs for food applications (Appendix B),

mechanisms of INPs altering ice morphology (Appendix C) and radiodensity distribution change of ice phase by INPs (Appendix D).

CONTENTS

LIST OF FIGURES

LIST OF TABLES

I. Scientific Rationale

Freezing related food processing offers the advantages of high quality nutritious foods with long term storage life. Among these freezing processes, technologies like freeze concentration and freeze drying are well-established food preservation methods. By freezing foods and separating the ice from the frozen matrices, freeze concentration and freeze drying processes are frequently used for producing valuable intermediate ingredients or final products. Due to the low temperature processing environment, these technologies can successfully preserve taste, color, aroma and nutritional values of the original products. For example, freeze concentration process shows tremendous advantages in concentrating aroma-rich liquid foods, such as fruit juice, coffee and tea. And freeze drying process has been favored for dehydrating perishable materials, such as proteins, enzymes, microorganisms and other bio-active compounds.

Although succeeded in maintaining high product quality and extending shelf life, these freezing technologies are relatively expensive processes as compared to other separation processes. The relatively high cost comes from two aspects of the processes. One is the equipment investment for the ice formation during freezing step. The other one is the energy cost related to the subsequent separation step, such as complicated mechanical separation of ice crystals from liquid concentrate or long duration of ice crystals sublimation from the frozen products (Geidobler & Winter, 2013; Spicer, 1974).

To reduce the process cost of freezing step, different parameters have been previously investigated, among which the control of ice nucleation showed great potential. However, current methods to control ice nucleation, such as scraped surface nucleation, ultrasound nucleation, or pressure-shift nucleation, are not efficient enough and required additional equipment investment, as well as extra energy cost. Besides these nucleation methods, efficient ice nucleation can also be achieved by adding ice nucleating agents. Among the current ice nucleating agents, biogenic ice nucleation proteins have been demonstrated as the most effective one and have shown great potential for food applications.

In addition, previous studies on controlling freezing step failed to further investigate the effect of ice nucleation on the subsequent separation steps and related energy cost. It has been empirically suggested that the efficiency of separation step is strongly dependent on the parameters during freezing step. Ice nucleation is suggested as one of the determinant factors during freezing step for its significant influence on the formation of ice morphology. However, these statements still lack of sufficient scientific proof. Thus, the further investigation of ice nucleation effect on efficiency of separation step after freezing is required. **This study aims to evaluate the potential of using ice nucleation proteins as an effective approach to improve the efficiency of both freezing and separation steps in freezing technologies, including freeze concentration and freeze drying processes, and to explore related mechanism on ice morphology.**

II. Literature review

1. Freezing technologies

Freezing technologies have been applied in food industry for product manufacturing, preservation and storage. The subzero temperature slows down many chemical reactions and inhibits the growth of microorganisms. Thus, freezing technologies have been widely used to preserve product quality, assure food safety and extend shelf life. Separation processes like extraction, dehydration or fractionation, are one of the important categories in food processing and are used for manufacturing intermediate ingredients or producing final products. This study is going to focus on freezing related separation processes including freeze concentration and freeze drying.

1.1. Freeze concentration

Freeze concentration is a separation process to remove water from a product. This process is to partially freeze solutions to form ice crystals in the solid phase while solute or impurities are expelled during ice crystal growth and remained in the liquid phase. The subsequent solid-liquid separation can be operated by centrifugation, filtration, and gravity. Many materials can be separated by freeze concentration process, such as water from seawater, concentrated milk from raw milk to produce milk powder, or concentrated apple juice (Deshpande, Cheryan, Sathe, & Salunkhe, 1984; Zhang & Hartel, 1996). Over the past decades, this process has achieved great success in industrial applications for preserving volatile flavors and heat sensitive nutrients in concentrated products due to its low temperature processing environment

(Sanchez, Hernandez, Auleda, & Raventos, 2011; Sanchez, Ruiz, Auleda, Hernandez, & Raventos, 2009). In addition, freeze concentration theoretically consumes only one seventh energy cost compared to distillation processes according to the latent heat required during phase transition. Due to its lower energy cost, this process was recently suggested as a potential application for desalination to help address water shortage for both human daily consumption and food production (Fujioka, Wang, Dodbiba, & Fujita, 2013; Luo, Chen, & Han, 2010).

Currently, there are three types of freeze concentration techniques, including suspension crystallization (Sanchez et al., 2009), film or layer freeze concentration (Jusoh, Yunus, & Abu Hassan, 2009; Sanchez et al., 2011) and block freeze concentration (Moreno, Robles, Sarmiento, Ruiz, & Pardo, 2013; Petzold, Moreno, Lastra, Rojas, & Orellana, 2015). In the conventional suspension freeze concentration, ice crystallization step forms individual ice crystals and enlarges their size by Ostwald ripening in the recrystallization tank. The subsequent separation step is to extract ice crystals from a mash of solution and crystals. The recently developed methods, like layer freeze concentration and block freeze concentration, have much simplified crystallization process by combining ice nucleation and growth in one step. For example, layer freeze concentration is used to form an ice layer on the cold surface of vertical or tubular equipment. The moving fluid and ice phase are separated without further assistance. And block freeze concentration is used to partially or completely freeze liquids with static contact to cold surface then the ice phase is separated by

additional techniques, such as vacuum or centrifugation (Moreno et al., 2013; Petzold et al., 2015; Sanchez et al., 2011). Thus, both processes use a similar ice crystallization mechanism to form an ice layer on a cold surface, which simplifies the freezing step, and also eases the following separation by removing mother liquid from the front of ice phase.

1.2. Freeze drying

Freeze drying is a dehydration process by direct sublimation of ice crystals from a frozen product. The process involves two major steps, including freezing process to form ice crystals inside frozen food matrixes and subsequent drying process to remove ice crystals by transforming them indirectly into gas. Because of its low temperature processing condition, freeze drying has been widely applied in products that contain sensitive materials and demand high quality, including biological materials, fine chemicals, food and pharmaceutical products (Geidobler & Winter, 2013). In the food area, freeze drying has been favored by different kinds of liquid and solid foods, such as powdered beverages like coffee and dehydrated snacks like dried vegetables and fruits. With the application of freeze drying, these products exhibit advantages of better flavor retention and nutrition preservation, faster rehydration compared to other drying methods, as well as cheaper transportation and longer shelf life. These benefits make freeze drying an appealing technology to provide consumers with products of convenience and better sensory profile.

A typical freeze dryer is consisted of a vacuum pump and a condenser. The

vacuum pump is used for reducing the gas pressure inside the chamber containing the samples, so ice is removed through sublimation as water vapor and condensed on the cooled surface of the condenser. Based on the interface of dried material with a condenser, there are three types of freeze dryers including manifold freeze-dryer, rotary freeze-dryer and tray style freeze-dryer. In manifold freeze-dryers, dried samples are placed in multiple containers and connected to a condenser by a circular tube. In rotary and tray freeze-dryers, samples are placed inside a single large reservoir which is connected to a condenser.

1.3. Economic considerations

Although these freezing technologies exhibit significant advantages in producing high quality products, they are relatively expensive as compared to other separation processes. The cost majorly comes from two aspects: equipment investment related to freezing step and energy consumption related to the separation step.

The freezing equipment consists of refrigerator (including compressor, heat exchanger, piping and instruments) and crystallizer. Based on the cost analysis for a system capacity of 1000 kg water removal, the cost for the refrigerator and crystallizer takes up 46% to 53% of the total investment cost (Spicer, 1974). Developments have been attempted to lower the equipment cost for the freezing step. For example, a fluidized-bed heat exchanger was developed for suspension freeze concentration, which is a less expensive compared to the typical surface scraped heat exchanger (Sanchez et al., 2009). Besides, layer and block freeze concentration methods have

been developed recently for its simplicity for both construction and operation of its freezing equipment. Such simplicity can reduce the necessary investment cost by 35% to 60% as compared to suspension freeze concentration (Sanchez et al., 2009). For both freeze concentration and freeze drying, the control of freezing parameters, such as supercooling level, can also lead to reduction of capital and operation cost of refrigeration. With smaller degree of supercooling during ice nucleation, a less expensive plain heat exchanger can be used, and higher coolant temperatures can result in less thermal energy required for cooling the feed stream and removing heat input from the environment (Sanchez et al., 2009). Therefore, the control of ice nucleation during freezing step might be an effective approach to reduce the process cost.

Another aspect of process cost relates to the energy consumption for ice removal during the separation step. For freeze concentration, the efficient removal of solute residue in the ice phase needs to be assisted by vacuum, filtering centrifuge or sophisticated wash column, which makes the ice removal at very high cost (Sanchez et al., 2011). For example, during layer freeze concentration, one of its economic obstacles is the cost related to the limited efficiency of separating solute from ice phase (Williams, Ahmad, Connolly, & Oatley-Radcliffe, 2015). In industrial freeze drying, the major part of the energy consumption is caused by the removal of the vast volumes of water vapor released by the product (Spicer, 1974). The relatively long duration of drying cycle result in high energy cost from the refrigeration unit of ice

condensers, which usually accounts for 50% of the total energy consumption (Ciurzyńska & Lenart, 2011; Rudy, 2009). The long time drying process can further lead to increased labor cost. Therefore, the high energy consumption and the long drying time result in expensive separation steps and approaches to make these separation steps more efficient are desired (Moejes & van Boxtel, 2016). Since the separation step is closely related the previous freezing step, the control of ice nucleation might also affect the cost of separation step, which has never been studied before.

2. Freezing and control of ice nucleation

2.1. Freezing and ice nucleation

During all these freezing technologies, freezing is the most crucial step for the entire process. Freezing of water is a process of ice crystallization from supercooled water. This phase transition of turning liquid water into solid ice follows a first-order thermodynamic transition when the temperature drops below the freezing point. The process of freezing water consists of two major stages, ice nucleation and ice crystal growth. Ice nucleation step involves the gathering of water molecules to form water clusters as initial nucleus and ice crystal growth is the subsequent step of further attachment of water molecules to the initial nucleus after it achieves the critical cluster size.

Ice crystallization that initiated by self-nucleation is called homogeneous ice nucleation. Homogeneous ice nucleation was reported to be initiated at temperature

lower than -35^{o}C, due to the metastable state of supercooled water (Wolber, 1993). Supercooled water could maintain in liquid state under freezing point, because of the free energy barrier built up by the existence of an interfacial layer between water and ice phases. This supercooling stage with free energy barrier can be overcome, when a critical ice embryo is produced and can grow spontaneously. This can only be achieved at relatively low subzero temperatures under an ideal homogeneous ice nucleation situation (Goff, Dutcher, & Marangoni, 2005). On the other hand, heterogeneous ice nucleation occurs when ice nucleation active materials are presented, such as silver iodides, dust particles and ice active bacteria or proteins, which are capable of binding water to overcome the supercooling stage and enable the formation of critical ice embryo at much warmer subzero temperatures up to -2^{o}C (Wolber, 1993).

The growth of ice crystals is the further addition of water molecules onto ice nucleus formed during ice nucleation. This exothermic process is macroscopically governed by the rate of latent heat removal as the heat transfer and the diffusion rate of water molecules towards the ice nuclei surface as the mass transfer. Since these physical terms are temperature dependent, the supercooling degree, which affects ice nucleation temperature, is supposed to further affect the macroscopic ice crystal growth. The effect of supercooling on the single ice crystals grown from initial ice nuclei has been observed under microscope with polarized light. The optical results showed that the shape of these single ice crystals grown from the critical ice embryo is strongly dependent on the initial supercooling level (Shibkov, Zheltov, Korolev, & Leonov,

2003). However, the effect of supercooling on macroscopic morphology of ice crystal is still unclear.

2.2. Technologies to control ice nucleation

Recently, several technologies have been introduced for controlling ice nucleation, including ice fog technique, electro-freezing, ultrasound-controlled ice nucleation, and high pressure freezing.

Ice fog technique is to initiate ice crystallization by forcing ice fog into the product. When the product temperature is decreased to the desired ice nucleation temperature, a dense ice fog is produced by passing nitrogen gas through copper coils immersed in liquid nitrogen (Chakravarty, Lee, DeMarco, & Renzi, 2012). However, the nucleation temperature and related ice structure might not be uniform in all the products, due to Ostwald ripening caused by the variation of nucleation time between products (Patel, Bhugra, & Pikal, 2009).

Electro-freezing has also been used for controlling ice nucleation. The technique is to apply strong electric field between electrodes immersed in the solution to induce ice crystallization at a desired supercooling level. It was suggested that ice nucleation temperature increased with the increase of applied voltage (Orlowska, Havet, & Le-Bail, 2009). The mechanism of this technique is that under the applied voltage, the dipoles of water molecules are polarized and their direction is aligned with the electric field from the native random state. These changes of water molecular dynamics could influence the free energy of the solution system that related to ice nucleation process

(Xanthakis, Havet et al. 2013). However, current application of electro-freezing for commercial manufacturing is still impractical, due to the need of individual electrodes in each sample and variation of voltage settings between different food systems (Anuj, 2012). Besides, the up-scaling of this technique requires optimized electrodes for larger installations and high voltage source with less energy demand (Xanthakis, Havet, Chevallier, Abadie, & Le-Bail, 2013). Also, electro-freezing cannot be used directly for products containing ionic molecules (e.g., NaCl) (Anuj, 2012).

It has been reported that ultrasound can activate and control the nucleation step during freezing of aqueous solutions (Nakagawa, Hottot, Vessot, & Andrieu, 2006). Although the exact mechanism is not yet well known, it is assumed that the collapses of cavitation bubbles might induce the nucleation of ice. Ultrasound can be applied at different degree of supercooling to initiate the ice nucleation process. It has been suggested that large crystals will be formed if ultrasound is applied at a low degree of supercooling while small crystals will be formed if ultrasound is applied at higher degrees of supercooling (Petzold & Aguilera, 2009). However, the further application of this technique is largely dependent on the availability of industrial equipment. It is also difficult to determine the optimal intensity for ultrasound treatment. Inappropriate intensity might lead to inconsistent nucleation among the samples and fragmented ice crystals in the already frozen samples. In addition, the up-scaling of ultrasound technique might also be quite difficult (Geidobler & Winter, 2013).

The use of high-pressure freezing also facilitates the nucleation step. The sample

is first cooled to subzero temperature under pressure. When the pressure is released to atmospheric pressure, the equilibrium freezing point of water increases and ice nucleation takes place. With this technique, very rapid freezing is achieved with a very fine ice structure (Sanchez et al., 2009). After pressure release, there is no difference between high-pressure freezing and classical freezing following the same course of temperature profiles. However, the further application of this technique is limited by the availability of equipment that can withstand the high pressure and related capital costs (Geidobler & Winter, 2013).

Although ice nucleation can be controlled to certain extent by the technologies mentioned above, their commercial applications are still limited, due to the variation of nucleation temperature and additional requirement of machinery investment as well as extra energy cost. Besides these nucleation methods, ice nucleation process can also be controlled with the addition of ice nucleation agents (Passot et al., 2009b). Ice nucleation agents can control ice nucleation efficiently without additional equipment requirement, which might be a promising option for commercial applications if a potential food grade agent can be obtained. In addition, these technology studies majorly focused on studying their effect on ice nucleation for the freezing part, but lacked of investigations on the effect of ice nucleation on the subsequent ice crystal growth and related ice morphology change. The potential alteration of ice morphology by ice nucleation agents could have a significant effect on the following processing steps.

2.3. Ice nucleators

Ice nucleators are defined as substances that can initiate ice crystallization at higher subzero temperatures under heterogeneous ice nucleation. These substances include inorganic and organic compounds. Inorganic ice nucleators, such as silver iodide, soil or mineral particles, are insoluble particles and consisted of the majority of atmospheric ice nucleators (Atkinson et al., 2013). The recent findings of global aerosol model suggested that mineral particles like feldspar ice nuclei are widely distributed and are consisted of the majority of ice nuclei in atmosphere for ice nucleation below -15 ^{o}C (Atkinson et al., 2013). Organic ice nucleators, especially biogenic ice nucleators, can be found in a wide range of biological sources and comprise a variety of chemical structures including proteins, saccharides, and lipids (Pummer et al., 2015). For example, proteinaceous ice nucleators have been discovered in living organisms such as freeze-tolerant animals, fungus and bacteria. Currently, the mechanism for the production of biogenic ice nucleators is still plausibly suggested (Lundheim, 2002). In the case of bacteria, the purpose for such production was previously suggested to access the nutrient by frost damage to their hosts. However, recent study has pointed out the production of biogenic ice nucleators may represent an important component of these microorganisms life cycle to provide a way to induce precipitation and their own precipitation from the atmosphere (Morris et al., 2014). This can be recognized as a dispersal strategy for these cells, allowing them to disseminate to new hosts via snow and rain (Christner, 2010). In

freeze-tolerant animals, such production is thought to help animals survive through the exposure to low temperature environment by controlling ice formation. The study regarding the specific location of INA in wintering plant tissues suggested that high INA in blueberry stems contributed to initiation of freezing in extracellular spaces of bark as subfreezing temperature sensor (Kishimoto et al., 2014).

2.4. What makes a good ice nucleating agent

The ice formation influences our daily life and a variety of scenarios ranging from climate change to intracellular freezing. Under most circumstances in nature, ice is formed through heterogeneous ice nucleation, thanks to the existence of impurities including dust particles, biological compounds and crystalline surfaces (Fitzner, Sosso, Cox, & Michaelides, 2015). Such diversity of ice nucleators leads to the question: what makes a good ice nucleating agent? Although many experimental and theoretical researches have been undertaken trying to answer this question, our current understanding regarding this question is still far from satisfactory. Recently, a number of experimental studies and computer simulation at the molecular level have been trying to characterize the ice nucleation activity of different materials by measuring their nucleation rates and temperatures, which provide the knowledge to further decipher the mechanism of ice nucleation (Fitzner et al., 2015). Based on the results so far, there are two most likely requirements for an efficient ice nucleating agent. First, it is suggested that to enable ice formation to take place, an ice nucleating agent needs to have ice lattice-liked structure to make water molecules cluster into an

ice-like pattern so that nucleation can be initiated (Lundheim, 2002). However, recent simulation investigation pointed out that lattice mismatch, which has been regarded as the most crucial requirement for a good ice nucleating agent, might be most desirable rather than a requirement (Fitzner et al., 2015). The second attribute is the water-surface interaction or hydrophobicity/hydrophilicity of a surface. Previous study has indicated that an increase in hydrophilicity led to the adverse effects on ice nucleation ability by using molecular dynamic simulations to add OH groups and this hypothesis has also been tentatively supported by some recent experimental results (Lupi & Molinero, 2014; Whale, Rosillo-Lopez, Murray, & Salzmann, 2015). There is increasing evidence that hydrophobic interactions are important, which exhibit a significant role in initiating ice formation. It has been suggested that the balance between the morphology of surface and its hydrophobicity can greatly affect the ice nucleation rate and lead to formation of different faces of ice on the same substrate (Fitzner et al., 2015). It is known that hydrophobic groups on protein surface are important for high affinity between ice and protein, which might be the determinant factor for the arrangement of OH groups that restrict polar interactions or the hydrogen-bond formation during the ice nucleation step (Davies, 2014). It was also suggested that ice nucleators needs to carry certain functional groups at the proper position to be effective (Pummer et al., 2015). In other words, it might not involve the entire surface of an ice nucleator to participate in ice nucleation, but only certain sections, which are considered as active sites. Currently, the correlation between the

surface hydrophilicity/ hydrophobicity and their ice nucleation activity is still under debate, since studies investigating the surface morphology of ice nucleators indicated that it is difficult to disentangle the effect of hydrophobicity from other factors like lattice mismatch and surface morphology.

3. Ice nucleation proteins

3.1. Origin and classification of ice nucleation proteins

Biological ice nucleators have been discovered in the atmosphere, soil, rain and snowfall, in various forms of life including certain strains of bacteria, fungus, algae, animals and plants (Christner, 2010; Iannone, Chernoff, Pringle, Martin, & Bertram, 2011; Morris et al., 2014; O'sullivan et al., 2014). Recent study has suggested that more and more fungal species are discovered with efficient ice nucleation activity and major compounds are thought to be proteins (Scheel et al., 2016). The chemical composition of these ice nucleators are majorly macromolecules, such as proteins, polysaccharides, lipids, and their hybrids, both as singular molecules as well as in aggregated form (Pummer et al., 2015). Proteinaceous compounds have been characterized in a variety of ice nucleators from bacterial, fungal, animal species, while polysaccharides are more commonly found in plant generated ice nucleators (Pummer et al., 2015). Among these biogenic ice nucleators, the ice nucleation proteins found in ice nucleation active bacteria show exceptional high activity with active nucleation temperatures above -5 ^{o}C (Atkinson et al., 2013; Guriansherman & Lindow, 1993).

Almost all the ice nucleating bacteria belong to gram negative genera and are mesophilic or psychrotrophic bacteria. Previous isolation study found 11 strains of ice-nucleating bacteria out of 135 strains from the bacterial collection stock at Ross Island in the McMurdo Dry Valleys region of Antarctica (Kawahara, 2002). These biogenic ice nucleators are a number of proteins that are able to catalyze the nucleation of ice formation at higher subzero temperature, which are considered as cold shock proteins (Wilson & Walker, 2010). Studies on the *ina* genes from these bacteria have revealed that ice nucleation proteins are large outer membrane proteins with a highly repetitive amino acid sequence responsible for ice nucleation activity (Kozloff, Turner, & Arellano, 1991; Turner, Arellano, & Kozloff, 1991; Warren & Wolber, 1991).

INPs can be classified into three groups with different nucleating activity within different temperature range. For instance, type 1 ice nuclei can catalyze the nucleation process of water at -2 to -5 ℃; while type 2 and type 3 ice nuclei can catalyze nucleation at -5 to -7, -7 to -10 ℃, respectively (Nemecek-Marshall, Laduca, & Fall, 1993). Accordingly, structure analysis of these ice nuclei also indicated different chemical composition between each other. Previous study predicted that type I ice nuclei had covalent linkage to cell membrane through a mannose-PI (phosphatidylinositol) with a major component of lipoglycoprotein (Kozloff, Turner, Arellano, & Lute, 1991). It was suggested that Phosphatidylinositol might be a major element of the ice nucleating site on the outer membrane of two bacteria (Kozloff, Lute, & Westaway, 1984). Type II was supposed to have sugar residues like glucose,

mannose, and attached to the protein core. And type III was the complex aggregation with only proteins (Muryoi, Matsukawa, Yamade, Kawahara, & Obata, 2003). It was also mentioned that *Erwinia herbicola* secreted liposomes with embedded INPs to produce cell-free ice nuclei in the medium rather than anchoring the protein on the cell membrane (Lorv, Rose, & Glick, 2014).

3.2.Molecular structures

Based upon the amino acid sequences of INPs, three domains were identified by modeling, including an *N*-terminal unique region, a highly repeated central region mostly consists of alanine, glycine, serine and threonine residues, and a *C*-terminal unique region (Kawahara, 2002). The functions of each protein domain were identified by the mutation of ice nucleation genes, which were suggested to be consistent with previous model studies. Previous study indicated that the *N*-terminal unique region was mainly responsible for aggregation of single INP into large aggregates and *C*-terminal unique region played an important role in protein folding (Abe, Watabe, Emori, Watanabe, & Arai, 1989). The repeated central region was suggested to work as ice template by binding water molecules (Warren & Wolber, 1991). The results showed that the deletion of *N*-terminal unique region only affected the nucleation activity of type I and II ice nuclei, while the deletion of *C*-terminal unique region and repeated central region could severely damage ice nucleation activity of all three ice nuclei types (Wolber, 1993). The further investigation regarding the molecular structure of INPs is limited by current biochemistry purification method, since it is still challenging

to purify ice nucleation protein with one specific molecular weight due to their complex aggregation effect. Besides, the presence of partial bacterial membranes might be required to have the appropriate structure for the nucleation activity of INPs, which makes their identification and isolation more difficult. Therefore, due to the complexity of protein aggregation and membrane fraction involved for activity, the comprehensive understanding of the molecular structure of INPs and their nucleating active site is still not clear yet.

Besides INPs, organisms living under subzero temperature also produce other types of ice active proteins, such as antifreeze proteins (AFPs), to defense against cold temperature stress and survive through freezing periods (Bar-Dolev, Celik, Wettlaufer, Davies, & Braslavsky, 2012). AFPs have been found in fish, plants, insects, fungus and bacteria (Graether & Sykes, 2004). They are able to prevent ice crystal formation by depressing the freezing point and inhibiting ice recrystallization (Hassas-Roudsari & Goff, 2012). In the bacterial strain of *Pseudomonas fluorescens* KUAF-68 isolated from Antarctic, the production of both INPs and AFPs was observed with the simulation of adding different amino acids (Kawahara et al., 2004). As suggested by previous studies, one of the significant characters that distinguish those two proteins was the molecular size difference. The molecular size of AFPs is generally within 30kDa, when the highly aggregated complexes of INPs have molecular mass over 600kDa with the combination of other components in most nucleation-efficient cells (Kawahara et al., 2004; Raymond, Janech, & Fritsen, 2009). Although these two

protein groups have different functions, it is likely that they might contain some similar structures which can interact with ice. So studies regarding AFPs molecular structures might shed some light on the INPs structures.

Based on the data of nuclear magnetic resonance (NMR) and X-ray experiments on highly active AFPs from two types of insects, the secondary structure was identified as a highly regular β-helix from the repetitive amino acid sequence and being stabilized by either hydrophobic core, or disulphide and hydrogen bonds (Liou, Tocilj, Davies, & Jia, 2000). The folding of the protein was also stabilized by the parallel β-sheets formed between the loops and the flat β-sheets. The structure of parallel β-sheets was proposed as the putative ice-binding surface, which contained most surface accessible threonine arraying in a regular TXT motif (Graether et al., 2000). It was suggested that the steric conformation of hydroxyl groups on the side chains of threonine perfectly matched the ice lattice pattern and thus explained the possible principle underlying the ice binding ability of AFPs as their mimicry of ice structure (Liou et al., 2000).

Recent studies suggest a similar way of functioning with water molecules between INPs and AFPs or IBPs (Bäumer, Duman, & Havenith, 2016; Davies, 2014). So the advances in the modeling of INP structure could be achieved by comparing with newly determined insect AFP structures indicated above. The comparison suggested that both AFPs and INPs might contain a similar β-helical folding, which interacted with water molecules through the repetitive TXT motif and the richness in neutral hydrophilic side chains like threonine provided the formation of hydrogen bonds with

water molecules (Graether & Jia, 2001; Kajava, 1995). Previous study indicated that the OH groups of threonine side chains matched the position of oxygen atoms in the ice lattice, which was likely to be the initial position for ice formation (Pummer et al., 2015). The possible factor that significantly distinguishes AFPs and INPs might be the size of the ice interacting surface because of their significant molecular size difference. Most previous structure modeling of INPs suggested the formation of largely planar extended macromolecules with the aligned aggregation of single molecule (Guriansherman & Lindow, 1993; Kajava & Lindow, 1993). Such aggregated structure enlarged the surface of planar arrayed hydrogen binding groups, which could be served as a template for turning water molecules into an ice lattice. Thus, it is likely that the ice binding surface area of INPs is large enough to stabilize a critical ice embryo and promotes ice crystal growth; while AFPs are small enough for only binding to ice crystal surface without further growth of ice crystals.

3.3. Food application of INPs

Based on current studies, the application of INPs in food industry is very promising. The addition of biogenic INPs into different food systems have showed significant effect on controlling supercooling stage during freezing processes, as compared to other ice nucleators (Li, Izquierdo, & Lee, 1997; Li & Lee, 1995). They have also been investigated for applications in food processes like freeze concentration and freeze drying to control the nucleation temperature (Watanabe & Arai, 1987, 1994; Michiko Watanabe & Arai, 1995). The results of these studies have demonstrated their

significant influence on the freezing step by suppressing the supercooling stage. Besides elevating nucleation temperatures, the addition of INPs also markedly affected ice formation pattern and can be used for freeze texturing (Arai & Watanabe, 1986; Li & Lee, 1998). In addition, INPs exhibited cryoprotective function on protein and cells during freezing process. Previous study suggests that the gel formation ability of fish actomyosin can be better retained with INPs during freeze/thaw cycles (Zhu & Lee, 2007). Also the yeast viability can be improved by INPs during long term storage study (Shi, Yu, & Lee, 2013). Further, the immobilization studies on different carriers provide feasible and flexible approaches to apply INPs in food products and processes. The immobilization of INPs on packaging materials, such as polyethylene films and modified zein films, indicates great potentials for frozen food applications like frozen dough (Gezgin, Lee, & Huang, 2013; Shi, Yu, Jin, & Lee, 2013). The immobilization of INPs on magnetic nanoparticles provides a feasible way of applying INPs in processes like freeze concentration (Zhou, Jin, Yue, & Lee, 2014).

4. Ice morphology

The term “ice morphology” has frequently appeared in the discussion part of papers working on freezing technologies, suggesting that their efficiency is largely depended on the morphology. So if ice nucleation could influence the ice morphology, it is very likely to be the mechanism for the influence of ice nucleation on the process efficiency of freezing technologies. However, current description of ice morphology is usually qualitative rather than quantitative and is often based on anecdotal evidences,

which leads to the ambiguity about ice morphology's relationship with different factors, such as ice nucleation and process efficiency. One of the crucial reasons for such vagueness is the lack of proper analysis tool to quantify ice morphology properties.

4.1. Ice crystal morphology

Morphology is defined as the forms of things, which includes the physical structure of a material. For ice morphology, the term can be characterized from a crystal lattice dimension to a large substance's size and shape. In the case of ice in nature, ice morphology can be described and measured at different scales, including crystal lattices, supra-crystalline structures like plates and columns, as well as macrostructures like icebergs and glaciers. At atomic level, there are nine known crystalline polymorphic structures of ice stable under different temperatures and pressure ranges. These microscopic structure differences can further develop into "macroscopic polymorphism" including a wide variety of macroscopic patterns or structures of ice crystals. The final ice crystal morphology is determined by the conditions when the crystals were formed and grown, such as temperature, crystal growth rate and the presence of solutes (Petzold & Aguilera, 2009).

In this study, the term "ice morphology" will be referred to the parameters that allow characterization of the ice structures influenced by the freezing factors that are relevant to their functions in freezing technologies.

4.2. Role of ice morphology in freezing technologies

In freeze concentration, the efficiency of ice crystal separation from concentrated liquid is suggested to be largely depended on its ice morphology. Previous study indicated that the inefficient separation was caused by the solute residue inside ice phase and the solute distribution was strongly influenced by the three-dimensional structure of the ice/liquid interface (Nagashima & Furukawa, 1997). Some studies had tried to reduce the solute residue by producing larger ice crystals, since larger ice crystals had smaller specific surface area so that the solute residue on ice crystal surface could be minimized (Kobayashi, Shirai, Nakanishi, & Matsuno, 1996; Shirai, Wakisaka, Miyawaki, & Sakashita, 1999; Smith & Schwartzberg, 1985). Another important factor related to the inefficient separation of solute from ice crystals is the shape of ice crystals formed during ice crystallization (Mahdavi, Mahvi, Nasseri, & Yunesian, 2011). The shape of ice crystals can be affected by different factors, such as the speed of crystal growth, environmental temperature and the existence of certain impurities, which can result in various ice crystal shapes from tabular to prismatic to acicular (Hartel, 2013). It was suggested by some studies that the formation of ice crystals in the shape of dendrites, which contained crystal branches extended into the solution, could cause higher solute entrapment in the ice fraction (Caretta, Courtot, & Davies, 2006; Petzold & Aguilera, 2009; Shibkov, Golovin, Zheltov, Korolev, & Leonov, 2003; Shirai et al., 1999; Wathen, Kuiper, Walker, & Jia, 2004). Besides, the orientation of ice crystals could also affect the freeze concentration efficiency (Okawa,

Ito, & Saito, 2009).

In freeze drying, the efficiency of drying process is governed by ice sublimation rate, which is also suggested to be strongly depended on its ice morphology. The ice sublimation rate is determined by the heat and mass transfer rate across dried layers, which is affected by the pore size and shape, and the connectivity of the porous matrix. The structure of the dried matrix is determined by the morphology of ice crystals formed during freezing (Passot et al., 2009a). Recent mathematical modeling analysis has confirmed that the morphological parameters of ice phase can strongly influence the mass transfer during freeze drying (Nakagawa, Hottot, Vessot, & Andrieu, 2007). Some experimental studies had also been conducted to investigate the relationship between ice crystal size and sublimation rates with indirect examination of crystal size using optical microscope (Geidobler & Winter, 2013; Petzold & Aguilera, 2009). It was found out that larger and dendritic ice crystals prepared by annealing of frozen samples, could lead to a higher mass transfer rate and thus a faster sublimation rate, as compared to frozen samples with smaller ice crystals prepared by liquid nitrogen immersion (Searles, Carpenter, & Randolph, 2001). Larger ice crystals were suggested to increase sublimation rate by leaving behind larger-sized pores, which had less resistance to water vapor flow during sublimation (Tang & Pikal, 2004). For freeze drying, ice morphology is also important for product quality. The batch homogeneity is an important issue during scale-up process development, so ice morphology with narrow ice crystal size distribution and similar crystal shapes is

desired to maintain the consistency between each batch (Nakagawa et al., 2007).

However, these observations and theories about the relationship between ice morphology and the efficiency of freezing technologies are largely depended on the evidence of indirect morphology observations and are somehow speculative (Sanchez et al., 2009). The descriptions about morphology characterizations were vaguely stated and mostly qualitative. For example, the description of “large ice crystal” was frequently used. But how to compare the size of two ice crystals if they don’t have similar shapes or how to define “large” if the crystals are under anisotropy growth. Therefore, more precise analysis of ice morphology properties and their relationship with process efficiency is required.

4.3. Relationship between ice nucleation and ice morphology

Nucleation is defined as the first step during the formation of a new thermodynamic phase via self-assembly. So ice nucleation means the formation of ice nucleus to initiate the ice crystallization process. Based on thermodynamic theories, the ice nucleation temperature, also known as supercooling degree, is supposed to influence the growth of ice crystals for different heat removal rates (Jiang, Wang, & Hou, 2012). This can further influence the orientation and structural pattern of ice crystals during the ice crystallization process (Deville et al., 2010; Miyawaki, Liu, Shirai, Sakashita, & Kagitani, 2005).

Previous studies have investigated the morphology of ice crystals grown from supercooled water in laboratory set-up space. Under supercooling degree ranging

from 0.1 °C to about 30 °C, microscopic ice structure changed from disk, to a branching morphology, to dendrite, to needle and needle branch, and to platelet (Petzold & Aguilera, 2009; Shibkov, Golovin, et al., 2003; Shibkov, Zheltov, et al., 2003). A computer simulation study also suggested that heterogeneous ice nucleation using ice nucleating agents may not only enhance the ice nucleation rate, but also alter the macroscopic structure of ice crystals (Cox, Raza, Kathmann, Slater, & Michaelides, 2013). In the field of biomedical engineering, scaffolds can be prepared by ice templating method and their architecture is suggested to be determined by ice nucleation (Pawelec, Husmann, Best, & Cameron, 2014; Schoof, Bruns, Fischer, Heschel, & Rau, 2000). In other freeze texturization studies, it was suggested that ice nucleation happened at different temperatures could result in ice morphology of wide ice crystal size distribution and various crystal shapes between each batch (Petzold & Aguilera, 2009). Besides, these evidences regarding the relationship between ice nucleation and related ice morphology are generally speculative based on thermal dynamic study rather than the observation of the real structure.

Further, the ice morphology formed at reduced supercooling degree was also proposed. Ice nucleation at lower level of supercooling was suggested to lead to the formation of larger ice crystals because of slower heat removal rate (Kobayashi et al., 1996; Shirai et al., 1999; Smith & Schwartzberg, 1985). Also, at lower degree of supercooling, the formation of ice crystals in dendritic shape, which can cause solute entrapment, could be avoided (Caretta et al., 2006; G. Petzold & Aguilera, 2009;

Shibkov, Golovin, et al., 2003; Shirai et al., 1999; Wathen et al., 2004). These proposed characteristics of ice morphology at reduced degree of supercooling show some similarities with the morphology positive for improving efficiency of freezing technologies.

However, there were also some studies reporting that ice nucleation had little influence on the formed ice structures. These studies investigated the effect of supercooling on the ice morphology grown on a cold surface, but the characterizations of ice morphology were vaguely described as “dense” or “sparse” without precise determination (Matsumoto, Akimoto, & Teraoka, 2010; K. Matsumoto, Inuzuka, Teraoka, Hayashi, & Murahashi, 2012). Therefore, quantitative approaches to measure and analyze ice morphology are required to further investigate the relationship between ice nucleation and ice morphology.

4.4.Imaging analysis method for ice morphology

Ice morphology studies have been conducted by using different methods, such as freeze fixation, optical microscopy with fluorescence or episcopic coaxial lighting, optical interferometry (Petzold & Aguilera, 2009). Methods like freeze fixation are considered as indirect methods and have the concerns of introducing artifacts due to the sample preparation. Other methods like microscope observation require cutting the samples for taking images at different locations, which might cause drainage of liquid from the ice matrix and lead to inaccurate results as well as the reconstructed structure based on that. In recent studies of sea ice internal structure, the method of

X-ray computed tomography (CT) has been applied as the non-destructive measurement of ice structure in three dimensions (Obbard, Troderman, & Baker, 2009).

X-ray CT is a technology that combines X-ray microscopy with tomographic algorithms. It generates X-ray images by the differences in X-ray attenuation based on the differences of material density without cutting samples. Tomographic algorithms exhibit three dimensional distribution of material density by reconstructing images of contiguous slices of X-rays passing through a specimen in different angles. It provides three dimensional imaging of sample microstructure under their original state and quantitative techniques can be used to precisely characterize different morphology properties (Schoeman, Williams, du Plessis, & Manley, 2016). Although X-ray CT is commonly used for qualitative comparison in medical diagnosis, it can be used quantitatively based on the intensity of the transmitted X-ray beam expressed as radiodensity (Kawamura, 1990). Radiodensity refers to the property of being relatively resistant to the passage of electromagnetic radiation, especially X-rays. X-rays are part of the electromagnetic spectrum, having a wavelength ranging from 0.01 to 10 nm (Florez, Evans, & Daly, 1998). The radiodensity is defined as $HU = 1000(\mu - \mu_w)/\mu_w$, where μ and μ_w are the attenuation coefficients of a substance of interest and water (Tanaka, Nakano, & Ikehara, 2011). So the Hounsfield scale is linearly transformed from the original attenuation coefficient, where water has a value of 0 HU and air has a value of -1000 HU. Since the coefficient of a material μ is proportional to its density,

the change in the Hounsfield unit represents the change in density. Therefore, in the radiographic images, dense materials that inhibit the passage of X-rays show relatively opaque white appearance, when less dense materials that allow X-rays to pass exhibit darker appearance. In the case of frozen solution, the concentrated liquid is denser than ice, and thus less transparent in the radiographic images as compared to ice.

Although the application of X-ray CT is still relatively new in the food science area, it has already been extensively applied in material science research, such as studies of internal structures of rock, ceramic and metal (Mousavi, Miri, Cox, & Fryer, 2007; Obbard et al., 2009). Recent development of higher resolution and contrast agent has enabled X-ray CT to measure ice morphology directly under its frozen state instead of freeze dried samples, and thus provides a non-destructive approach of analyzing frozen samples without artifacts from sample preparation. Recent development of imaging analysis related to X-ray CT has advanced with successful differentiation of crystal morphology and solute distribution inside ice matrix, as well as the determination of liquid volume fraction, fluid permeability, porosity and fractional connectivity (Golden et al., 2007; Pringle, Miner, Eicken, & Golden, 2009). Therefore, X-ray CT is a promising tool for investigating ice morphology in this study.

III. Objective

The objective of this study is to investigate the effect of ice nucleation proteins on process efficiency of freezing technologies and explore the related mechanism of ice morphology alteration. To achieve the objective, the specific aims and approaches of this study are listed below:

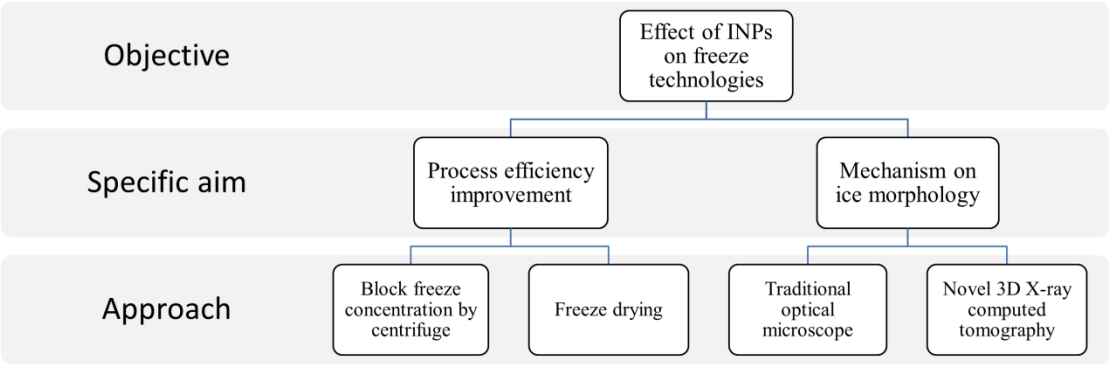

IV. Effect of INPs on process efficiency of freeze concentration and related mechanism of ice morphology

The work cited in this chapter has been published in the title of "A Novel Approach to Improve the Efficiency of Block Freeze Concentration Using Ice Nucleation Proteins with Altered Ice Morphology" in Journal of Agricultural and Food Chemistry (Volume 65, Issue 11, Pages from 2373 to 2382) on March 22, 2017.

1. Abstract

Freeze concentration is a separation process with high success in product quality. The remaining challenge is to achieve high efficiency with low cost. This study aims to evaluate the potential of using ice nucleation proteins (INPs) as an effective method to improve the efficiency of block freeze concentration while also exploring the related mechanism of ice morphology. Our results show that INPs are able to significantly improve the efficiency of block freeze concentration in a desalination model. Using this experimental system, we estimate that approximately 50% of the energy cost can be saved by the inclusion of INPs in desalination cycles while still meeting the EPA standard of drinking water (<500ppm). Our investigative tools for ice morphology include optical microscopy and X-ray computed tomography imaging analysis. Their use indicates that INPs promote the development of a lamellar structured ice matrix with larger hydraulic diameters, which facilitates brine drainage

and contains less brine entrapment as compared to control samples. These results suggest great potential for applying INPs to develop an energy saving freeze concentration method via the alteration of ice morphology.

2. Introduction

Freeze concentration is a separation process to remove water from a product. During this process, water is frozen into solid ice crystals and separated from the concentrated solution. Over the past decades, freeze concentration has achieved great success in industrial applications for preserving volatile flavors and heat sensitive nutrients in concentrated products due to its low temperature processing environment (Sanchez et al., 2011; Sanchez et al., 2009). In addition, due to its lower energy cost as compared to evaporation, this process was recently suggested as a potential application for desalination to help address water shortage for both human daily consumption and food production (Fujioka et al., 2013; Luo et al., 2010). However, current freeze concentration methods still face the challenge to achieve high concentration efficiency with low cost (Bruin & Jongen, 2003; Sanchez et al., 2009). In conventional suspension freeze concentration, high concentration efficiency was obtained using a scraped-surface heat exchanger to form ice nuclei and a recrystallization tank for ice growth. Unfortunately, this equipment requires a costly investment in machinery for the crystallization step (Otero, Sanz, Guignon, & Sanz, 2012). Recently, another type of freeze concentration method called block freeze concentration was developed to freeze water completely or partially, on a cold surface, into a porous ice block. Then the

concentrate is removed from this ice block through gravity or other external forces (Moreno et al., 2013; Petzold et al., 2015). This method significantly reduced the initial capital cost with its simplified crystallization step (Sanchez et al., 2011). However, the concentration efficiency of current block freeze concentration is not yet comparable to suspension freeze concentration and thus needs further improvement (Petzold et al., 2015). In suspension freeze concentration, the control of ice nucleation was suggested to improve its efficiency with fewer loss of entrained concentrate (Bruin & Jongen, 2003). The control of ice nucleation might also be important to improve the process efficiency of block freeze concentration, which has not been studied before.

To examine the effect of ice nucleation on the efficiency of block freeze concentration, an efficient method to control ice nucleation is required. Ice nucleation proteins (INPs) that have been studied in our lab for years, are a number of proteins that are able to catalyze the nucleation of ice formation at higher subzero temperatures by reducing the supercooling level (Li & Lee, 1995). These INPs are produced by a group of microoganisms, such as some strains in the genera of *Pseudomonas*, *Xanthomonas* and *Erwinia*, considered the most effective amongst the ice nucleation agents currently known (Kozloff, Schofield, & Lute, 1983; Li & Lee, 1998; Watanabe & Watanabe, 1994). Previous studies on the *Ina* genes from these bacteria revealed that ice nucleation proteins are large outer membrane lipoglycoproteins with a highly repetitive amino acid sequence responsible for ice nucleation activity (Kozloff et al., 1991; Warren & Wolber, 1991). Without changing other functionalities or the original flavor

profile of the products, it was demonstrated that these microbial INPs had a significant influence on suppressing supercooling level and shortening freezing time during freezing processes of food systems (Li, Izquierdo, & Lee, 1997; M. Watanabe, Watanabe, Kumeno, Nakahama, & Arai, 1989). Besides elevating nucleation temperatures, the addition of INPs also markedly affected ice formation pattern and can be used for freeze texturing (Arai & Watanabe, 1986; Li & Lee, 1998). The effect of INPs on process efficiency of block freeze concentration has not been investigated until now.

It is thought that freeze concentration efficiency is closely related to ice morphology and brine distribution formed during the freezing process (Petzold & Aguilera, 2009). Thus, to further understand the mechanism of concentration efficiency, the morphology of ice formed inside frozen samples should be characterized. Microscopy is often used for ice morphology studies but is plagued by artifacts formed during sample preparation (such as liquid drainage in the frozen state, or deformed voids in the freeze dried state) (Petzold & Aguilera, 2009). X-ray computed tomography (CT) combines micro-radiography with tomographic algorithms to generate three-dimensional images based on the radiographic density of a material. It provides three dimensional imaging of sample microstructure in their original state and quantitative techniques that can accurately characterize different properties (Schoeman et al., 2016). Although this technique is still relatively new in the field of frozen food studies, it has already been extensively applied in other material research,

such as studies of the internal structure of rock, ceramic and metal (Delattre, Bai, Ritchie, De Coninck, & Tomsia, 2013; Obbard et al., 2009). Recent developments of higher resolution and contrast agents have enabled X-ray CT to measure ice morphology directly in its natural state instead of in freeze dried samples (Golden et al., 2007; Obbard et al., 2009; Pringle et al., 2009). Thus, X-ray CT is an excellent tool to investigate ice morphology in this study.

Therefore, in the current study, the effects of biogenic INPs on the efficiency of block freeze concentration and the related mechanism on ice morphology are investigated (schematized in Figure 1). Since water shortages have been identified as a major concern for the food industry in the coming decade, the model of desalination via freeze concentration is used in this study (Mancosu, Snyder, Kyriakakis, & Spano, 2015). The effect of INPs on the freeze concentration process was investigated from two aspects, including the process efficiency at different variables and mechanism on ice morphology through different approaches. Firstly, process efficiency was measured using block freeze concentration assisted centrifugation at different variables, including INP concentrations and freezing temperatures, as well as separation conditions. After obtaining results at these parameters, process efficiency was further evaluated in practical application using desalination cycles to obtain fresh water. An estimation of potential energy savings was calculated based on the results from desalination cycles. Secondly, the mechanism on ice morphology was explored by both a traditional optical microscope and novel three dimensional X-ray computed tomography. The

characteristics of ice morphology, such as crystal size, shape and phase distribution, were observed and measured to identify morphology factors related to process efficiency.

3. **Materials and methods**

3.1. Materials

E. herbicola subsp. Ananas, obtained from the American Type Culture Collection (ATCC; ATCC Cat. No.11530), was used as the source of microbial INPs in these studies. Yeast extract was obtained from BD Biosciences (Franklin Lakes, NJ, USA). Sucrose (>99.9%), sodium chloride, Tris (Hydroxymethyl) aminomethane, potassium sulfate (K_2SO_4), magnesium sulfate ($MgSO_4$), and calcium chloride ($CaCl_2$) were obtained from Fisher Scientific (Fair Lawn, NJ, USA). L-serine, L-alanine and magnesium chloride ($MgCl_2$) were purchased from Sigma-Aldrich (St. Louis, MO, USA). All reagents were of analytical grade, and deionized water from Milli-Q was used throughout the experiments. Seawater was prepared artificially in the lab by dissolving 26.73g NaCl, 2.26g $MgCl_2$, 3.25g $MgSO_4$ and 1.15g $CaCl_2$ in 1L of deionized water.

3.2. Preparation and purification of ice nucleation proteins

Erwinia herbicola was stored frozen at -60 ℃ and grown in yeast extract (YE) media (20g/L), containing sucrose (10g/L), L-serine (2g/L), L-alanine (2g/L), K_2SO_4 (8.6g/L) and $MgSO_4$ (4g/L). Following culture expansion to a density of 10^8/L, the cells

were collected by high-speed centrifugation (10,000×g 20 mins @ 4 ^{o}C), and the resulting pellet was re-suspended in 20mM Tris buffer containing 20mM $MgCl_2$. The suspension was then sonicated on ice, using three brief (10 sec) sonication bursts generated by a Brandson sonicator (Danbury, CT) set at the 4.5 power output setting. Following sonication, the suspension was centrifuged again as described above and the supernatant was isolated and ultra-centrifuged at 4 ^{o}C and 160,000×g for 2h. Finally, the resultant pellet was re-suspended in 20mM Tris buffer with 20mM $MgCl_2$, and freeze-dried to obtain the INP powder. Lyophilized INPs isolated in this manner were stored at -18 ^{o}C prior to use.

3.3. Centrifugal freeze concentration procedures

The artificial seawater (40mL) used in this study was frozen in plastic centrifuge tubes (internal diameter of 29mm) by radial freezing using a static cooling bath containing a mixture of water and ethylene glycol. The samples were then removed from the cooling bath, and rapidly subjected to refrigerated centrifugation, using different speeds and times (delineated below) to separate the brine from the ice matrix. After centrifugation, the frozen ice fractions were thawed and the total dissolved salt (TDS) was measured at ambient temperature using a conductivity meter (model 09-326-2, Fisher Scientific). The volume of the solutions was also determined. The desalination rate was calculated using the following equation:

$$R_d = \frac{C_0 - C_{ice}}{C_0} \times 100\%$$

Where R_d is the desalination rate (%); C_0 is the TDS of the original seawater; C_{ice} is the TDS in the melt ice fraction.

To evaluate the effect of INPs on the efficiency of freeze concentration, the freeze concentration procedures above were performed using different variables to determine the desalination rates. The experimental variables tested in our study were INP concentration, freezing temperature, and centrifugal time and speed, all of which were identified, by other studies, as the main factors that could affect concentration efficiency (Luo et al., 2010; G Petzold & Aguilera, 2013). The levels of tested variables and controlled variables during each freeze concentration experiment are listed in Table 1. For example, the tested variable of the experiment group 1 was INP concentration. The controlled variables of group 1 were freezing temperature at -18 ^{o}C and centrifugation condition at 500 rpm for 5 mins. The salt concentration of seawater in nature (i.e. 33.3 g/L) was used as the initial salt concentration during the experiments of these four variables (i.e. experiment groups 1 to 4). For desalination cycles (i.e. experiment groups 5&6), both control and INP samples started at the concentration of seawater in nature (i.e. 33.3 g/L). The initial concentration of each subsequent cycle was based on the salt concentration in melted ice of its previous cycle. The desalination cycles ended, when the salt concentration in the melted ice fraction was less than the Environmental Protection Agency (EPA) standard of drinking water (i.e. 0.5 g/L). All experiments were performed in triplicates.

3.4. Ice crystal size determination

The evaluation of ice crystal structure was conducted using a 10× Olympus lens (0.25 N.A.) (Olympus, Tokyo, Japan) and a Q imaging 2560×1920 pixel CCD camera (Micropublisher, Surrey, Canada) equipped with a Linkham temperature-controlled imaging stage (LTS120, Linkham, Surrey, England). In a typical experiment, samples of seawater containing INP concentrations ranging from 10^{-7} mg/mL to 10^{-2} mg/mL were frozen in petri dishes. The frozen preparations were then placed on the microscope stage, which had been adjusted to -18 ^{o}C, and digital images of the ice crystal structure were collected by focusing on the ice surface. The average size of the ice crystals was determined using ImageJ software (version 1.46r, NIH, Bethesda, MD), using Feret's diameter calculation (Wang, Agyare, & Damodaran, 2009; Wang & Damodaran, 2009).

3.5. Evaluation of ice morphology using X-ray Computed Tomography

Three dimensional imaging analysis of frozen seawater samples was obtained using the Albira PET/CT Imaging System (Bruker, Billerica, MA) at standard voltage and current settings (i.e., 45kV and 400μA) at the Molecular Imaging Center at Rutgers University. A set of 400 image projections was then captured throughout a 360^{o} rotation of the sample. Reconstruction of X-ray data produced 3D images in which the air, ice and brine pockets could be differentiated based on differences in X-ray attenuation properties.

The morphology of ice structures within different growth heights was studied to

determine interface evolution in both control and INP samples. The samples were frozen on a cold surface at -18 ^{o}C until the vertical length of frozen matrix reached our targeted growth height. The frozen samples were then removed from the cold surface to pour out the remaining liquid and kept in the freezer at -18 ^{o}C before imaging analysis. A KI contrast agent was included in the solutions prior to freezing the samples for better differentiation between ice and brine phases. The morphology of ice crystals in both horizontal and vertical directions was characterized by the measurement of crystal dimension and brine inclusion width. The hydraulic diameter in the cross sections at different growth heights of the entire frozen sample was calculated based on flow mechanic theory, in order to compare the brine flow rate in control and INP samples (Nguyen & Wereley, 2002; Yamaguchi, 2008). The hydraulic diameter with different INP concentrations was determined at the same growth height. The hydraulic diameter of different channel shapes is given by:

$$\mathrm{D}_h = \frac{4 \times \text{Cross Section Area}}{\text{Wetted Perimeter}} = \frac{4\mathrm{A}}{\mathrm{P}}$$

For rectangular cross section:

$$\mathrm{D}_h = \frac{4\mathrm{ab}}{2(\mathrm{a}+\mathrm{b})} = \frac{2\mathrm{ab}}{\mathrm{a}+\mathrm{b}} \qquad (1)$$

For triangular cross section:

$$\mathrm{D}_h = \frac{4 \times \frac{\mathrm{b}}{2} \times \left(\mathrm{a}^2 - \frac{\mathrm{b}^2}{4}\right)^{1/2}}{2\mathrm{a}+\mathrm{b}} \qquad (2)$$

Where D_h = hydraulic diameter; a = ice crystal dimension in the cross section; b = maximum width of brine inclusion between two ice crystals.

Frozen samples for the brine distribution study were prepared in centrifugal tubes as previously described in the centrifugal freeze concentration procedures and placed in a cooling bath at the subzero temperature of -18 ^{o}C until completely frozen. Segmentation for imaging processing is done using thresholding techniques where the volume is partitioned into voxel groups of each region of interest (ROI) inside the sample. Volumes of the brine inside frozen samples were determined using VivoQuant image analysis software (version 1.23, inviCRO LLC, Boston MA). In a typical study volumes of the entrapped brine liquid were resolved and determined using a threshold range of 80 to 150 Hounsfield Units (Golden et al., 2007; Obbard et al., 2009).

3.6. Statistical analysis

One-way ANOVA was performed using Data Processing System software v.9.50. Differences among mean values were established by the least significant difference (LSD) at 5%.

4. Results and discussions

4.1. Effect of INPs on the supercooling point of seawater

The effect of INPs isolated from *E. herbicola* on the supercooling point of seawater was investigated using differential scanning calorimetry (Figure 2A). The supercooling point was determined as the lowest temperature that the supercooled solution could reach before the phase transition from water to ice took place, with the release of latent heat (as indicated in Figure 2B). With the addition of INPs at final

concentrations of 1mg/mL, the supercooling point of the seawater samples was elevated to -6.24 ^{o}C, as compared to the supercooling temperature of -21.38 ^{o}C for the control samples. Even at the lowest INP concentration of 10^{-6} mg/mL, the supercooling point increased to -11.36 ^{o}C. As suggested by Jung *et al*., the nonlinear relationship between INP concentrations and supercooling point might mainly be due to the dependence of ice nucleation activity on the degree of protein aggregation (Jung, Park, Park, Lebeault, & Pan, 1998). In the theory of heterogeneous ice nucleation, a larger nucleating site leads to a higher threshold temperature of ice nucleation activity (Schmid et al., 1997). Therefore, the variation of ice nucleation activity at the supercooling point (threshold temperature), shown by the DSC measurement, is likely to be the result of protein aggregation into different sizes of ice nuclei. Such aggregation process was suggested to be limited by stochastic chain-terminating events in the growing ice nucleus rather than the availability of INP concentration range (Southworth, Wolber, & Warren, 1988). The results indicate that INPs can function as effective ice nucleators for controlling the supercooling level of seawater even at low concentrations. The elevated nucleation temperature also suggests significant energy savings for the freezing step, which will be further discussed in the energy saving section.

4.2. Effect of INP concentration on desalination rate

The effect of INPs on freeze concentration efficiency as a function of desalination rate was investigated at different INP concentrations using block freeze concentration

assisted by centrifugation (Figure 3). In this technique, concentrated solute drains through the porous ice block and is separated from the ice under centrifugal force. The addition of INPs at a concentration of 10^{-6} mg/mL increased the desalination rate by 14% as compared to the control sample. This rate continued to increase from 48% to 53% with increases in INP concentrations from 10^{-6} mg/mL to 10^{-2} mg/mL. The results demonstrate that INPs can increase desalination rates, indicating that INPs can improve concentration efficiency and thus reduce related energy cost.

4.3. Desalination rate by INPs at different freezing temperatures and centrifugation conditions

To examine the practical application of INPs to the production of drinking water from seawater, the effect of these agents on desalination rates at different conditions, including freezing temperature and centrifugation speed or time, were investigated. INP concentration of 10^{-2} mg/mL was utilized in the subsequent experiments.

The effect of INPs on desalination rate at different freezing temperatures was determined (Figure 4). The results show that INPs can improve concentration efficiency at freezing temperatures of -13 ^{o}C and -18 ^{o}C compared to the control samples. At the temperature of -8 ^{o}C, INPs were able to freeze samples while seawater controls remained liquid. This elevation in the freezing temperature induced by INPs is associated with a 36% increase in the desalination rate, which was two-fold higher than the effect of INPs on the desalination rate of samples frozen at -18 ^{o}C. This increased desalination rate observed at the higher subzero temperature (-8 ^{o}C) is

thought to be due to the higher diffusion rate of solute under warmer temperature that then leads to less solute entrapment as compared to samples with INPs at lower freezing temperatures.

The effect of INPs on desalination rate at different centrifugation conditions was also characterized. Here, desalination rates were determined while varying centrifugation times (Figure 5A). For these studies, frozen samples of the control seawater and seawater containing INPs were centrifuged at 500rpm for increasing periods of time (i.e., 5, 10, 15, 20 and 30 mins). The results show that INPs exhibit marked effect on desalination rates at the lower centrifugation times of 5, 10 and 15 minutes, with increases ranging from 16% to 20% as compared to control samples under the same conditions. Since there was no significant difference ($P<0.05$) between the maximum desalination rate for controls at 30 mins and the desalination rate achieved by the INP sample at 15 mins, the same desalination effect can be achieved by INPs with only half the centrifugal duration. In other studies, the effect of INPs on desalination rates of frozen seawater was investigated by centrifugation for 10 mins at increasing speeds (i.e., 500 rpm, 1000 rpm, 2000 rpm and 4000 rpm). As shown Figure 5B, the difference in desalination rates between the control and INP samples was substantial at 18% at 500 rpm, but diminishing to 6% at a centrifugation speed of 4000rpm. Since there was no significant difference ($P<0.05$) between the maximum desalination rate for control samples centrifuged at 4000 rpm and the desalination rate attained by INP samples at 2000 rpm, the same desalination effect

can be achieved by INPs with only half the centrifugal speed. These results were used in further studies involving the application of INPs to the production of drinking water.

4.4. Effect of INPs on desalination rate of different salt concentration

The effect of INPs on the desalination rate was investigated in solutions with different initial salt concentrations (Table 2). At each salt concentration, INP samples have higher desalination rate with less salt residue in the melted ice fraction, as compared to control samples. Between control and INP samples, the difference in salt concentration of the melt ice fraction is more significant at higher salt concentration. For example, at the initial salt concentration of 33.3 g/L, there is a salt concentration difference of 2.2 g/L between INP and control samples, whereas such difference drops to 0.2 g/L at the initial concentration of 3.3 g/L. The results show that INPs could increase the desalination rate, with less concentrate in the ice phase, at each salt concentration. This indicates the ability of INPs to improve efficiency under wide range of initial concentrations. Therefore, the effect of INPs on desalination rate is independent of initial salt concentration.

4.5. Desalination cycles for obtaining fresh drinking water

To explore the potential use of INPs for obtaining drinking water in a more energy efficient desalination process, the effect of INPs on desalination rate of continuous desalination cycles was investigated. Cycles of INP samples were conducted under

higher subzero freezing temperatures and lower centrifuge speeds based on results from the studies above. Comparing the results of desalination cycle 1 from both control and INP samples (shown in Table 3), INP samples contained much less residual salt inside the ice phase, even though they were separated at a lower centrifuge speed. At the following desalination cycles, with lower initial salt concentrations, INP samples also had a significantly higher desalination rate as compared to controls. For instance, the third cycle of control samples and the second cycle of INP samples (Table 3) had very close residual salt amounts (i.e. 0.9 g/L) in the melted ice fraction. But the initial salt concentration of INP samples (i.e. 3.33 g/L) was much higher than control samples (i.e. 1.8 g/L). When the fourth cycle of control samples and the third cycle of INP samples both had initial salt concentrations near 0.9 g/L, the desalination rate of INP samples (i.e. 60%) was significantly higher than control samples (i.e. 50%). At the end of cycle 3, INP samples reached the target of containing salt less than 0.5 g/L in the melt ice; while at the end of cycle 3 of control samples, the concentration in melted ice was 0.9 g/L, that was still higher than EPA standard and thus needed an extra cycle to reach the goal of 0.5 g/L. Therefore, these results above suggest that fewer desalination cycles with less energy cost, are needed with the addition of INPs during a continuous desalination process, to meet the drinking water standard. This also strongly supports that INPs have the ability to improve efficiency during freeze concentration cycles with different initial solute concentrations. The mechanism for such improvement is further explained in the ice

morphology section follows.

4.6. Energy saving by INPs to obtain drinking water

The energy savings realized from using INPs in freeze concentration to obtain drinking water is thought to originate from three aspects of the overall process. Firstly, by freezing at a higher subzero temperature with INPs, the thermostats of freezing units could be adjusted to warmer settings. Previous studies indicate that a freezer consumes less electricity if its thermostat is set to a higher subzero temperature (Saidur, Masjuki, & Choudhury, 2002). The energy saving is due to the decreased frequency of compressor cycles, which decreases the overall running time needed to maintain the desired temperature. Other studies suggest that for each degree of decrease in freezer temperature, energy consumption is increased by 6.5-8% (Hasanuzzaman, Saidur, & Masjuki, 2008; Saidur, Masjuki, Mahlia, & Nasrudin, 2002). Assuming an energy reduction of 6.5% for each degree of increase, the energy cost associated with freezing during each desalination cycle could be reduced by almost 50%, by freezing at -8^{o}C rather than -18^{o}C with INPs. Secondly, by centrifugation at lower speeds with INPs, the amount of energy consumed during the separation process would be reduced. The Affinity Laws of pump indicate that the power requirement (kW) varies by the cube of the change in speed, which means that at two times the speed, a centrifuge would consume eight times the power. Based on this projection, the energy cost associated with centrifugal separation for samples containing INPs at 2000rpm would only require one eighth of that needed for control

samples at 4000rpm. Moreover, decreasing the centrifugation speeds required for desalination could also greatly reduce the initial installation costs as well as the costs associated with equipment repair and wear (Spicer, 1974). Thirdly, our study above on desalination cycles suggests that INP required only three cycles to reach the drinking water standard while control samples needed four cycles. Analysis of estimated energy cost to obtain drinking water through desalination cycles in this study was calculated based on laboratory equipment specifications during freezing and separation steps (Table 4). By combining the energy consumption for each step with cycle numbers and final yield, the total energy saving by INPs could be approximately 50% for obtaining fresh drinking water. Therefore, the application of INPs in freeze concentration suggested great potential for energy savings.

4.7. Effect of INPs on ice morphology

To examine the influence of INPs on ice morphology, the pattern of individual ice crystal was first characterized using an optical microscope (Figure 6). The boundaries of ice crystals in the images could be visually defined by the brine veins, or brine channels, which contained concentrated salt solutions (Figure 6A). Such structures within ice are known to result from solute accumulation at the solid-liquid interphase during the growth of ice crystals (Junge, Eicken, & Deming, 2004; Junge, Krembs, Deming, Stierle, & Eicken, 2001; G Petzold, Niranjan, & Aguilera, 2013). Since the ice crystals appeared irregular in shape, the Feret's diameter determination was used in this study. We measured an object's size along a specific direction, instead of

assuming crystal cross-sections are normalized circles with defined dimensions. Using this method of analysis, the size of ice crystals in the visual field was found to increase significantly with increasing concentrations of INPs (Figure 6B). It must be noted that the size of crystals formed in the presence of higher concentrations of INPs tested (>10^{-3} mg/mL) was not calculated since most crystals that appeared in the field were not intact. However, increases in crystal size in these samples were obvious with the increase of INP concentration (see Figure 6A images f&g). With the addition of INPs at the concentration of 10^{-7} mg/mL, the average size of ice crystals significantly increased to 37.6 μm as compared to control samples at 30 μm. Between INP concentrations from 10^{-7} to 10^{-5} mg/mL, the increase of ice crystal size was relatively small, with only a 2 μm increase between every concentration increase. At the concentration of 10^{-4} mg/mL, the average size of ice crystals was 48.1 μm, which is a significant increase from the size of 42.1 at 10^{-5} mg/mL. Although INP concentrations higher than 10^{-3} mg/mL were not measured quantitatively, the increase of ice crystal size was obviously significant, suggesting that ice crystal size increased more significantly at higher INP concentrations between 10^{-4} to 10^{-2} mg/mL. It is well to recognize that for freeze concentration processes, larger ice crystals are desired as they improve concentration efficiency by minimizing the surface area at interphase and thus reduce the solute entrapped within the ice (Petzold & Aguilera, 2009; Spicer, 1974). Studies have been conducted by other investigators to generate larger ice crystals through other methods, such as modifying the operation conditions or the

equipment used for crystallization process, and have demonstrated optimized separation process with improved concentration efficiency (Kobayashi et al., 1996; Smith & Schwartzberg, 1985). Therefore, it is very likely that the formation of larger ice crystals by INPs helped improve concentration efficiency.

However, such ice morphology of the thin layer observed under microscope is limited to a small and two dimensional scale, that is inadequate to represent the actual morphology of the frozen matrix subjected to the freeze concentration process. The evaluation of INP effect on three dimensional morphology of ice block within different growth heights was conducted using X-ray CT to scan both control and INP samples (i.e., 10^{-2} mg/mL) frozen on cold surface. The radiographs (Figure 7A) show that the periphery of the ice block (initial ice layer close to the cold surface) is composed of a zone in which solute and randomly oriented ice crystals were finely commingled. The thickness of this peripheral layer, described as “transitional region” by other investigators (Delattre et al., 2013), was significantly decreased in samples containing INPs. The average length of the transitional region for control and INP samples in this study was measured to be 13.0 mm and 3.6 mm respectively for a total crystal growth length of 20 mm (Figure 7B). The lamellar structure of ice crystals emanating from this region extended in the direction of crystal growth as indicated by the white arrows in Figure 7A. Since this region is homogeneous across all the vertical slices of the samples, the fraction of lamellar ice structure can be calculated based on their length along the freezing direction. Therefore, in the current study,

within an ice crystal growth length of 20 mm, the lamellar ice structure consists of roughly 35% of the volume in control samples compared to 82% of INP samples. Such parallel ice structures are suggested to occlude less solute and work as drainage channels toward the freezing front (Waschkies, Oberacker, & Hoffmann, 2011). This difference in ice matrix morphology made by INPs might also have a significant impact on other freeze concentration processes, such as progressive freeze concentration. The thickness of the ice layer grown on the cold surface in recent progressive freeze concentration studies is approximately 5 to 15mm, which is within the range of crystal growth length (20mm) in this study (Miyawaki et al., 2005; Sánchez, Ruiz, Raventos, Auleda, & Hernandez, 2010). Therefore, the results of this study are likely to be applicable to freeze concentration processes that involve growing ice crystals on cold surfaces.

Besides the longitudinal growth direction, the morphology of longer ice crystal dimension and parallel ice plate was also observed in the cross sections of INP samples (i.e., 10^{-2} mg/mL) (Figure 8A). With the measurement of crystal dimension and brine inclusion width, the hydraulic diameter was calculated at different growth heights of the frozen sample to indicate the brine flow rate in both control and INP samples. The cross section of INP samples contains parallel ice plates so that the brine flow inside goes through rectangular shaped pores, while in control samples the pores are closer to triangularly shaped. Based on the equations (1) and (2) in the method, the hydraulic diameters in control and INP samples are shown in Table 5. The INP

samples with rectangular shaped pores have a significantly larger hydraulic diameter at different heights through the entire frozen sample as compared to controls. Since the flow rate is proportional to the hydraulic diameter, it is mechanically easier for the liquid inside INP samples to be expelled (Nguyen & Wereley, 2002). As shown in Figure 8B, the ice morphology in cross sections changes at different INP concentrations. Further measurement of these radiographs suggests that ice crystal dimension increases with the increase of INP concentration. The solute inclusion width between ice crystals also changes at different INP concentrations (as shown in Table 6). Based on the equations (1) and (2) in the method, the hydraulic diameter is calculated using the results of crystal dimension and inclusion width, suggesting an increase of hydraulic diameter with the increase of INP concentration (Table 6 and Figure 8C). Thus, the concentrated solutes can be more easily drained through these larger hydraulic pores along the longitudinal channels in INP samples, when compared to the crystal morphology in control samples of this study. Therefore, the increased concentration efficiency in INP samples is very likely to be closely related to those ice morphology alterations.

4.8. Brine distribution

Since the solute distribution in frozen sample is dominated by ice morphology, X-ray computed tomography was also used to observe the brine distribution in both control and INP samples, to shed more light on mechanism of efficiency improvement. Illustrations of horizontal and vertical 2D slices of original radiographs and processed

images with region of interest (ROI) are shown in Figure 9A. The 3D graphs with ROI shown in the same figure were reconstructed by combining a series of 2D radiographs.

For this analysis, a range of pixel intensities reflecting the radiographic density of brine pockets were assigned a false color (i.e., yellow) and analyzed (Figure 9A). Using this method the distribution of the brine pockets inside the ice matrix, as well as the volumes of the entrapment concentrated salt solution could be determined directly. Comparison of the images show that samples containing INPs exhibited the colored brine pockets mainly close to the center of the frozen matrix, while in control samples these pockets were distributed throughout the sample from center to edge. Since radial freezing was utilized to generate these samples, this observation indicates an improved exclusion of brine liquid at the ice-brine interphase during the freezing process in the INP samples. Quantitative volumetric analysis of the false-colored brine pockets within the three-dimensional images confirmed that less brine was entrapped inside the ice matrix of INP-containing samples (Figure 9B), which might contribute to improvement of efficiency. Moreover, upon examination of the radiographs of centrifuged INP sample after brine removal (see Figure 10), the lamellar structure (indicated by the red arrow) on the interfacial surface can also be observed. This confirms the formation of liquid channel in INP samples during the freezing step in this study. Conversely, after centrifugation control samples exhibited tortuous crystal morphology at the interfacial surface, suggesting a non-oriented

crystal and solute mixture during the freezing process.

4.9. Textural analysis

The influence of INPs on ice morphology might also affect the mechanical properties of ice matrix, which is also closely to the efficiency of ice-brine separation step. Thus, the effect of INPs on mechanical property of frozen seawater was investigated by determining the compression strength of frozen seawater at different INPs concentrations. As shown in Figure 11, the compression strength was indicated by measuring the distance of the probe penetrating into the frozen seawater samples under consistent compression force. With the increase of INP concentrations, the distance under same compression force increased, which indicated that the addition of INPs reduced the ice strength and made the frozen seawater much easier to be compressed. This influence by INPs might be closely related to the alteration of ice structure observed in the X-ray study above. The structure of highly aligned ice layers in INP samples consisted of more connected brine inclusion and these areas would lose its stiffness more easily by fast expelling the brine inclusion between the ice layers (Lau, Jones et al. 2008). Between different compression forces, the moderate force of 5524g exhibited the most significant difference between the control and INPs samples. The reason for this might be that the lower compression force drove the brine out of the ice matrix very slowly so that the difference between control and INP samples was not significant; while the higher compression force might not only expel the brine but also break down some thin ice crystals and thus showed more significant compression

distance with relatively large deviations. The compression distance here was measured by alumina cylinder with diameter of 10mm. In order to verify the effect of INPs on this alteration, alumina cylinder with bigger diameter of 25mm was also performed and showed the same trend. The influence of INPs on the compressive strength as the mechanical property suggests the faster brine drainage from frozen seawater by INPs, which positively supports the reduced requirement of centrifugal intensity observed in the previous experiments of the effect of INPs on centrifugation conditions.

4.10. Effect of INPs on concentration efficiency in food systems

The effect of INPs on the freeze concentration efficiency of different food systems was investigated at different freezing temperatures as compared to seawater (Figure 12). Juice and milk were chosen as they are commonly freeze concentrated in food industry.

At -18^{o}C, INPs significantly improved the concentration efficiency of seawater, juice and milk as compared to control samples under the same separation conditions. Under higher subzero freezing temperature of -8^{o}C, INP samples were able to overcome supercooling stage when controls were unable to freeze. At -8^{o}C, INPs increased the concentration efficiency of seawater, juice and milk by 21%, 23% and 15% respectively, as compared to controls at -18^{o}C. By freezing at -8 ^{o}C instead of -18 ^{o}C, the energy cost can be significantly reduced for the freezing step as well. These results suggest the same trend of easier and faster solute removal from frozen matrices by INPs. This further indicates that such improvement of concentration

efficiency by INPs is not limited to seawater and could possibly be expanded for wide applications in freeze concentration with lower process cost. The effect of INPs on solute distribution inside juice and milk was also been studied using X-ray CT (Figure 13). The quantitative analysis of concentrate entrapment volume inside ice matrix was determined by calculating the pixels with grey value between 20 and 40. The results show less concentrate inclusion inside frozen seawater, juice and milk with INPs by 29%, 9% and 13% respectively. The results suggest that better exclusion of concentrated solution during freezing can be achieved by INPs in different liquid system, which is independent with the solute inside the liquid systems and probably is related to their ability to alter the ice structure.

In conclusion, the present study demonstrates that INPs can significantly improve the efficiency of block freeze concentration with altered ice morphology. Our results indicate that approximately 50% of the energy cost associated with freeze concentration can be saved by the inclusion of INPs in desalination cycles to obtain fresh water. The imaging analysis indicates that INPs can alter ice morphology by inducing the growth of larger sized ice crystals and a lamellar structured ice matrix with a larger hydraulic diameter that facilitates brine drainage and contains less entrapped solute as compared to control samples. The results of this study suggest that INPs have the potential to improve the desalination process as well as other freeze concentration related processes with enhanced efficiency and reduced cost. Further, the use of X-ray computed tomographic analysis in this study indicates its

applicability to study internal structures of frozen food matrixes. It is also worthy to further investigate the effect of INPs on other morphology affected freezing processes.

Table 1 Experimental design for investigating the effect of INPs on freeze concentration efficiency under different variables

experiment group	tested variable	variable levels		
		INP concentration (mg/mL)	freezing temperature (^{o}C)	centrifuge condition
1	INP concentration	0, 10^{-6}, 10^{-4}, 10^{-2}	-18	10 mins @ 500 rpm
2	Freezing temperature	10^{-2}	-18, -13, -8	10 mins @ 500 rpm
3	Centrifuge time	10^{-2}	-18	5, 10, 15, 20, 30 mins @ 500 rpm
4	Centrifuge speed	10^{-2}	-18	10 mins @ 500, 1000, 2000, 4000 rpm
5	DC of control	0	-18	10 mins @ 4000 rpm
6	DC of INPs	10^{-2}	-8	10 mins @ 2000 rpm

*DC represents desalination cycle.

Table 2 Desalination rate of control and INP samples with different initial concentrations [a]

samples	initial concentration (g/L)	salt concentration in melted ice (g/L)	desalination rate %
control	3.3	1.2 ± 0.18	63.94% ± 5.55%
	8.3	2.9 ± 0.19	65.27% ± 2.26%
	33.3	6.5 ± 2.31	80.50% ± 6.94%
INPs	3.3	1.0 ± 0.10	69.79% ± 3.10%
	8.3	2.3 ± 0.13	72.13% ± 1.63%
	33.3	4.3 ± 0.85	86.99% ± 2.54%

[a] Samples for each initial salt concentration were frozen at -18^{o}C and centrifuged at 4000rpm for 10mins

Table 3 Comparison of desalination cycles between control and INP samples [a]

samples	cycle number	initial concentration (g/L)	initial volume (mL)	concentration of melted ice (g/L)	melted ice volume (mL)	desalination rate %	yield %
control	1	33.3	40	6.5 ±2.31^{a}	24.9 ±2.9^{c}	80.50 ±6.94^{d}	62.25 ±7.13^{c}
	2	6.5	40	1.8 ±0.18^{bc}	35.4 ±0.8^{a}	73.07 ±2.72^{c}	88.44 ±1.88^{a}
	3	1.8	40	0.90 ±0.05^{bc}	36.4 ±0.6^{a}	50.08 ±2.84^{a}	91.00 ±1.57^{a}
	4	0.9	40	0.45 ±0.05^{c}	37.2 ±0.3^{a}	50.02 ±5.96^{ab}	92.92 ±0.72^{a}
INPs	1	33.3	40	3.3 ±0.38^{b}	20.8 ±0.6^{d}	89.99 ±1.14^{e}	51.88 ±1.44^{d}
	2	3.33	40	0.94 ±0.16^{bc}	29.8 ±2.9^{b}	71.82 ±4.88^{c}	74.38 ±7.25^{b}
	3	0.94	40	0.38 ±0.03^{c}	33.9 ±1.0^{a}	59.88 ±3.67^{b}	84.69 ±2.58^{a}

[a] Control samples for each cycle were frozen at -18^{o}C and centrifuged at 4000rpm for 10mins and INP samples for each cycle were frozen at -8^{o}C and centrifuged at 2000rpm for 10 mins.

* Values with no common letters are significantly different ($p < 0.05$).

Table 4 Comparison of energy cost between control and INP samples for obtaining fresh water

steps	samples	control	INPs
freezing	cooling output (kW)	0.2	0.1
	freezing time (hr)	1	1
	energy cost (kWh)	0.2	0.1
separation	maximum power required for centrifuge used in this study at 14,000rpm is 2.0kW		
	centrifuge speed (rpm)	4000	2000
	centrifuge power (kW)	0.0467	0.0058
	centrifuge time (hr)	0.3333	0.3333
	energy cost (kWh)	0.0156	0.0019
desalination	energy of each cycle (kWh)	0.2156	0.1019
	cycle number	4	3
	total energy cost (kWh)	0.8623	0.3058
	final yield (10^{-3} m^3)	0.7448	0.5228
	final energy cost (kWh/m^3)	1157.7	585.0

Table 5 Effect of INPs on hydraulic diameter at different growth height

samples	growth height (mm)	crystal dimension (mm)	inclusion width (mm)	hydraulic diameter (mm)
control	11.6	3.0 ±0.5[a]	0.75 ±0.17[a]	0.66 ±0.15[a]
	17.0	5.2 ±0.8[b]	0.76 ±0.20[a]	0.69 ±0.18[a]
	24.7	6.3 ±0.8[c]	0.79 ±0.18[a]	0.74 ±0.16[a]
INPs	8.6	8.4 ±1.1[d]	0.54 ±0.08[b]	1.02 ±0.15[b]
	20.0	10.8 ±0.5[e]	0.63 ±0.14[ab]	1.19 ±0.22[c]
	24.2	12.2 ±1.7[f]	0.63 ±0.11[ab]	1.20 ±0.21[c]

* Values with no common letters are significantly different ($p < 0.05$).

Table 6 Effect of INP concentration on morphology of frozen seawater matrix

INP concentration (mg/mL)	crystal dimension (mm)	inclusion width (mm)	hydraulic diameter (mm)
0.00E+00	2.79 ± 0.12[a]	0.61 ± 0.01[a]	0.55 ± 0.01[a]
1.00E-06	3.02 ± 0.48[a]	0.83 ± 0.07[b]	0.72 ± 0.06[b]
1.00E-04	4.19 ± 0.28[b]	0.82 ± 0.06[b]	0.74 ± 0.05[b]
1.00E-02	11.02 ± 1.12[c]	0.54 ± 0.06[a]	1.02 ± 0.02[c]

* Values with no common letters are significantly different ($p < 0.05$).

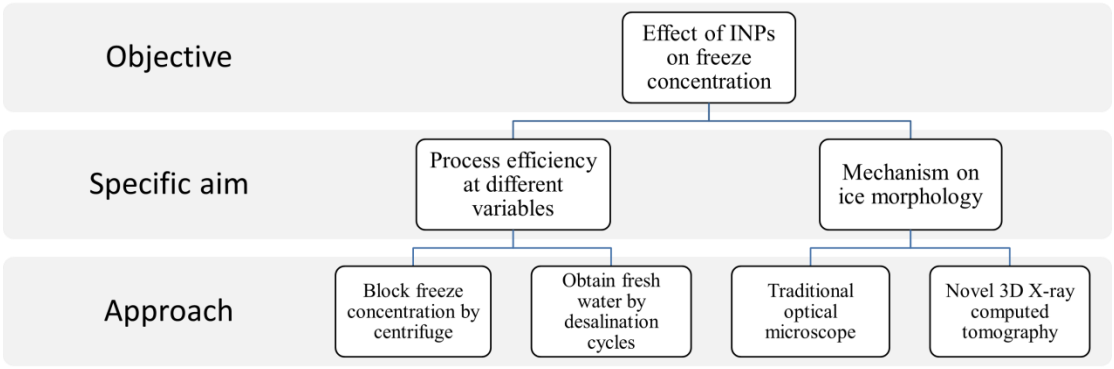

Figure 1 The diagram of objectives and approaches to study the effect of INPs on freeze concentration process including process efficiency and related mechanism on ice morphology

A

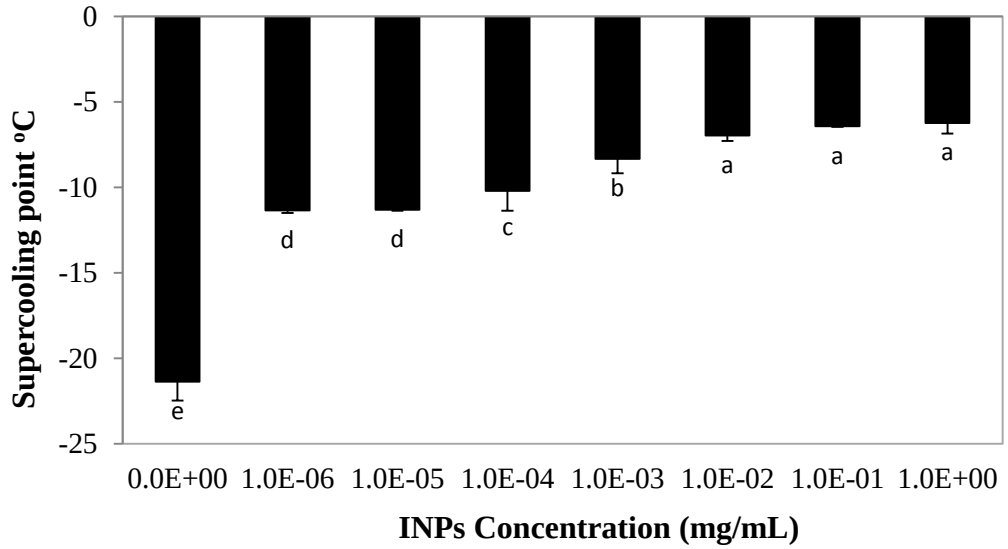

B.

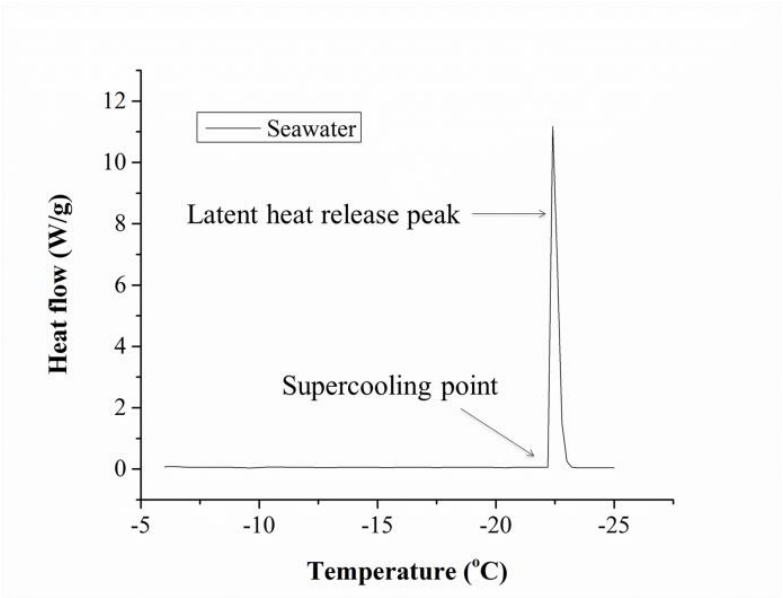

Figure 2 (A) Effect of increasing INP concentrations on the supercooling point of seawater. The letters on the top of error bars indicate the result of statistical analysis. Values with no common letter are significantly different ($P < 0.05$). (B) DSC thermogram of freezing of artificial seawater solution at a cooling rate of 1 ^{o}C/min.

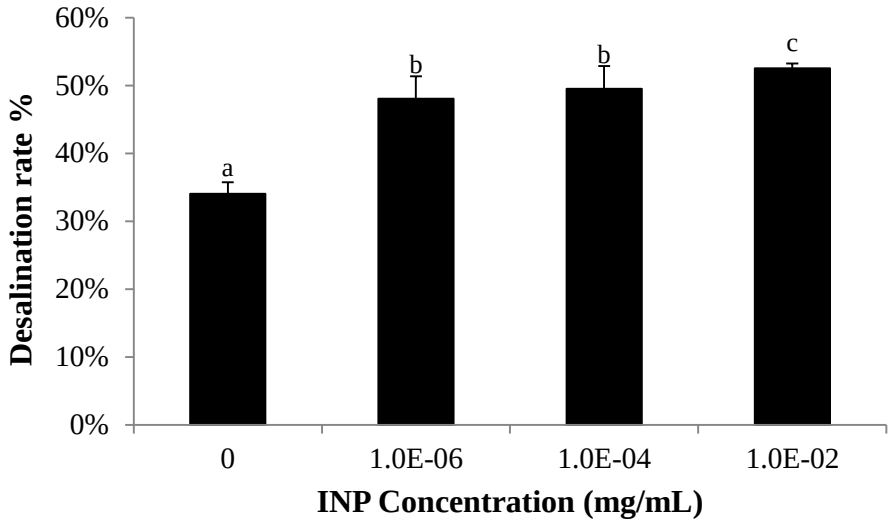

Figure 3 Effect of increasing INP concentrations on desalination rate. Values with no common letter are significantly different ($P < 0.05$)

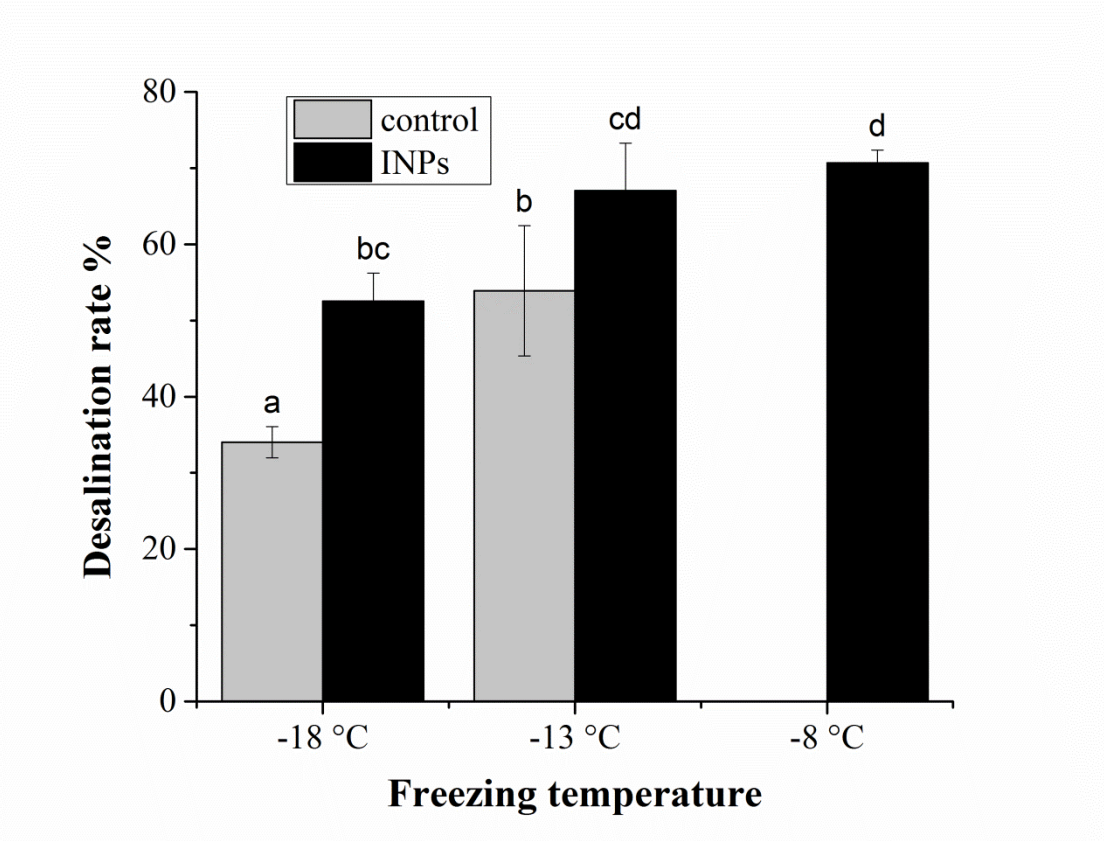

Figure 4 Effect of INPs on desalination rate of samples under different freezing temperatures. The letters on the top of error bars indicate the result of statistical analysis. Values with no common letter are significantly different ($P < 0.05$)

A

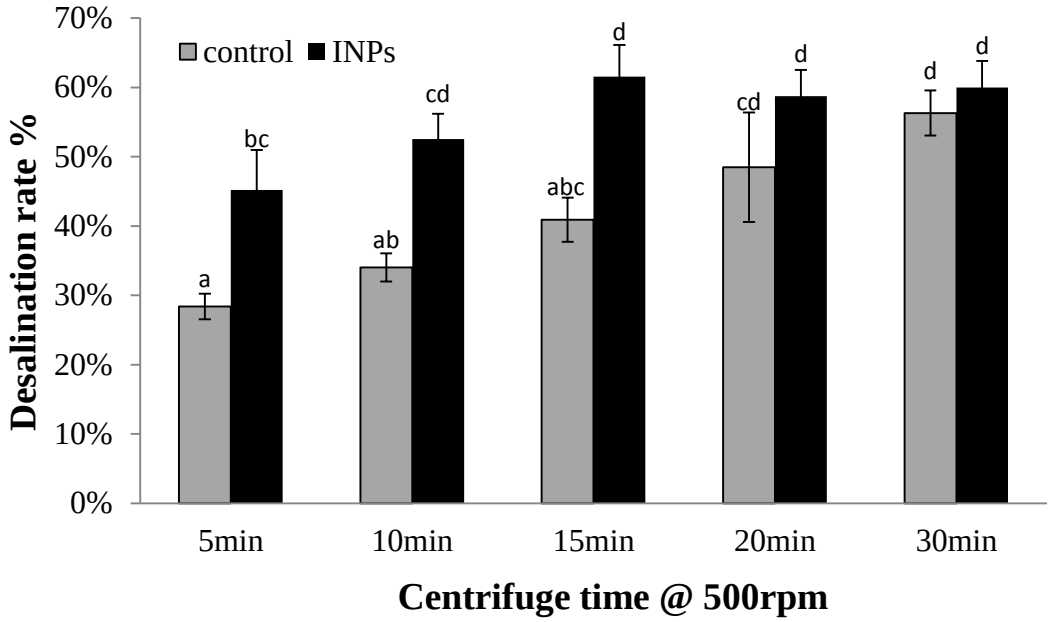

B

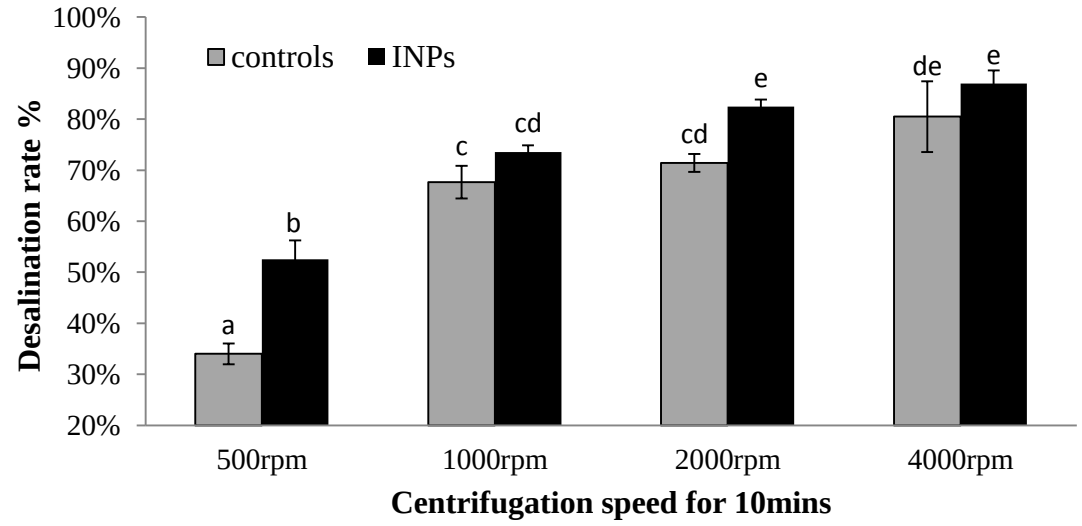

Figure 5 Effect of INPs on desalination rate under different conditions. (A) Effect of INPs on desalination rate of samples subjected to increasing centrifugation time at 500rpm. (B) Effect of INPs on desalination rate of samples subjected to increasing centrifugation speed for 10 mins. The letters on the top of error bars indicate the result of statistical analysis. Values with no common letter are significantly different ($P < 0.05$).

A

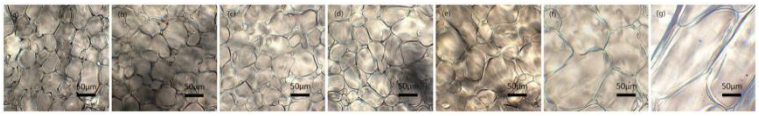

B

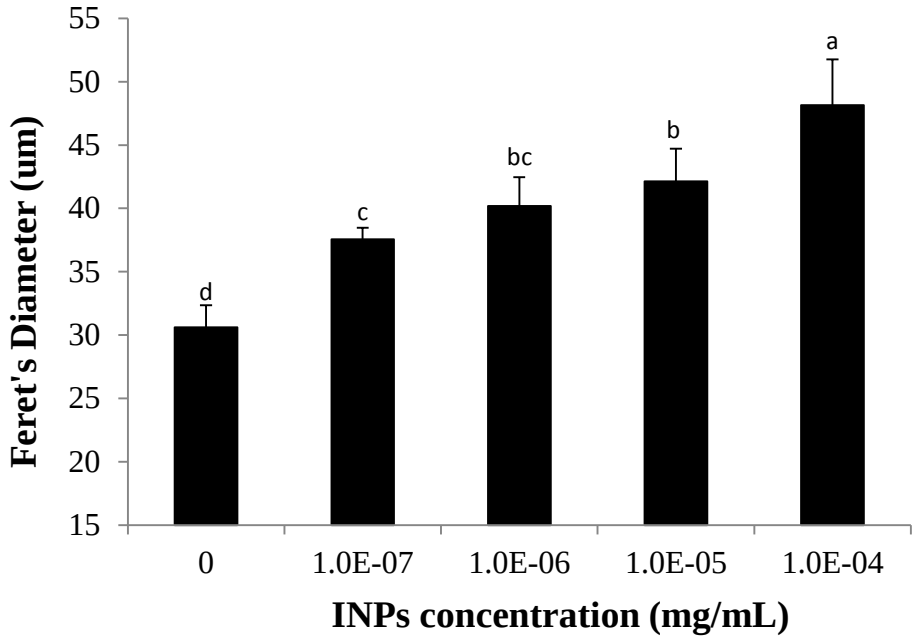

Figure 6 Effect of INP concentrations on ice crystal size in frozen seawater. (A) Bright field images of seawater containing INPs at (a) 0 mg/mL, (b) 10-7 mg/mL, (c) 10-6 mg/mL, (d) 10-5 mg/mL, (e) 10-4 mg/mL, (f) 10-3 mg/mL and (g) 10-2 mg/mL. (B) Quantitative determination of ice crystal size in frozen seawater. The letters on the top of error bars indicate the result of statistical analysis. Values with no common letter are significantly different ($P < 0.05$).

A

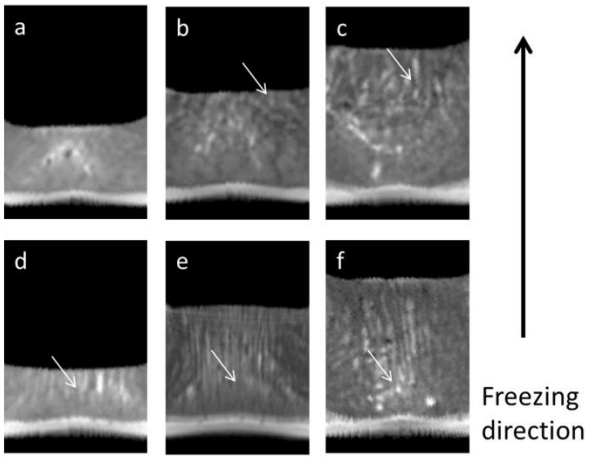

B

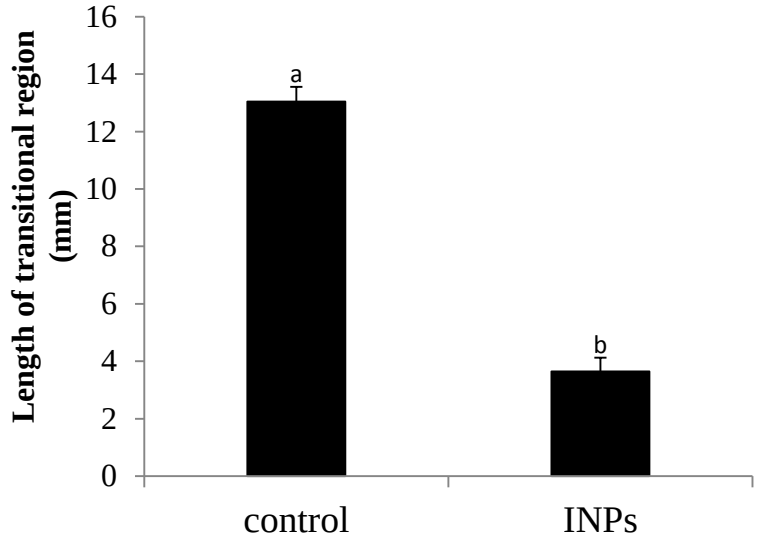

Figure 7 Effect of INPs on ice structure along the freezing direction. (A) Radiographs of control samples at different growth height (a, b, c); Radiographs of INP samples at different growth height (d, e, f). The white arrows indicate the lamellar structure of ice crystals emanating from the transition region. (B) Effect of INPs on the length of the transitional region before turning into lamellar structure.

A

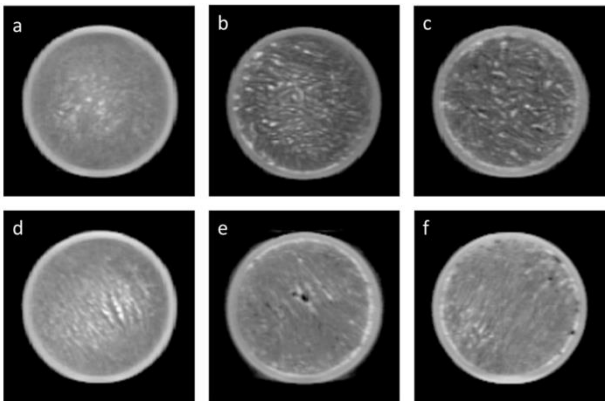

B

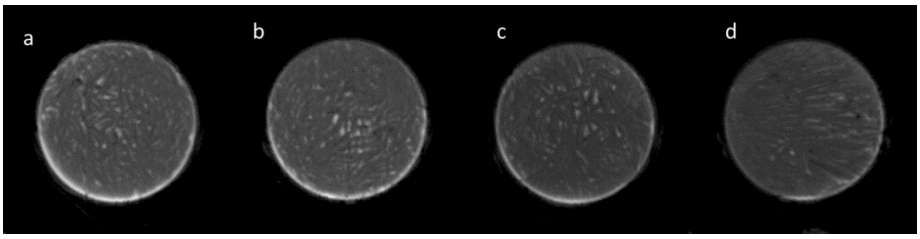

C

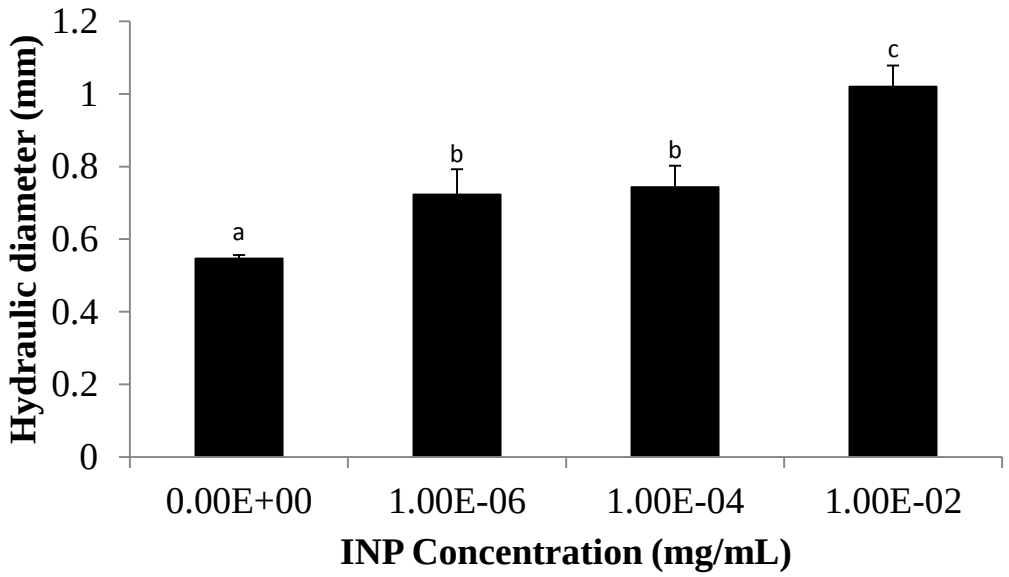

Figure 8 (A) Effect of INPs on ice morphology across the freezing direction at different growth height in both control (a, b, c) and INP (d, e, f,) samples. (B) Radiographs of ice morphology across the freezing direction with INP concentration at (a) 0 mg/mL, (b) 10^{-6} mg/mL, (c) 10^{-4} mg/mL of INPs, (d) 10^{-2} mg/mL. (C) Effect of INP concentration on hydraulic diameter. The letters on the top of error bars indicate the result of statistical analysis. Values with no common letter are significantly different ($P < 0.05$).

A

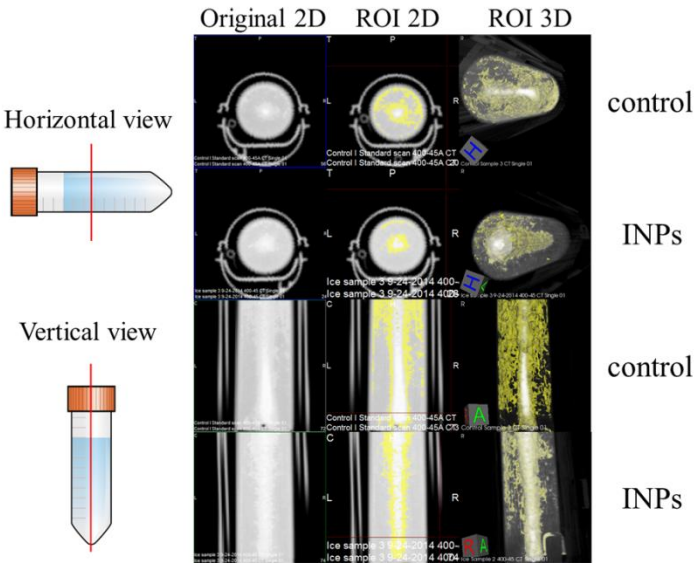

B

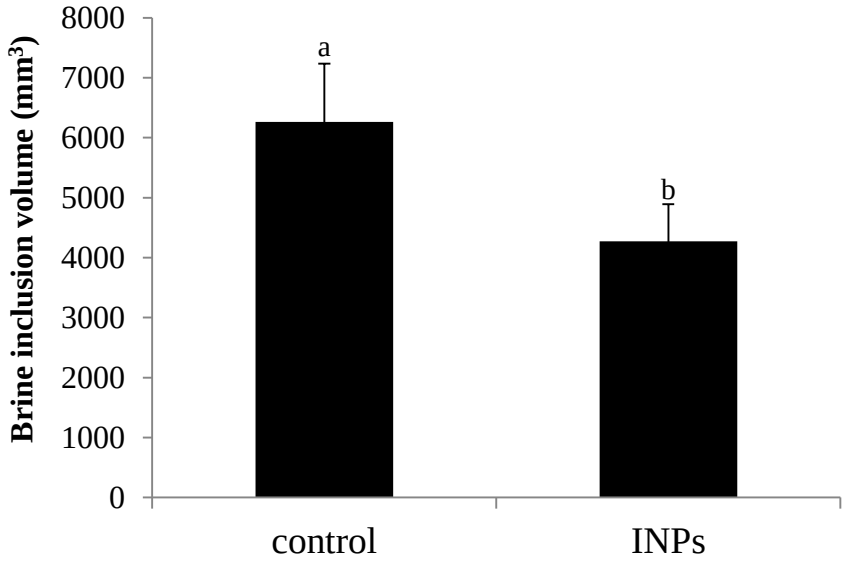

Figure 9 Effect of INPs on brine distribution inside frozen seawater. (A) Horizontal (upper two rows) and vertical (bottom two rows) views of CT images for brine distribution inside frozen seawater without (1st and 3rd rows) and with INPs (2nd and 4th rows). The original 2D views are shown on the left. The 2D views with brine distribution highlighted as ROI are shown in the middle. The corresponding ROI in the 3D views are shown on the right. (B) Quantitative analysis of brine inclusion volume highlighted in the CT images of controls and INP samples. The letters on the top of error bars indicate the result of statistical analysis. Values with no common letter are significantly different ($P < 0.05$).

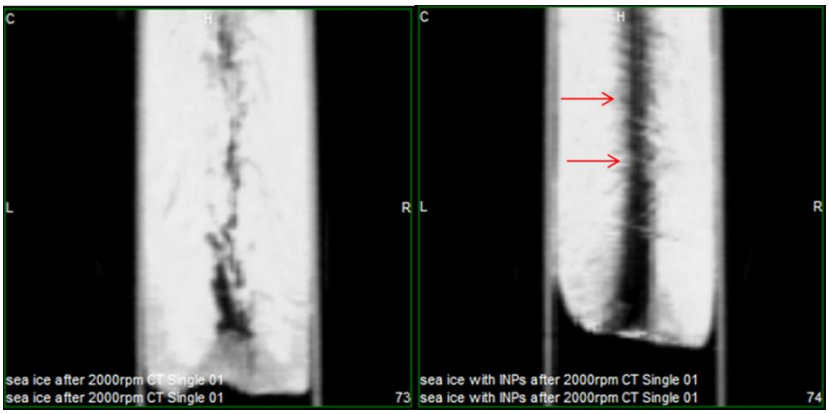

Figure 10 Radiographs of centrifuged frozen seawater without (left) and with INPs (right). The red arrows indicate the lamellar structure on the interfacial surface of centrifuged INP sample after brine removal

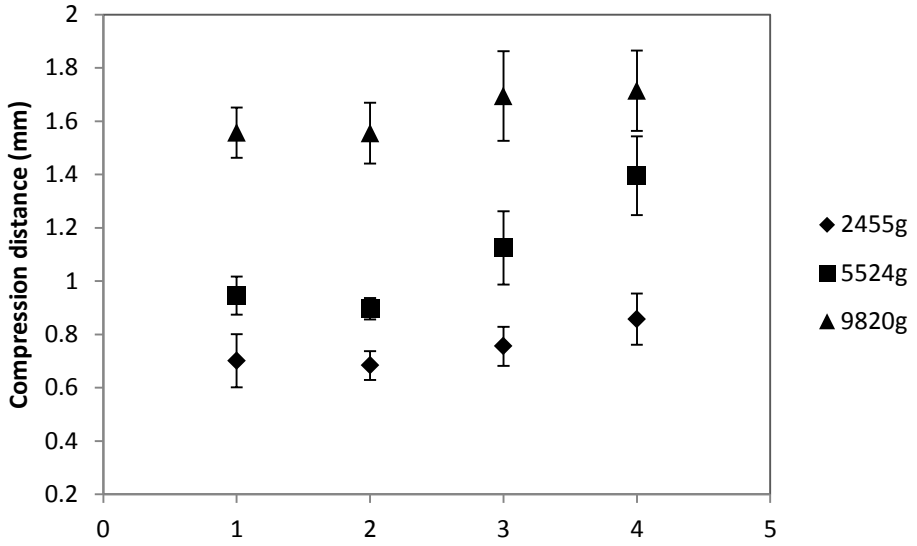

Figure 11 Effect of INPs concentration on compression distance of frozen seawater (1: control; 2: 10^{-6} mg/mL INPs; 3: 10^{-4} mg/mL INPs; 4: 10^{-2} mg/mL INPs)

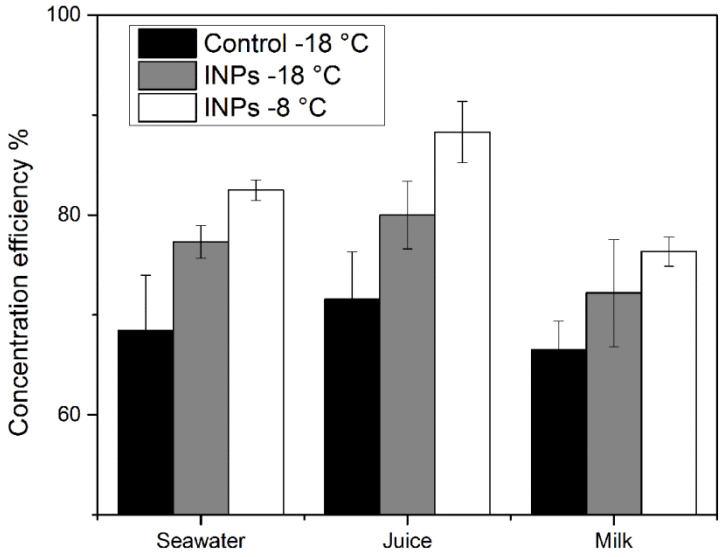

Figure 12 Effect of INPs on concentration efficiency of seawater, juice and milk at different freezing temperatures (i.e. -8 ℃, -18 ℃).

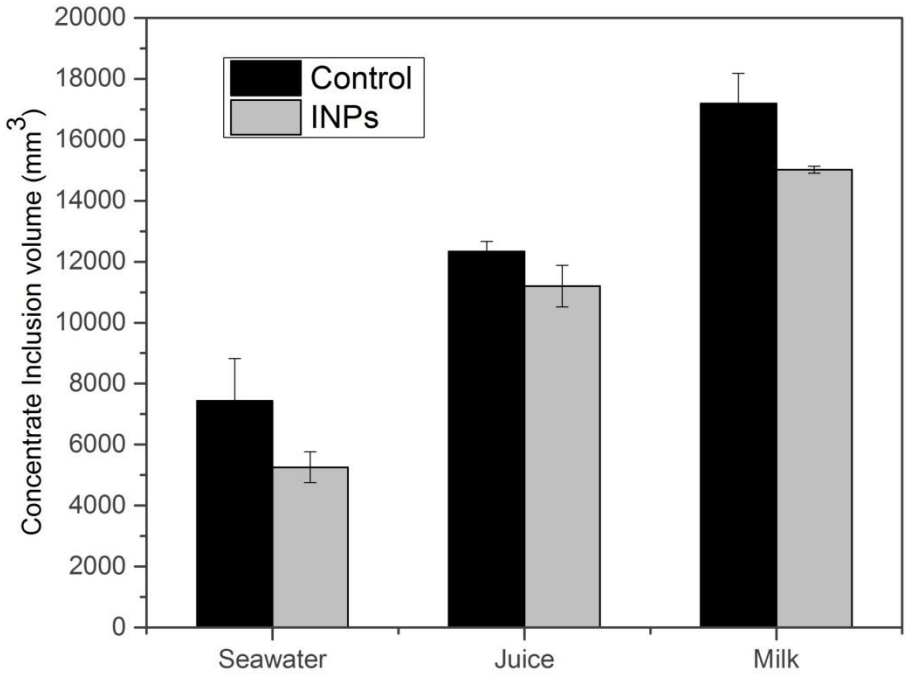

Figure 13 Effect of INPs on concentrate distribution inside frozen food systems. Quantitative analysis of concentrate inclusion volume highlighted in the X-ray CT images of controls and INPs samples

V. Effect of INPs on process efficiency of freeze drying and related mechanism of ice morphology

The work cited in this chapter has been published in the title of "Improved Freeze Drying Efficiency by Ice Nucleation Proteins with Ice Morphology Modification" in Food Research International (Volume 160, April 2018, Pages from 90 to 97).

1. Abstract

This study aims to use ice nucleation proteins (INPs) as a novel approach to improve the efficiency of freeze drying process and investigate the related mechanism of ice morphology. Our results show that INPs can significantly improve freeze drying efficiency with increased primary drying rate under the increase of INP concentration from 0 to 10^{-2} mg/mL. Moreover, such improvement was more significant at higher subzero freezing temperatures with the addition of INPs, when the control samples were unable to freeze. Those improvements further lead to reduced total drying time, which suggests an estimated total energy saving of 28.5% by INPs. Our ice morphology results indicate the ability of INPs to alter ice morphology with lamellar ice structure and larger crystal size, which both show linear relationships with primary drying rate. The results further suggest that these ice morphology characteristics induced by INPs are very likely to facilitate the water vapor flow and improve the sublimation rate. Additionally, the increase of freeze

drying efficiency can also be achieved by INPs in other food systems like coffee and milk with elevated primary drying rate. The results of this study suggest great potential of using INPs to improve the efficiency of freeze drying process for a wide range of food products and other related applications. This study also provides new insights into the relationship between process efficiency and ice morphology.

2. Introduction

Freeze drying is a dehydration process by direct sublimation of ice crystals from a frozen product. Because of its low temperature processing condition, freeze drying has been favored by different kinds of liquid and solid foods, such as powdered beverages like coffee and dehydrated snacks like dried vegetables and fruits. With the application of freeze drying, these products exhibit advantages of better flavor retention and nutrition preservation, faster rehydration compared to other drying methods, as well as cheaper transportation and longer shelf life (Ciurzyńska & Lenart, 2011). However, currently freeze drying is only utilized in food products with high commercial value or high demand for sensory attributes. Such limitation is majorly due to the high cost, since lyophilization is a very time- and energy-intensive drying process (Cohen & Yang, 1995; Kasper & Friess, 2011). A conventional freeze drying cycle consists of three steps, including freezing, primary drying, and second drying (Ciurzyńska & Lenart, 2011; J. C. Kasper & Friess, 2011). Among these three steps, primary drying has the longest duration. Along the primary drying step, the sublimation rate gradually decreases, because the internal transfer rate of heat and mass declines when the

thickness of the dried layer increases. This leads to long duration processing and related high process cost due to the energy cost from the maintenance of the compressor and refrigeration units for the ice condensers. Previous studies suggested that the sublimation step accounts for about 50% of the total energy consumption in a freeze-drying cycle (Ciurzyńska & Lenart, 2011; Rudy, 2009). The longtime drying process can also lead to increased labor cost. Therefore, the long sublimation step and related high energy consumption during primary drying result in an expensive process, and thus approaches to make primary drying step more efficient are desired (Moejes & van Boxtel, 2016).

The ice sublimation rate during primary drying step is governed by the heat and mass transfer rate across the front dried layers, which is strongly depended on the morphology of these dried porous matrices. The structure of porous layers is determined by the morphology of ice crystals formed during freezing step (Passot et al., 2009b). Thus, the control of freezing step might be very crucial for the performance of freeze drying process, but recent studies suggested that the importance of freezing step has rather been neglected in the past (Kasper & Friess, 2011; Julia Christina Kasper, Winter, & Friess, 2013). Among the factors of freezing step, the control of ice nucleation is probably the most important, since it determines the initial nucleation temperature and crystallization rate when ice crystals are formed (Searles, Carpenter, & Randolph, 2001). Previous studies have suggested that the control of ice nucleation might affect the efficiency of primary drying step (Geidobler & Winter,

2013; Passot et al., 2009b). During these studies, methods like ice fog, ultrasound ice crystallization, vacuum induced surface freezing, gap freezing etc., have been applied to control ice nucleation during freezing step, but most of them remain empirical with poor scalability or repeatability for not controlling nucleation temperature directly. Here, the addition of ice nucleation agents like biogenic ice nucleation proteins (INPs) might be an effective way to directly control ice nucleation. INPs are produced by a group of Gram-negative microorganisms, such as *Pseudomonas syringae*, *Xanthomonas campestris*, and *Erwinia herbicola*. Studies on the *ina* genes from these bacteria have revealed that ice nucleation proteins are large outer membrane proteins with a highly repetitive amino acid sequence responsible for ice nucleation activity (Kozloff et al., 1991; Warren & Wolber, 1991). The food applications of INPs have been studied in our lab for many years, which exhibited efficient control on ice nucleation by reducing the supercooling degree during the freezing of different food systems (Li et al., 1997; Li & Lee, 1998). Our recent study regarding the effect of INPs on freeze concentration process also indicated improved process efficiency (Jin, Yurkow, Adler, & Lee, 2017). However, the effect of INPs on the efficiency of freeze drying is still unknown.

To further understand the related mechanism of freeze drying, investigation regarding the relationship between ice morphology and process efficiency is required. Recent methods of observing ice structure in freeze drying studies include optical or electron microscopy, which provides limited observation under two dimensional

(Hottot, Vessot, & Andrieu, 2007; Nakagawa et al., 2006; Petzold & Aguilera, 2009). Besides, most of these morphology studies only examined the morphology of freeze dried samples without comparing it to the initial structure under the frozen state (Hottot, Nakagawa, & Andrieu, 2008; Peters, Molnár, & Ketolainen, 2014). Such interpretation of the mechanism only based on the morphology of dried samples might be insufficient and inaccurate, since the morphology can be altered during drying process by shrinkage and collapse (Khalloufi et al., 2015). In addition, the sample preparation involved in these microscopy approaches might introduce artifacts. Among the recent novel methods for morphology studies, X-ray computed tomography (CT) can measure ice morphology under frozen state without sample preparation, as well as providing three dimensional imaging analysis (Kiani & Sun, 2011). X-ray CT is a technology that combines micro-radiography with tomographic algorithms to generate three-dimensional images based on the radiographic density of the material. This imaging method has been used for qualitative and quantitative studies for the internal structures of different materials, such as sea ice, rock, ceramic and metal (Mousavi et al., 2007; Obbard et al., 2009). Recent development of higher resolution and contrast agents has enabled X-ray CT to measure ice morphology directly under its frozen state instead of freeze dried samples. Thus, in this study, the ice morphology will be investigated using non-destructive three-dimensional X-ray CT.

In this study, the effect of INPs on the efficiency of freeze drying and the related

mechanism on ice morphology were investigated. 10% sucrose solution was used as the food model, since sugar is the major dissolved solids in most beverages. The effect of INPs on primary drying rate as the efficiency indicator was examined at different INP concentrations and freezing temperatures. The total drying time needed for control and INP samples at different freezing temperatures was also determined. Further, the ice morphology of both control and INP samples was studied by three dimensional X-ray CT. The ice morphology characteristics were analyzed based on the 3D reconstructed images, to identify morphology patterns that related to process efficiency. The effect of INPs on primary drying rate and dried cake morphology of different food systems was also evaluated.

3. Materials and methods

3.1. Materials and reagents

Erwinia herbicola subsp. Ananas, obtained from the American Type Culture Collection (ATCC; ATCC Cat. No.11530), was used as the source of microbial INPs in these studies. Yeast extract was obtained from BD Biosciences (Franklin Lakes, NJ, USA). Sucrose (>99.9%), tris (Hydroxymethyl) aminomethane, potassium sulfate (K_2SO_4), magnesium sulfate ($MgSO_4$), and calcium chloride ($CaCl_2$) were obtained from Fisher Scientific (Fair Lawn, NJ, USA). L-serine, L-alanine, magnesium chloride ($MgCl_2$), potassium iodide (KI) and bovine serum albumin (BSA) were purchased from Sigma-Aldrich (St. Louis, MO, USA). All reagents were of analytical grade, and deionized water from Milli-Q was used throughout the experiments. Nescafe coffee and

Nestle instant dry milk were purchased from the local supermarket.

3.2. Preparation and purification of ice nucleation proteins

Erwinia herbicola was stored frozen at -60 ℃ and grown in yeast extract (YE) media (20g/L), containing sucrose (10g/L), L-serine (2g/L), L-alanine (2g/L), K_2SO_4 (8.6g/L) and $MgSO_4$ (4g/L). Following culture expansion to a density of 10^8/L, the cells were collected at 4 ^oC and 9000 rpm for 20 mins by Beckman Coulter Avanti J-E Centrifuge (Brea, CA), and the resulting pellet was re-suspended in 20mM Tris buffer containing 20mM $MgCl_2$. The suspension was then sonicated on ice, using three brief (10 sec) sonication bursts generated by a Brandson sonicator (Danbury, CT) set at the 4.5 power output setting. Following sonication, the suspension was centrifuged again as described above and the supernatant was isolated and ultra-centrifuged at 4 ^oC and 47500 rpm for 2h using Beckman L8-70 Ultracentrifuge (Brea, CA). Finally, the resultant pellet was re-suspended in 20mM Tris buffer with 20mM $MgCl_2$, and freeze-dried to obtain the INP powder. Lyophilized INPs isolated in this manner were stored at -18 ^oC prior to use

3.3. Primary drying rate

10% sucrose solution was prepared as the model of liquid food for this freeze drying study. 5mL volume of sucrose solutions were added into each bottle and INPs were added at concentrations of 10^{-6}, 10^{-4} and 10^{-2} mg/mL. All solutions were subjected to directional freezing by exposing the bottom surface of the samples to the freezing

bath set at constant temperatures of -8 or -13 or -18 ^{o}C until complete frozen. For food systems, 5% bovine serum albumin, coffee and milk were prepared as the systems with typical food biopolymers and INPs were added at concentrations of 10^{-2} mg/mL. Solutions of each food systems were subjected to directional freezing under constant temperatures of -8 or -18 ^{o}C until complete frozen. Then all the frozen samples prepared above were transferred into the chamber of VirTis Freezemobile R5L Freeze Dryer (Stone Ridge, NY) for the drying process. Primary drying rate was determined as the average weight loss rate during the time interval when 20-50% of the crystalized water had sublimed. In this study, the time interval is 3hs when almost 40% ice had sublimed.

3.4. Total drying time

5mL volume of 10% sucrose solutions were added into each bottle and INPs were added at the concentration of 10^{-2} mg/mL. All the solutions were incubated in the cooling bath set at the subzero temperature of -18 ^{o}C or -8 ^{o}C under unidirectional freezing from bottom to top until the solutions were completely frozen. Then the frozen samples were transferred into the freeze dryer chamber for the drying process. The moisture content of frozen samples was measured at different drying time intervals to determine end point of the drying process. The total drying time was determined when the weight loss of the dried products reached 90%.

3.5. X-ray Computed Tomography

Aliquots of control and INP solutions, containing potassium iodide (KI, 30mg/mL) as the imaging contrast agent, were prepared at the temperature of -18 ^{o}C under the same freezing procedures as described above. INPs were added at the concentrations of 10^{-6}, 10^{-4} and 10^{-2} mg/mL. The frozen samples were then scanned using the Albira PET/CT Imaging System (Bruker, Billerica, MA) set at standard voltage and current settings (i.e., 45kV and 400 μA, respectively) at the Molecular Imaging Center at Rutgers University. A set of 600 image projections was then captured throughout a 360^{o} rotation of the sample. Crystal morphology in the reconstructed 3D X-ray images was differentiated based on their boundaries highlighted by the contrast agent, which exhibited a higher X-ray attenuation coefficient. The crystal morphology was characterized and measured in three dimensions using VivoQuant image analysis software (version 1.23, inviCRO LLC, Boston MA, USA) and ImageJ software (version 1.46r, NIH, Bethesda, MD).

3.6. Statistical analysis

One-way ANOVA was performed using Data Processing System software v.9.50. Differences among mean values were established by the least significant difference (LSD) at 5%.

4. Results and discussions

4.1. Effect of INPs on primary drying rate

The process efficiency was determined by measuring the primary drying rate, since the primary drying step is typically the most time consuming stage of the freeze-drying and thus the time consumed at this stage is closely related to process economics (Parker et al., 2010). The effect of INPs on primary drying rate of 10% sucrose solutions was investigated at different INP concentrations (Figure 14). With the addition of INPs to sucrose solutions at final concentration of 10^{-6}, 10^{-4} and 10^{-2} mg/mL, the primary drying rate was elevated respectively by 3.5%, 8.3% and 21.0%, as compared to the control samples. The increase of primary drying rate at INP concentration of 10^{-2} mg/mL was more significant than the increase at lower concentrations. The results demonstrate that INPs can increase the primary drying rate, indicating that INPs can improve freeze drying efficiency and lead to related energy cost reduction.

4.2. Primary drying rate at different freezing temperatures

The effect of INPs on primary drying rate at different freezing temperatures was also determined (Figure 15). The results show that the improvement of primary drying rate by INPs was more significant at higher subzero freezing temperatures (i.e., -13 ^{o}C and -8 ^{o}C). At -13 ^{o}C, the primary drying rate of INP samples was 24% higher than control samples frozen under the same temperature. At -8 ^{o}C, the primary drying rate of INP samples was further increased when the control samples were unable to freeze. The

increase of primary drying rate by INPs at -8 ^{o}C was 47% higher than control samples frozen at -18 ^{o}C, which was 2-fold higher than the drying rate of INPs samples frozen at -18 ^{o}C. Such elevated primary drying rate at -8 ^{o}C by INPs suggests great energy savings of the drying step and also indicates energy savings of the freezing step by freezing samples at much higher subzero temperature. These results suggest that INPs can effectively improve the primary drying rate at different freezing temperatures and the improvement is more significant at higher subzero freezing temperature, which can further lead to energy savings of both freezing and drying steps.

4.3. Effect of INPs on total drying time

To further indicate the potential reduction of process cost by INPs, the effect of INPs on total drying time at different freezing temperatures was measured. As shown in Figure 16, the total drying time needed for 90% weight loss of frozen samples under different conditions was showed by red solid line. At -18 ^{o}C, INP samples had larger weight loss at each time point than control samples frozen under the same temperature. INP samples frozen at -8 ^{o}C had larger weight loss at each time point than INP samples frozen at -18 ^{o}C. To reach the weight loss of 90%, control samples require 14 hrs when it's only 12 hrs for INP samples under same temperature and 10 hrs for INP samples at -8 ^{o}C. Thus, based on the decrease of required drying time, the potential energy saving of drying step is 14.3% with INPs at -18 ^{o}C and 28.6% with INPs at -8 ^{o}C. Further, by freezing samples at higher subzero temperature of -8 ^{o}C when control samples remained unfrozen, the energy cost related to refrigerator units can also be reduced because of

decreased frequency of compressor cycle and reduced overall running time (Saidur, Masjuki, & Choudhury, 2002). Based on the energy reduction of 6.5% for each degree of increase in freezer temperature, the energy cost associated with freezing could be decreased by almost 50% when freezing at -8 ^{o}C with INPs instead of -18 ^{o}C (Hasanuzzaman et al., 2008; Saidur, Masjuki, Mahlia, et al., 2002). As shown in Table 7, on the basis of laboratory equipment specifications during the freezing and drying steps, the total energy savings by adding INPs is approximately 28.5%. Therefore, the application of INPs in freeze drying suggests significant potential of energy savings.

4.4. Effect of INPs on related ice morphology

The effect of INPs on ice morphology of frozen samples before sublimation step was characterized and measured by X-ray computed tomography. In the radiographs of Figure 17, ice crystals are shown in black color and frozen solids are highlighted in green color. As shown in those radiographs, INPs markedly affect ice crystal morphology in different radiographic slices. Images of the ice morphology captured at the center of the longitudinal axis (Figure 17b), show a distribution of randomly oriented granular ice crystals at the bottom of the frozen matrices, which changed to aligned columnar ice crystals at the top. At lower INP concentrations, the transition from randomly oriented ice crystals to vertically elongated lamellar ice structure occurs at earlier stage of ice growth as compared to the control. This is indicated by the longer length of lamellar spacing in Figure 18. At the highest INP concentration (i.e. 10^{-2} mg/mL), such transition occurs at the initiation of ice growth very close to the bottom

edge, which is positively related to the significant increase of primary drying rate under the same INP concentration. Alternative off-center longitudinal image (Figure 17c) of each sample shows the same lamellar ice structure pattern at the off-center location, which indicates consistent formation of lamellar ice structure across the entire frozen sample along the longitudinal axis. CT images of the transverse sections of frozen samples (Figure 17a) show that INPs could induce the formation of columnar ice crystals with longer crystal length (Fig. 19A). Since there is almost no significant difference in crystal width between these samples (Fig. 19B), the increased crystal length by INPs suggests larger crystal size at the cross section, which indicates increased pore size in the dried sample layers. Besides, as shown in Figure 19C, the crystal orientation in the transverse sections has also been influenced by the increase of INP concentration, based on the standard deviation of crystal orientation angle in the images. If the crystals are more paralleled to each other, the deviation of orientation angle between each crystal should be smaller. In Figure 19C, the deviation of crystal orientation angle decreases with the increase of INP concentrations, which indicates more aligned ice structure by INPs. At the highest INP concentration (i.e. 10^{-2} mg/mL) with the smallest deviation, ice crystals become mostly aligned in the transverse sections as compared to the crystals in other samples. Thus, a dual structure of lamellar ice crystals in both vertical and horizontal dimensions has been developed by INPs under the freezing conditions in this study.

The relationship between ice morphology and freeze drying efficiency is further

indicated in Figure 20. The results demonstrate that the average crystal size at the cross section and the length of lamellar structure along the growth direction both show linear relationships with primary drying rate. This suggests that these ice morphology characteristics are positively related to the increase of primary drying rate. Previous study has suggested that during the drying step, samples containing larger ice crystals had less resistance to water vapor flow, since larger pores were left behind (Geidobler & Winter, 2013). Based on this, the larger sized columnar ice crystals induced by INPs in the cross sections are very likely to facilitate the water vapor flow and thus improve the drying efficiency. In addition, the presence of lamellar ice structure along the growth direction, which is same as the mass transfer direction, might also lead to faster drying rates because of higher void connectivity in the dried cakes. It was suggested that higher void connectivity in the dried matrix, which contains more direct vapor flow paths toward the top, can facilitate the heat and mass transfer and thus reduce the drying time with higher primary drying rate (Searles et al., 2001). Without monitoring ice nucleation, control samples tend to initiate freezing at higher supercooling stage, which leads to the formation of small and randomly oriented ice crystals with a high tortuosity structure that is more difficult for mass and heat transfer (Petzold & Aguilera, 2009). In INP samples, the lamellar ice structure toward the top of frozen samples can leave large pores with high connectivity after drying, which makes mass and heat transfer much easier as compared to the disconnected smaller pores in control samples (Patapoff & Overcashier, 2002; Rezanezhad et al., 2009). Therefore, the increased length of

lamellar ice structure along mass transfer direction in INP samples is very likely to be another crucial reason for the drying efficiency improvement.

Previous studies have indicated several mechanisms for the development of lamellar ice structures. First, lamellar ice structure can be developed by the strong growth anisotropy of ice crystals under certain temperature conditions. Similar structure has been observed during the studies of freeze drying and freeze texturization, which was investigating the relationship between nucleation temperature and crystal structures (Nakagawa et al., 2006; Pawelec et al., 2014). In the freeze drying study of mannitol solution, the anisotropic lamellar ice structure was developed along the temperature gradient of the liquid slurry, and the control of local nucleation temperature was recognized as the key factor to predict the growth of anisotropic ice crystals (Nakagawa et al., 2006). The aligned columnar crystals observed in the sea ice is another example of anisotropic crystal structure grown under natural environment, where the ice crystal morphology changes from randomly to uniformly oriented with horizontal c-axes (Bleil & Thiede, 2012). One of the mechanisms associated with such development of aligned columnar crystals of sea ice is the occurrence of thermal gradients (Stand, 1989). With the addition of INPs into the solution, the constitutional supercooling is controlled and thermal gradients occur at the freezing front with the release of latent heat (Stand, 1989). Therefore, these temperature-related mechanisms might also be the reason for the alteration of macroscopic crystal morphology by INPs. Besides the temperature factor, the molecular chemistry aspect of ice nucleation agents

might also lead to the development of lamellar ice morphology. During the molecular simulation study to understand heterogeneous ice nucleation, the clay mineral kaolinite was used as the model ice nucleating agent and was found to promote the growth of the prism plane over the basal plane, which was suggested to be able to further influence the macroscopic ice crystal structure (Cox et al., 2013). In addition, a previous study conducted by Nada *et al.* demonstrated the selective binding of *Xanthomonas campestris* INPs to the basal plane of ice crystal, leading to a faster growth rate of ice crystal in the prism face (Nada, Zepeda, Miura, & Furukawa, 2010). Thus, the mechanism for the lamellar structure developed by INPs might be the effect of INPs on the nucleation temperature and/or molecular growth of ice crystals.

For freeze drying, ice morphology is also important for product quality control. The batch homogeneity is an important issue during the scale-up process development and thus INPs might also help improve the product consistency with narrow ice crystal size distribution and similar crystal shape between each batch (Nakagawa et al., 2007). Besides, this study demonstrates that with the increase of INP concentration, ice morphology of frozen samples develops from a coarse lamellar structure with partially aligned columnar crystals into a well oriented and well-defined lamellar structure. This suggests that it is possible to control the growth of lamellar ice structure during freezing with different INP concentrations. In material science, such transition between randomly oriented ice crystals and lamellar ones might be a big interest. So the application of INPs might provide an effective approach for material preparations by

techniques like ice-templating, especially when continuous porosity is desired (Bareggi, Maire, Lasalle, & Deville, 2011; Deville et al., 2009; Lasalle et al., 2012).

4.5. Efficiency improvement by INPs in other food systems

The effect of INPs on the freeze drying efficiency of different liquid systems, including 5% BSA solution, coffee and milk, was investigated. BSA was chosen as the model for products containing proteins. Milk and coffee were selected as they are commonly freeze-dried in food industry.

As shown in Figure 21, INPs were able to increase the primary drying rate in the liquid systems of BSA solution, milk and coffee as compared to control samples under the same freezing temperature of -18 ^{o}C. The improvement was more significant when the solutions were frozen at -8 ^{o}C with INPs, when controls were unable to freeze. At -8 ^{o}C, the primary drying rate was increased by 28%, 11% and 15% for BSA, coffee and milk respectively, as compared to control samples frozen at -18 ^{o}C. By freezing at -8 ^{o}C instead of -18 ^{o}C, the energy cost can be significantly reduced for the freezing step as well. The results suggest that INPs can improve the efficiency of freeze drying in liquid systems with different compositions, strongly indicating their applications to a wide range of food product categories. The morphology of dried cakes from different liquid systems was shown in Figure 22. As indicated by the red arrows, the pore structure in the freeze dried cakes of different food systems also showed evidence of lamellar ice structure along the growth direction as well as the cross section. Such morphology observation in different systems suggests that the ice morphology alteration by INPs is

also very likely to be the major reason for the efficiency improvement. This also indicates that such ice morphology alteration by INPs is independent with the solute inside the liquid system.

This study demonstrated that INPs could improve the efficiency of freeze drying with significant energy savings, because INPs could change the ice morphology that facilitated the drying process. The results suggested that the addition of INPs can lead to faster primary drying rate and reduced total drying time in various food systems. This indicates significant potential of process cost savings and makes freeze drying process more competitive for a wide range of food applications. The X-ray CT results for mechanism investigation showed that INPs developed lamellar ice structure and larger crystal size that favored for sublimation process. The linear relationship between characteristics of ice morphology and process efficiency emphasizes the importance of controlling freezing step and related ice morphology. Further, this study demonstrates that INPs may not only facilitate the ice nucleation process, but also change the macroscopic ice structure. Based on the results of this study, other freezing technologies or frozen products might also benefit from the addition of INPs to effectively control ice nucleation and produce desired ice structure. Besides, further understanding of the mechanism for the lamellar ice structure developed by INPs is important to support the wide application of INPs.

Table 7 Comparison of energy cost between control and INP samples for freeze drying process

step	parameters	control	INPs
freezing	cooling output (kW)	0.2	0.1
	freezing time (h)	1	1.5
	energy cost (kWh)	0.2	0.15
drying	electric output (kW)	1.87	1.87
	drying time (h)	14	10
	energy cost (kWh)	26.18	18.7
total	final energy cost (kWh)	26.38	18.85

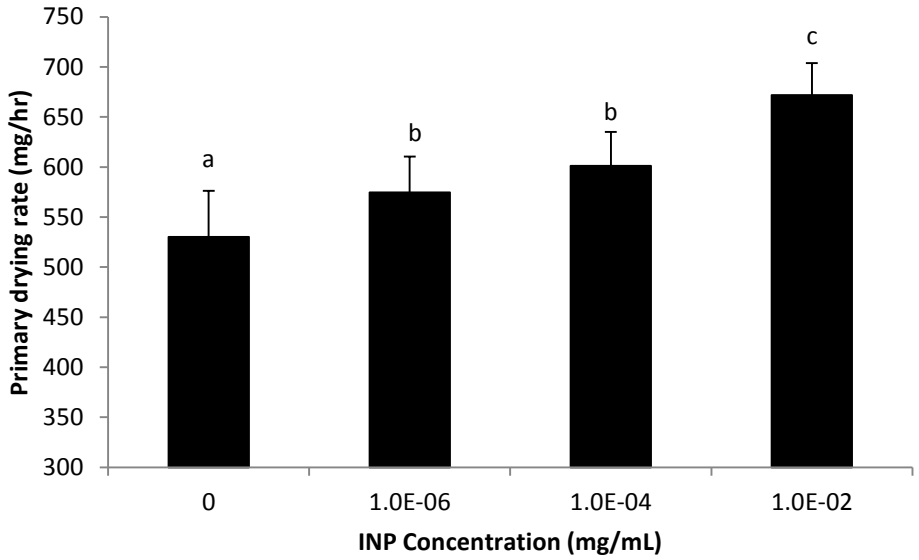

Figure 14 Effect of increasing INP concentrations on primary drying rate of sucrose solutions. Values with no common letter are significantly different ($P < 0.05$)

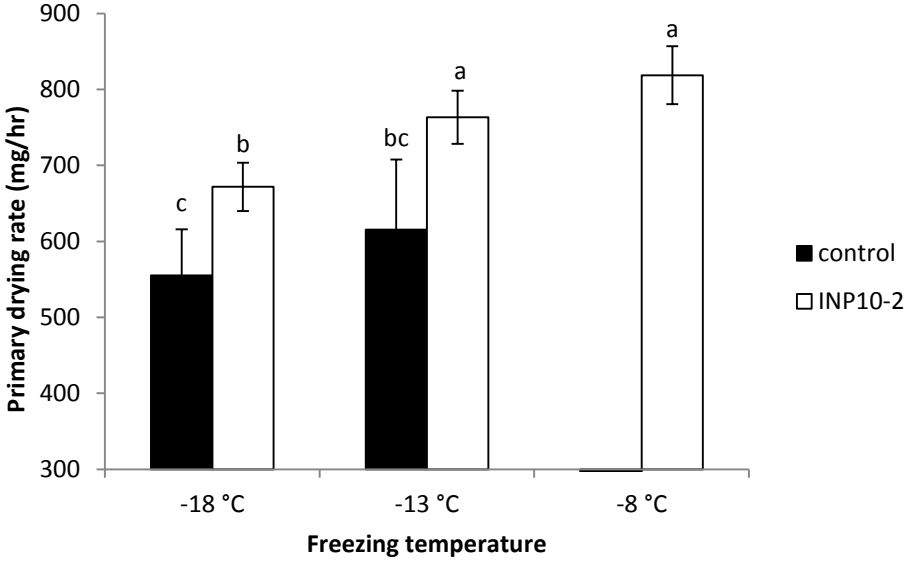

Figure 15 Effect of INPs on primary drying rate at different subzero freezing temperatures. Values with no common letter are significantly different ($P < 0.05$)

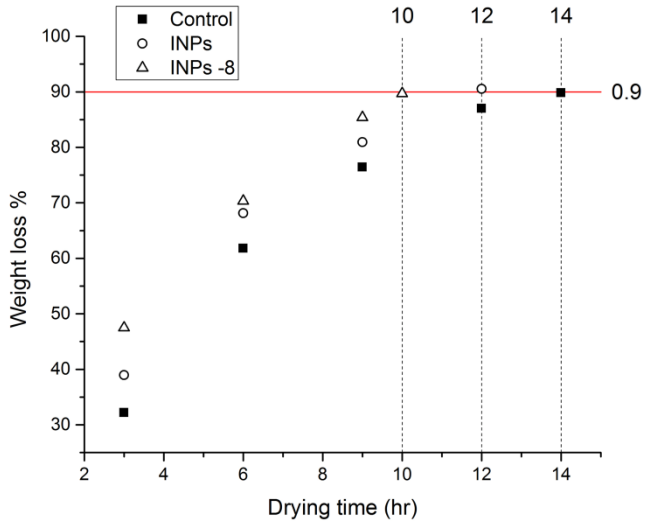

Figure 16 Effect of INPs on total drying time at different subzero freezing temperatures

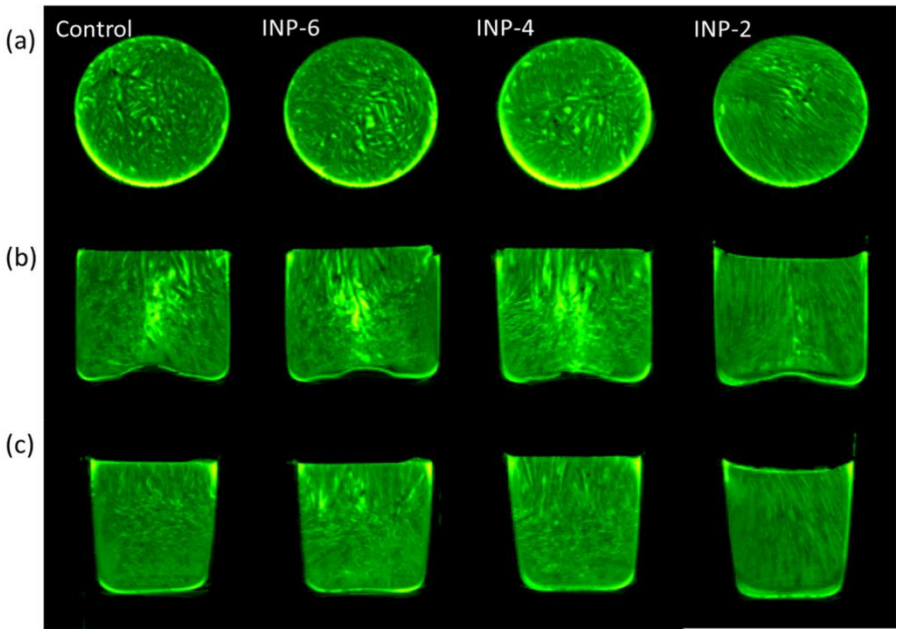

Figure 17 Effect of INP concentrations on macroscopic ice structure. The three dimensional slices from tomographic reconstruction: (a) transverse slice perpendicular to the growth direction; (b) longitudinal slice at the center of the ice; (c) off-center longitudinal slice parallel to the growth direction (1/4 diameter away from the center). KI (green) was used to image the boundaries of the crystals (dark).

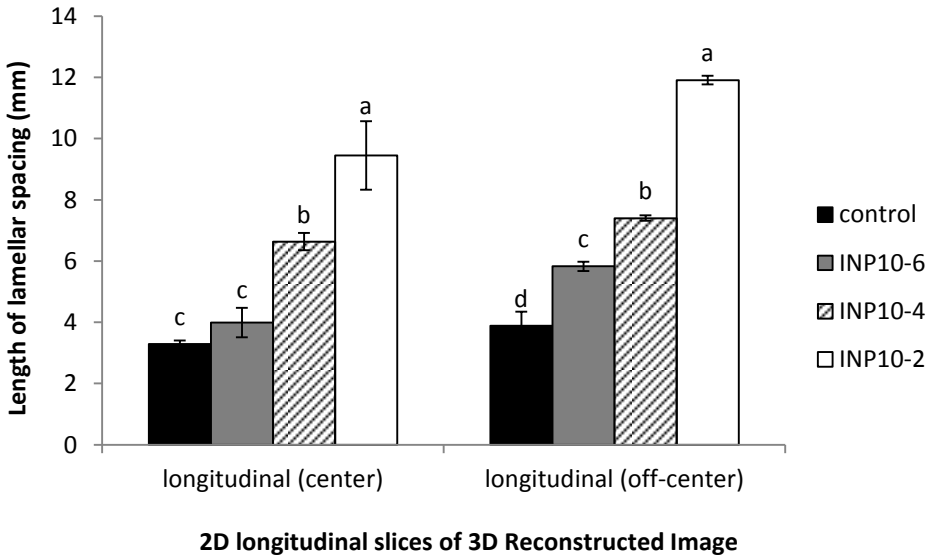

Figure 18 Effect of INP concentrations on the length of lamellar spacing in the 2D longitudinal slices of 3D Reconstructed Images. The letters on the top of error bars indicated the result of statistical analysis. Values with no common letter are significantly different ($P < 0.05$).

A

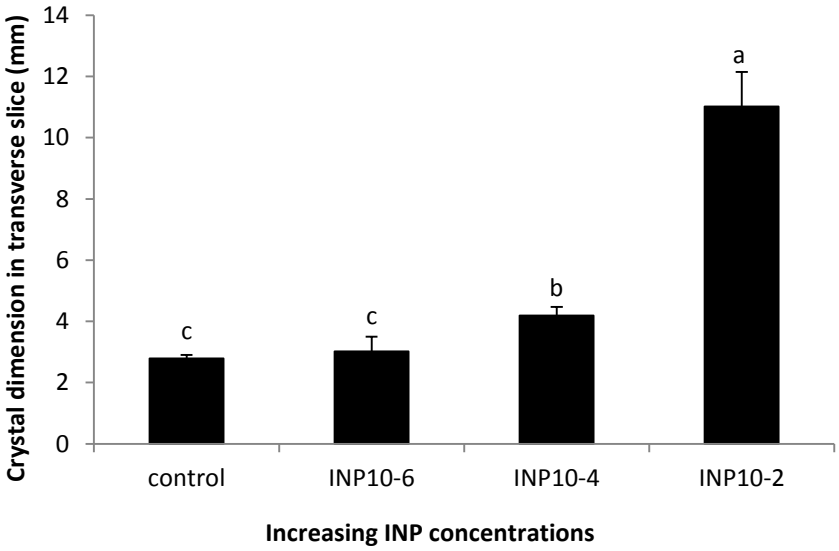
Crystal dimension in transverse slice (mm)
14
12
10
8
6
4
2
0
c
c
b
a
control
INP10-6
INP10-4
INP10-2
Increasing INP concentrations

B

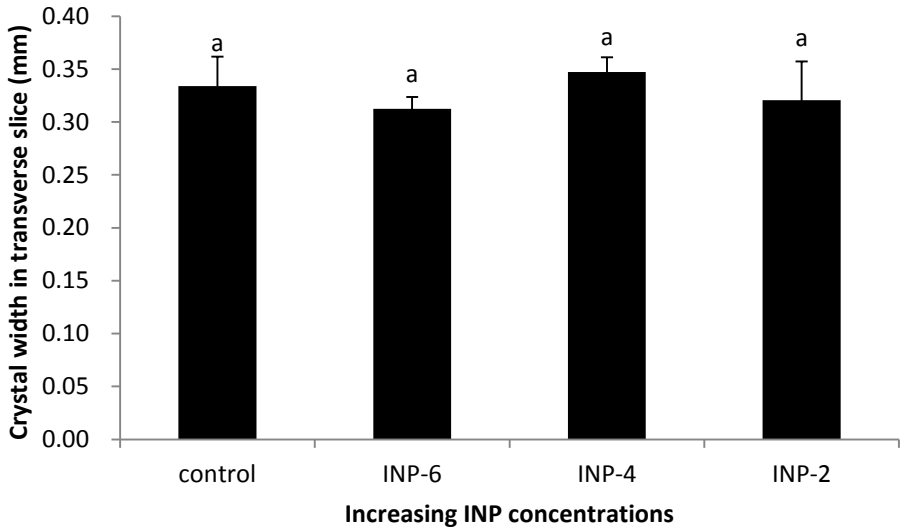
Crystal width in transverse slice (mm)
0.40
0.35
0.30
0.25
0.20
0.15
0.10
0.05
0.00
a
a
a
a
control
INP-6
INP-4
INP-2
Increasing INP concentrations

C

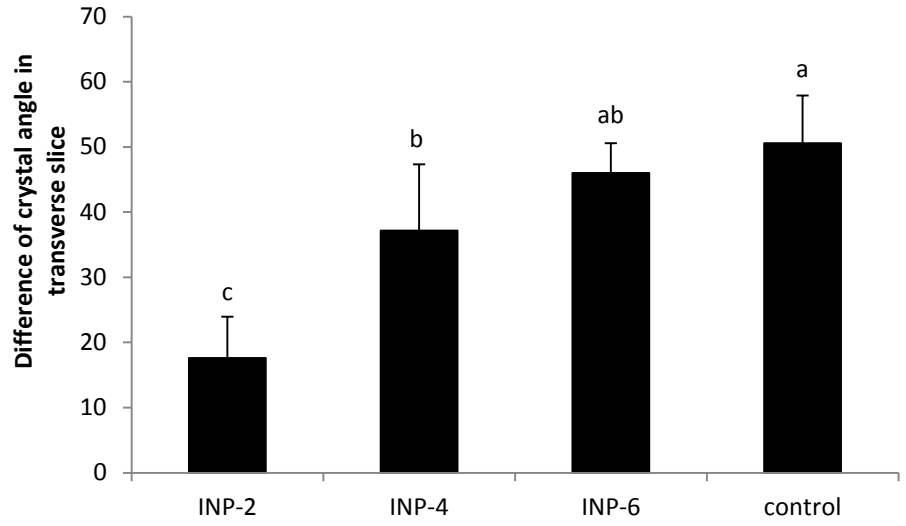

Figure 19 (A) Effect of INP concentration on crystal dimension in transverse slice; (B) Effect of INP concentration on crystal width in transverse slice; (C) Effect of INP concentration on crystal alignment in transverse slice. The letters on the top of error bar indicated the result of statistical analysis. Values with no common letter are significantly different ($P < 0.05$).

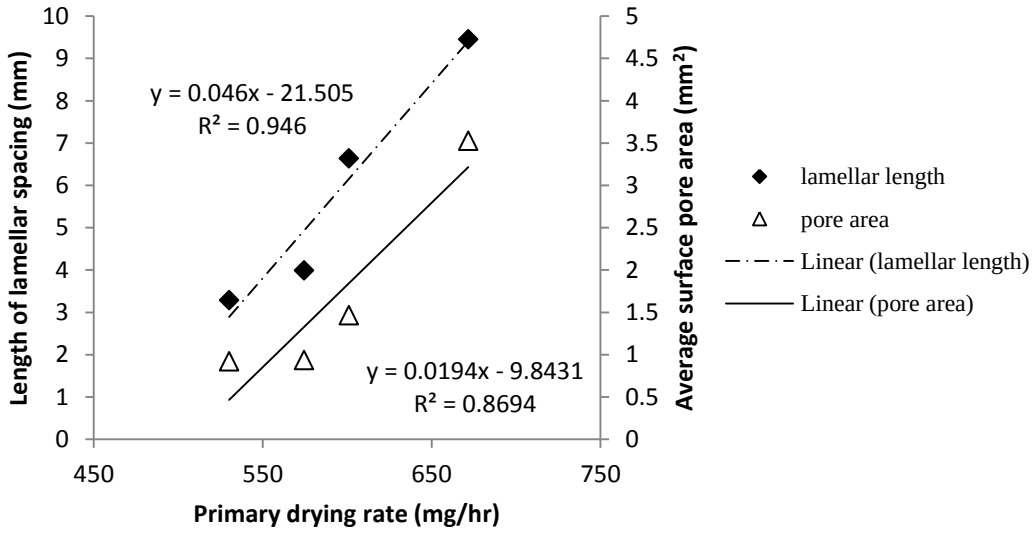

Figure 20 Linear relationship of primary drying rate with the length of lamellar spacing and surface pore area from X-ray CT results at different INP concentrations

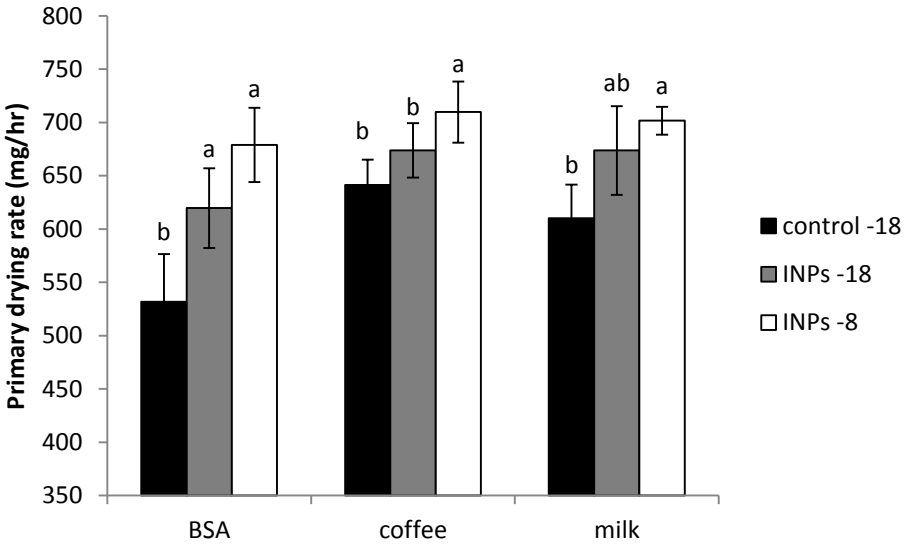

Figure 21 Effect of INPs on the primary drying rate in different food systems at different freezing temperatures. The letters on the top of error bars indicated the result of statistical analysis. Values with no common letter are significantly different ($P < 0.05$)

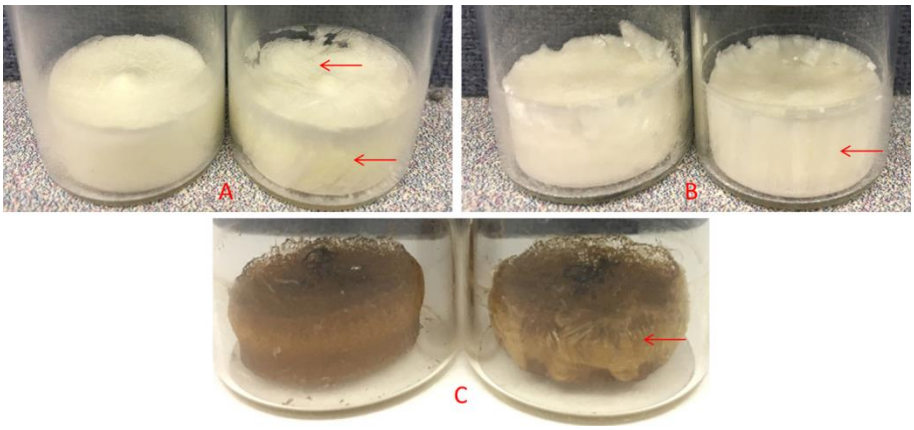

Figure 22 Morphology of freeze dried cakes from different food systems: (A) milk without (left) and with INPs (right), (B) 5% BSA without (left) and with INPs (right) and (C) coffee without (left) and with INPs (right). The red arrows indicate the lamellar structure along the ice growth direction as well as cross section

VI. Summary and future work

Due to the demand for nutritional food products with high quality, the interest in development of freezing technologies continues to grow. Under the low-temperature processing environment, the product quality, including heat sensitive nutrients and volatile aroma and flavors, can be maximally retained; while other major proposes of the process, such as extending shelf life, reducing the cost for packaging, storage and transportation, and food safety assurance, can also be achieved. Freezing related separation processes have promising applications beyond food industry. For example, the desalination process studied in this study will have a significant impact on human daily water consumption and agricultural production.

The remaining challenge for wide applications of freezing technologies is to achieve high efficiency with low cost. This research focuses on the improvement of the efficiency of freezing technologies, including freeze concentration and freeze drying processes, using biogenic ice nucleation proteins (INPs) as a novel approach and the further understanding of ice morphology alteration made by these biomaterials. The results of this research suggested that the application of INPs in block freeze concentration process showed significant efficiency improvement based on different parameters, including higher freezing temperature, lower separation speed, and significantly reduced total energy cost. The imaging analysis of frozen food matrices by X-ray computed tomography suggested that INPs promoted the

development of a lamellar structured ice matrix with larger hydraulic diameters and less solute entrapment, which facilitates the separation process. The results also suggested that the application of INPs in freeze drying process of different food systems showed significant efficiency improvement based on increased primary drying rate, which leads to the decrease of total drying time and great reduction of total energy cost. The imaging analysis from X-ray computed tomography demonstrated the modification of ice morphology by INPs and its linear relationship with primary drying rate, which suggests strong relationship between process efficiency and ice morphology.

This research is of major significance because it provides new evidence of three-dimensional ice structure, which offers new insights into the mechanism for efficiency improvement of freeze technologies. The results demonstrated significant potential of applying INPs for improving process efficiency of freezing technologies including freeze concentration and freeze drying processes. This leads to a broad range of food applications of INPs with the purpose of providing consumers with higher quality food products at lower cost. Further, the use of X-ray computed tomography in this research suggests its applicability to study internal structure of frozen food matrices. Last but not least, this is the first study to reveal that INPs could not only affect the nucleation temperature but also significantly change the macroscopic ice structure. This finding of INPs altering ice morphology can have significant impact on many practical applications in food, nutraceutical and

pharmaceutical industries

Meanwhile, further research could be performed to extend current study. Firstly, the ability of INPs to alter ice morphology can be applied in other areas that require precise control of porous material architecture and still remain difficult to achieve. For example, INPs could be used in ice templating to produce meat alternatives with desired texture, or to create tissue engineering scaffolds with functional structure and optimized permeability, or to fabricate porous metals and ceramics with unique structures.

Secondly, the mechanism for INPs altering ice morphology needs to be investigated. Future studies can measure the growth and melting of single ice crystal by nanoliter osmometer, crystal growth face by X-ray diffraction, and hydrogen bond network by terahertz spectrometry. Those experiments might shed some light on the interaction between INPs and ice crystals, which will definitely benefit the applications of INPs for morphology alteration with better prediction. Besides, the fundamental understanding of how INPs interact with ice can also help the application of INPs in consumer packaged goods. For example, if the function of INPs can be transferred from the surface to the center of the product, INPs only need to be put into the packaging materials instead of adding them into the product, which would ease the safety issues.

Last but not least, there has been increasing interest in ice nucleation research during the last decade (Coluzza et al., 2017). Ice nucleation proteins, as the most

effective ice nucleators, might be a good model to study the fundamental knowledge of ice nucleation processes. The basic understanding of INPs characterizations includes their specific surface morphology (e.g. surface charge, surface hydrophobicity, surface angle), or formation of favored ice habits. The related studies can also include their comparison with other ice nucleators, such as atmospheric ice nucleators, or ice nuclei from fungus, diatom or plants. These understandings will fill important gaps in ice nucleation mechanism and their impacts on scientific and commercial applications, such as engineering synthetic ice nucleators, climate and cryopreservation applications.

Appendix A: Effect of growth conditions on the activity of INPs and related surface hydrophobicity

This work is to provide supporting materials regarding the INPs preparation in this study. The effect of growth conditions on the activity of INPs is investigated and the relationship between ice nucleation activity and surface morphology is also suggested.

Abstract

Before applying INPs to freezing technologies, it is important to obtain INPs with sufficient ice nucleation activity (INA). To achieve sufficient INA, the preparation factors of temperature and extraction conditions were investigated. The results suggest that culture with higher ice nucleation activity can be achieved at lower growth temperature. Moreover, the cold shock effect can induce the ice nucleation activity of the cell culture, especially type I and II ice nuclei. The determination of surface morphology of cells and INPs suggests that the enhanced activity at lower temperature might be closely related to the increased surface hydrophobicity. The results of differentiation centrifugation indicate that the membrane fraction contains the highest ice nucleation activity.

Introduction

Ice nucleation proteins (INPs) can be produced by a group of Gram-negative plant pathogens, such as *Pseudomonas syringae*, *Pseudomonas fluorescens*, *Pseudomonas viridiflava*, *Xanthomonas campestris*, and *Erwinia herbicola*, during their invasion to

plant tissue at low temperature (Kozloff et al., 1983; Li & Lee, 1998; Watanabe & Watanabe, 1994). In order to obtain high level expression of INPs from these bacteria source, many studies have focused on monitoring environmental factors that related to the protein expression. Some attempts had been made to use different culture conditions, such as the variations in carbon source or fatty acid compositions, certain nutrient limitation and low temperature induction (Yu, Liu, Tao, & Zhu, 2013). As suggested in previous study, the expression of ice nuclei from *Erwinia herbicola* could be influenced by the growth temperature (Fall & Fall, 1998). In this study, bacterial cells grown at lower temperature between 18 to 22 ℃ produced more active ice nuclei, as compared to the cells grown at temperature above 22 ℃, which had dramatic decrease of ice nuclei activity. Besides, sudden decrease of growth temperature could also affect the ice nucleation activity of ice nucleating bacteria (Yamanaka, 1999). Previous study indicated that the shift of cell culture from higher to lower temperature incubation, described as cold shock effect, could improve the activity of ice nuclei at different threshold temperatures (Marentes, Griffith, Mlynarz, & Brush, 1993). For example, the appearance of type I and II ice nuclei in *Pseudomonas syringae* was observed under the low temperature induction (Fall & Wolber, 1995). Such change in temperatures was believed to affect the formation or aggregation of the ice nucleation sites on the cell surface (Nemecek-Marshall et al., 1993). Some studies had been reported that the ice nucleation activity decreased as the increase of cell membrane fluidity, due to the mechanism that the aggregation of ice nuclei favors cell membrane

with stable conditions (Palaiomylitou et al., 1998). One of the reasons for this might also be the change in membrane surface morphology, which influences the conformational structure and functional integrity of attached membrane proteins.

Based on ice nucleation theory, an ice nucleus requires three properties to mimic ice lattice, including size, slightly charged surface and hydrophobicity (Burke & Lindow, 1990). The hydrophobic surface is suggested to interact with the atomic spacing of the ice crystal planes. The extracellular INPs from *E. uredovara* KUIN-3 were suggested to be composed of lipid, protein, saccharide and polyamine. And polyamine was suggested to take part in the surface charge and hydrophobicity (Kawahara, 2002). Besides, the richness of threonine in the central region of INPs could also provide hydroxyl side chain for hydrogen bonding during hydrophobicity interaction. Among the methods for quantifying protein surface hydrophobicity, fluorescent probe has its advantages of simplicity, speed, ability to predict functionality, and use of small amounts of purified protein for analysis (Haskard & Li-Chan, 1998). Besides, this method is also capable of measuring average surface hydrophobicity of a protein mixture. The mechanism of this method is to measure the increase of fluorescence after binding these probes to accessible hydrophobic regions of proteins since these probes have low quantum yield of fluorescence by themselves in aqueous solution (Alizadeh-Pasdar & Li-Chan, 2000).

Cell fractionation is involved in protein purification and organelle isolation to better understand the subcellular location of target proteins and organelles inside cells.

It allows researchers to enrich specific cell components in large amount for further study in the functions and structures of cell organelles. Cell fractionation process contains two parts: homogenization and centrifugation. With the purpose of disrupting cells, homogenization is a critical step to efficiently break up the cells without the change of location and structure of cell components. Cells can be broken apart by several ways, such as mechanical methods, chemicals or enzymes methods, and structure damage methods (Geciova, Bury, & Jelen, 2002). For mechanical methods, cells are disrupted with homogenization by pressure, sonication and grinding, among which sonication is one of the most widely used disruption methods (Geciova et al., 2002). Differential centrifugation is a separation process based on different size and shape of organelles by repeatedly undergoing centrifugations with increasing centrifugal force (De Duve & Berthet, 1954). The force of centrifugation is much greater than force of gravity and therefore enables the precipitation of substances in the solution to the bottom. By spinning with increase of speed, the organelles with larger size will precipitate first.

Therefore, in this study, the INA of *Erwinia herbicola* grown at different temperatures was compared. The cold shock effect on ice nucleation activity of cell culture was conducted by exposing the culture to lower temperature incubation after harvest from different growth temperatures and related ice nucleation activity was determined. The relationship between temperature and surface morphology of cells and INPs was determined. The effect of extraction condition was investigated by

partially separating different fractions of bacterial cells via centrifuging sonicated bacterial solution at different centrifugation speeds.

Materials and methods

Materials

E. herbicola subsp. Ananas, obtained from the American Type Culture Collection (ATCC; ATCC Cat. No.11530), was used as the source of microbial INPs in these studies. Yeast extract was obtained from BD Biosciences (Franklin Lakes, NJ, USA). Sucrose (>99.9%), tris (Hydroxymethyl) aminomethane, potassium sulfate (K_2SO_4), and magnesium sulfate ($MgSO_4$), were obtained from Fisher Scientific (Fair Lawn, NJ, USA). L-serine, L-alanine, magnesium chloride ($MgCl_2$) and 1-(aniline)naphthalene-8-sulfonate (ANS) were purchased from Sigma-Aldrich (St. Louis, MO, USA). All reagents were of analytical grade, and deionized water from Milli-Q was used throughout the experiments.

Drop-freezing method and specific ice nucleation activity

The ice nucleation activity (INA) was measured by the drop-freezing method. Protein solutions were serially diluted in DI water and 20 droplets with constant volume of 10uL were placed on the alumina plate incubated at -8 ^{o}C for 3mins. Total numbers of frozen droplets were counted after that and the value between 5 and 18 were considered to be statistically significant. The corresponding dilution factor was used for calculation through the below formula:

$$ina\,(T) = -\frac{\ln(1-f)}{V_d} \times D$$

T: incubation temperature

f: ratio of frozen droplets

V_d: droplet volume

D: dilution factor

The unit of INA based on the equation is units/uL.

Protein concentration of each solutions were measure by the Bio-Rad Protein Assay and interpreted using the standard curve that established by measuring absorbance of BSA at different concentrations. And specific ice nucleation activity (units/mg) was calculated by dividing ice nucleation activity with the protein concentration.

Preparation of cell culture under different growth temperature

Erwinia herbicola was stored frozen at -60 ℃ and grown in yeast extract (YE) media (20g/L), containing sucrose (10g/L), L-serine (2g/L), L-alanine (2g/L), K_2SO_4 (8.6g/L) and $MgSO_4$ (4g/L). The cells were grown at temperatures of 30 ℃, 22 ℃, 18 ℃ and 10 ℃. They were collected when the cell density reached 10^8/L, and then went through cold shock stage by storing in the 4 ℃ fridge for 4hrs. The ice nucleation activity of each culture was determined by drop-freezing method.

Cell disruption and differential centrifugation

The cells were collected by high speed centrifuge at 4 ^{o}C, 10,000 x*g* for 25mins. The pellet was wash by re-suspending with 50 mL tris buffer containing 20mM $MgCl_2$ in each centrifuge tube and centrifuged at 4 ^{o}C, 10,000 x*g* for 15mins. The washed cells

were re-suspended in 40mL of the same buffer. Sonication was applied to the suspension on ice with output level of 4.5, 10s burst with 10s break for 3 times. The sonicated suspension was centrifuged again under 4 ^{o}C, 10,000 x*g* for 25mins to remove unbroken cells. The supernatant was centrifuged at 4 ^{o}C, 24,000 x*g* for 30mins to obtain the membrane fraction in the pellet. The supernatant was collected and ultra-centrifuged under 4 ^{o}C, 160,000 x*g* for 2h. The pellet, which represents the ribosomal fraction, was suspended in the Tris buffer and the cytoplasmic fraction remains in the supernatant. Each of the fractions collected by differential centrifugation above was measured with ice nucleation activity and protein concentration.

Measurement of surface hydrophobicity of INPs

ANS Stock solution of 8 X 10^{-3} M prepared in phosphate buffer (pH 7.0/7.4, 0.1M) Stored in dark, screw-capped container and minimum exposure to light by wrapping in aluminum foil at room temperature. Protein solution: 1.5% (w/v) protein were prepared in phosphate buffer (pH 7.0, I = 0.01 M). Prepare in duplicate. Then dilute to final of concentrations. Phosphate buffer (pH 7.0/7.4, 0.1M) is prepared and added 0.02% sodium azide. To successive samples containing 4 mL of buffer and 20 μL of ANS-stock solution were added 10, 20, 30, 40, and 50 μL of 1.5% protein solution (final protein range of 0.00375-0.01875% or 0.005%-0.025%). Relative fluorescence intensity (RFI) was measured at 30±0.5 °C and -5 °C with fluorometer. Excitation and emission wavelengths of 390 and 470 nm for ANS- and slit widths of 5 nm were used.

The RFI of each protein in buffer alone (no probe) was also measured at five concentrations. The net RFI for each sample with probe was then computed by subtracting the RFI attributed to protein in buffer. The initial slope (S_0) of the net RFI versus protein concentration (percent) plot was calculated by linear regression analysis and used as an index of the protein surface hydrophobicity. No time dependence of the fluorescence intensity was observed in the systems studied within 5-15 min after mixing. Each system was run at least in duplicate. From buffer bland, buffer plus probe and protein samples from lowest concentration to highest concentration and buffer with protein dilution.

Measurement of cell surface hydrophobicity

The surface hydrophobicity of cells was measured by bacterial adhesion to hydrocarbons (BATH) test. The cells were first washed by PUM or Tris buffer twice and diluted to an optical density at 550nm of 0.2. Triplicate samples (1mL) of the cell suspensions were mixed with 0.1mL hydrocarbons of octane or hexane in test tubes. Then the tubes were mixed on a vortex for 1min and allowed to stand for phase separation. The optical density of aqueous phase was measured. Hydrophobicity was calculated as the percentage loss in optical density relative to that of the initial cell suspension.

Results and discussions

Effect of growth and post growth temperature on INA of cells

The effect of growth temperature on the INA of cells was investigated by cell fermentation at different temperatures of 18 ℃, 22 ℃ and 30 ℃. As shown in the

Figure 23, the INA of cells decreases with the increase of growth temperature. Compared to the INA at 30 ℃, the INA of cells grown at 18 ℃ is more than 10^3 times higher. This result indicates that low growth temperature can significantly enhance the INA of bacteria cells. Thus, to achieve sufficient INA, the culture growth at low temperature is preferred.

The effect of post growth temperature, also known as cold shock effect, was also studied to identify the low temperature effect on the cellular INA. The cold shock effect was investigated by transferring the fermented cells at different growth temperature to lower temperature incubation. In Figure 24, the cells were first grown at 30 ℃ for 19h until early stationary phase and then incubated in the fridge (i.e. 4 ℃) for 4h and the INA was measured at -4, -6 and -8 ℃ respectively. The results indicate that INA was very low under the growth temperature of 30 ℃, especially that the type I and type II ice nuclei were even not detectable. However, after 4 hours incubation under 4 ℃, the activity increased significantly for each type.

The cold shock effect was also conducted on the cells grown at 18 ℃ using the same procedure (Figure 25). Although the cells grown at 18 ℃ had much higher INA of type II and III than the ones grown at 30 ℃, their INA at -4 ℃ was not detectable. After incubation in the fridge for 4h, the activity of type I ice nuclei in 18 ℃ samples increased dramatically. Such phenomena have also been observed in other studies when performing low temperature induction on *Pseudomonas syringae* and *Erwinia herbicola,* in which they concluded that the low temperature induction was most

notable on the type I ice nuclei (Fall & Fall, 1998; Muryoi et al., 2003). The activity increase of type I ice nuclei could even be repeatedly induced by low-temperature and high-temperature cycles (Muryoi et al., 2003). Low temperature induction was also conducted under 10 ℃ in this study for cells grown under 18 ℃, but the increase of INA was not significant, which indicates that the cold shock effect might require significant temperature shift. The measurement of protein concentration in culture supernatant before and after low temperature induction suggests no increase of protein amount, which indicated that the increase of INA might not be due to the release of synthesized new proteins but the formation of more ice nucleation site on the cell surfaces. Other studies added protein synthesis inhibitor into the culture before shifting to low temperature still observed the increase of INA. One possible explanation for this phenomenon might be that the lower membrane fluidity at lower surrounding temperature provides higher chance of protein aggregation on the cell surface and therefore form larger ice nucleation sites which are recognized as more active at warmer threshold temperature. During the nucleation event analysis, the appearance or disappearance of different types of ice nuclei were consistent with the aggregation model (Ruggles, Nemecek-Marshall, & Fall, 1993), which supported that low temperature was required to produce type I ice nuclei (Phelps, Giddings, Prochoda, & Fall, 1986).

Therefore, these results suggest that low temperature during growth and post growth plays an important role in achieving sufficient INA. The condition of low

growth temperature can improve the cellular ice nucleation activity. And the temperature shift to low temperature from the relatively high growth temperature can induce cellular nucleation ability at higher threshold temperatures.

Surface morphology of cells and INPs under temperature shift

As discussed previously, the cold shock effect has been proven to affect membrane morphology and related cellular function (Yamanaka 1999). In order to further understand the effect of low temperature on INA of bacteria cells, the surface hydrophobicity of bacterial cells before and after cold shock (Table 8) was measured by bacterial adherence to hydrocarbons (BATH). BATH is a quantitative assay generally for determining cell surface hydrophobicity (Rosenberg, 1984). This surface hydrophobicity measurement had been conducted to determine cell adhesion to certain materials or separation of cells with different surface properties (Koga et al., 1990; Vanhaecke et al., 1990). Two different buffer and hydrocarbons were used in this study to interpret the hydrocarbons adherence as cell-surface hydrophobicity. Generally, cells after temperature shift showed higher surface hydrophobicity in both buffer systems. The difference of cell adherence to hydrocarbon between original cells and shifted cells is more significant in the mixture with hexane. The increase of cell surface hydrophobicity after temperature shift accompanied with the INA enhancement might suggest that the surface hydrophobicity was one of the crucial factors for these cells exhibiting higher INA especially the activity of type I ice nuclei. The reason for this might be that surface hydrophobicity plays a key role in influencing the initial

interaction between INPs on the membrane and ice surface.

The measurement of protein surface hydrophobicity was also conducted to determine the relationship between temperature shift and surface hydrophobicity of INPs. Figure 26 shows the fluorescence emission spectrum of ANS with INPs and OVA in the concentration range from 0.00375% to 0.01875% in aqueous phosphate buffer at pH 7.0, 0.1M and 30 ^{o}C. The observed blue shift in maximum wavelength of ANS under the increase of INPs or OVA concentration indicates the increase in hydrophobicity of their environment upon binding between ANS probe and proteins. The reason for choosing OVA as the control is that the surface of OVA is also negatively charged like INPs. For each protein concentration, INPs showed more significant blue shift than OVA, which suggests higher hydrophobicity of binding sites of INPs. Besides, the more dramatic intensity increase of INPs also suggested more hydrophobic binding site on INPs surface.

Figure 27 shows the fluorescence emission spectrum of ANS with INPs and OVA in the concentration range from 0.00375% to 0.01875% in aqueous phosphate buffer at pH 7.0, 0.1M and -5 ^{o}C. Under the supercooled conditions, more significant blue shift was observed for both INPs and OVA, indicating the increase in hydrophobicity and related alteration of protein tertiary structure under supercooled conditions (Gabellieri & Strambini, 2003; Hawe, Sutter, & Jiskoot, 2008). For each protein concentration, INPs showed much more significant blue shift than OVA as compared to their difference at higher temperature, which suggested higher surface hydrophobicity of

INPs. Under supercooled conditions, the blue shift of ANS by INPs was more significant at low concentration. At the lowest concentration, the difference in maximum wavelength of bound ANS between INPs at -5 and 30 ^{o}C was 17nm when at highest concentration there was almost no difference, which might have reached the equilibrium. The intensity enhancement with the increase of INP concentration was also more significant in the supercooled liquid, suggesting the increase of ANS binding sites on INPs surface after temperature decreasing. Same trend in blue shift and intensity enhancement was also observed in OVA, but difference was much less than INPs.

The hydrophobicity is calculated based on the fluorescence intensity at different protein concentrations (Table 9). The result indicates that INPs show higher hydrophobicity compared to OVA as control. The hydrophobicity of both INPs and OVA increased with lowering environmental temperature. The increase of hydrophobicity of INPs under supercooled condition is more significant as compared to that of OVA.

Thus, the results suggest that both bacteria cells and INPs have hydrophobic surface regions, which might be crucial for their INA. The increased cell surface hydrophobicity after cold shock effect strongly suggests the importance of surface hydrophobicity for cellular INA. The increased surface hydrophobicity of INPs under subzero temperature, also indicates more hydrophobic sites were induced on INPs surface. This might be due to the disruption of protein tertiary structure, such as

instability of folded state at low temperature or protein-solutes and protein-protein interactions (Gabellieri & Strambini, 2003). The INP structure modeling study also suggested that hydrophobic contact along the dimerization interface might be closely related to the increase of ice-active surface area of the protein (Garnham, Campbell, Walker, & Davies, 2011).

INA of cellular fraction based on centrifugal speed

Besides growth conditions, the identification of subcellular location of ice nucleation proteins is another important factor to achieve sufficient INA. By centrifuging sonicated bacterial solution at different centrifugation speeds in this study, different fractions of bacterial cells can be partially separated and the major subcellular location of INPs can be figured out. According to the previous studies, INPs are majorly located on the cell outer membrane and certain portions of INPs are also secreted into the media with a relatively high INA (Kishimoto et al., 2014; Phelps et al., 1986).

In this study, three subcellular fractions, including membrane, ribosomal and cytoplasm, were collected by centrifuging sonicated bacterial solution at different centrifugation speeds. The INA of these three subcellular fractions was compared with the INA of extracellular fraction and whole cell. As shown in Figure 28, only the INA of membrane fraction is higher than that of whole cell, whereas ribosomal fraction has much lower INA and cytoplasm fraction has almost no INA. The INA of the media is also considerably high, which suggests that part of INPs are secreted into the media

and thus *Erwinia herbicola* strain used in our study contains both intracellular and extracellular INPs . However, the protein concentration in the media is relatively low when compared to other fractions, indicating relatively low preparation yield. The result suggests that the membrane fraction contains the highest specific INA when compared with other fractions.

In conclusion, cell culture with higher INA was obtained by growing cells in low temperature environment. The exposure of cells to low temperature after growth, also known as cold shock effect, could induce the activity of ice nuclei at higher threshold temperatures (i.e. -4 ^{o}C). In addition, cells with cold shock effect had higher surface hydrophobicity. The protein surface hydrophobicity results also indicated that INPs had higher surface hydrophobicity than OVA under different temperatures, especially under subzero temperature. Therefore, this study suggested that cold shock might an effective approach to obtain INPs with activity at higher threshold temperatures. Moreover, the results from cells and INPs suggest that surface hydrophobicity might play an important role in exhibiting INA.

Table 8 Determination of cell surface hydrophobicity before and after cold shock

Hydrocarbons	Octane		Hexane	
Buffer	PUM	Tris	PUM	Tris
Original	4.47 ± 0.42	3.99 ± 0.60	19.49 ±3.18	10.72 ± 0.32
Cold shock	4.95 ± 0.71	7.88 ± 0.32	29.04 ± 3.87	17.67 ± 5.88

Table 9 Determination of surface hydrophobicity of INPs and OVA at room and supercooled temperatures

Samples	INPs at -5	OVA at -5	INPs at 30	OVA at 30
Hydrophobicity (S_0)	8.7373	2.1288	4.5239	1.5994

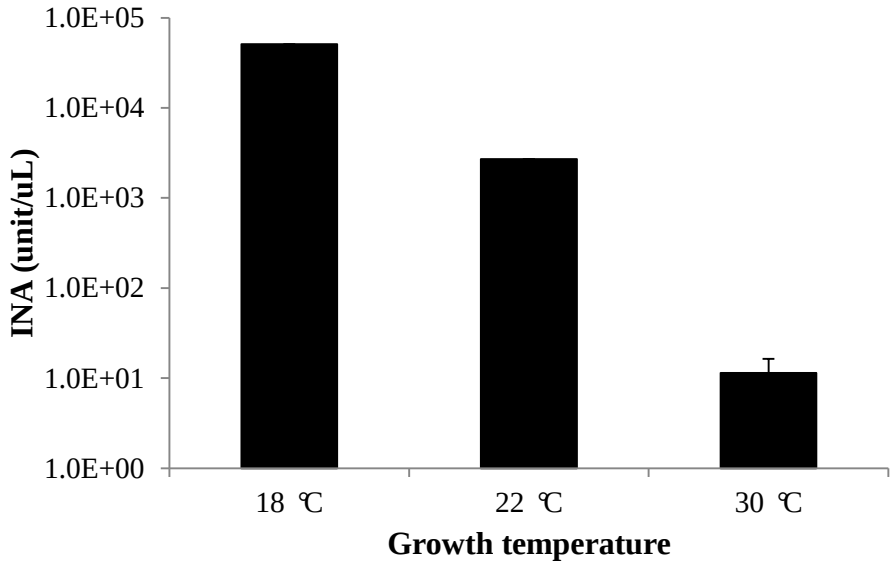

Figure 23 Effect of growth temperature on cellular ice nucleation activity

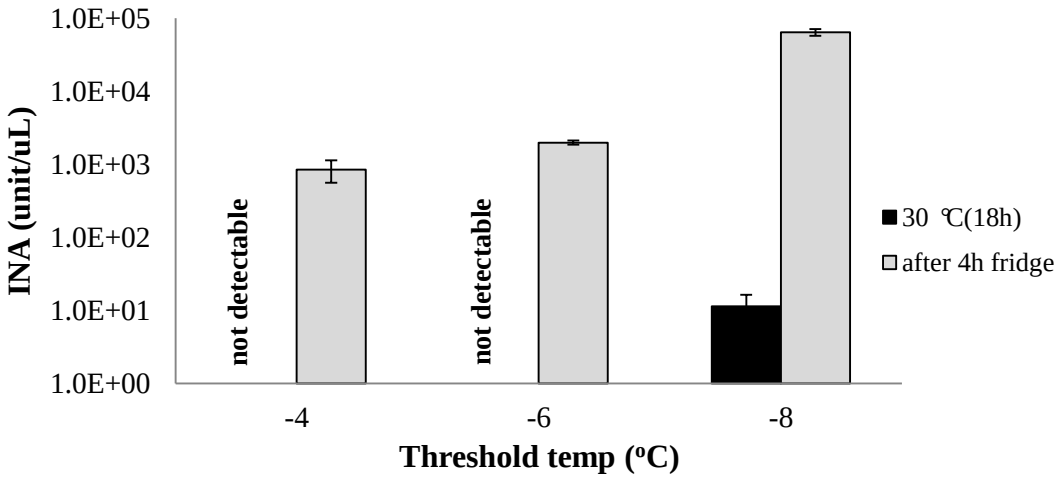

Figure 24 Post cold shock effect on INA at different threshold temperatures of cells grown at 30 ^{o}C

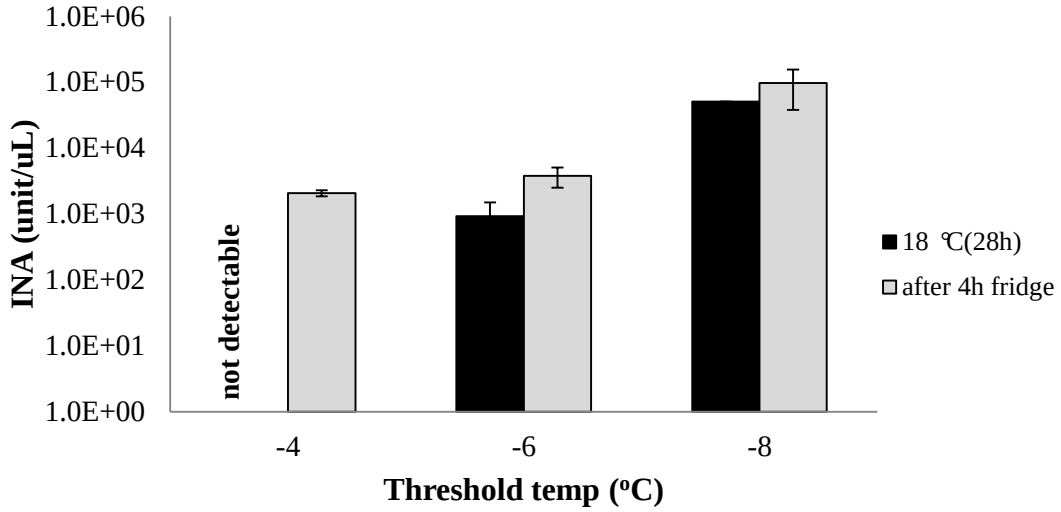

Figure 25 Post cold shock effect on INA at different threshold temperatures of cells grown at 18 ^{o}C

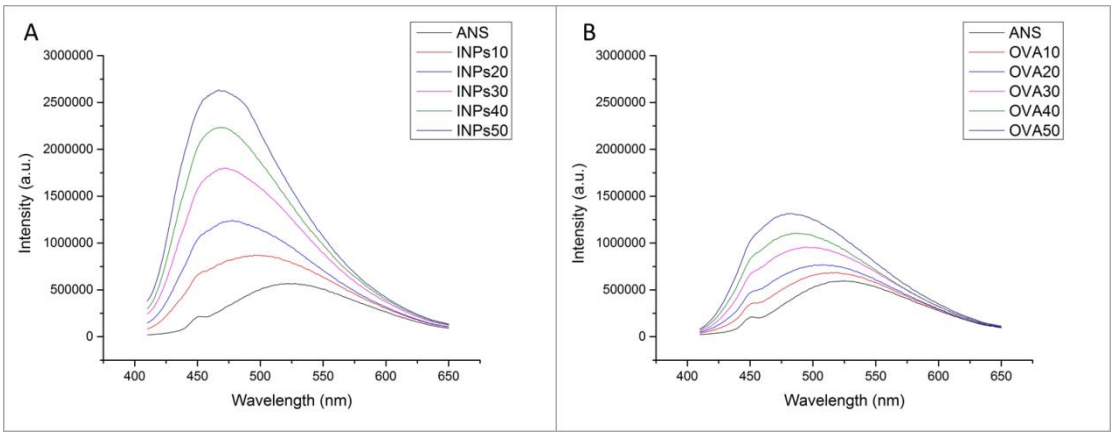

Figure 26 The fluorescence emission spectrum of ANS with INPs and OVA at different concentrations at 30 ^{o}C

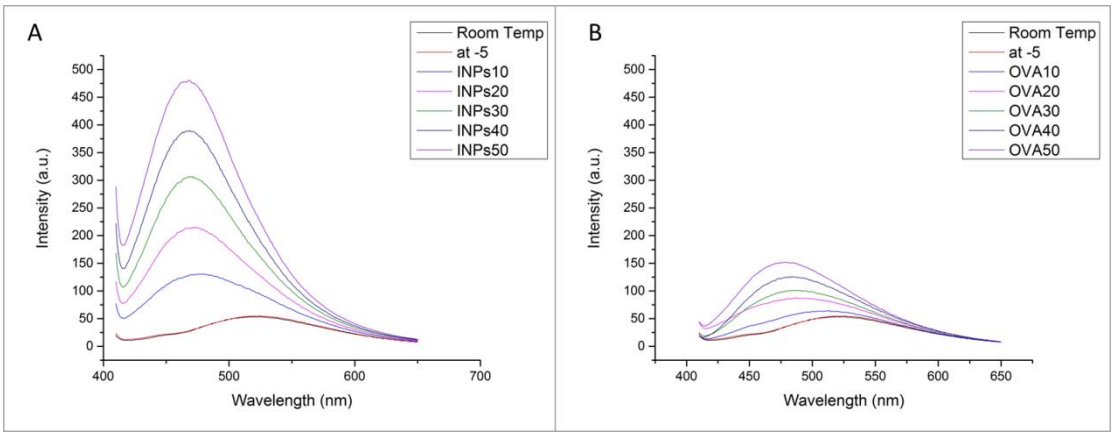

Figure 27 The fluorescence emission spectrum of ANS with INPs and OVA at different concentrations at -5 ^{o}C

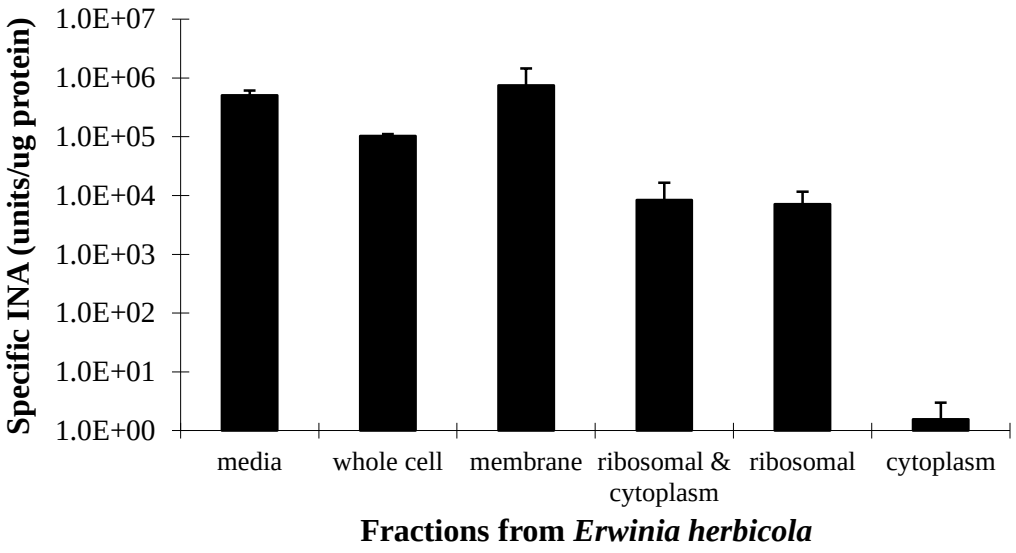

Figure 28 Specific ice nucleation activity of different fractions from Erwinia herbicola by differential centrifugation

Appendix B: Safety evaluation of INPs for food applications

This work is to address the safety concerns of INPs for food use by evaluating safety aspects of biogenic source, manufacturing procedures and dietary exposure, based on FDA regulatory requirements.

Abstract

According to FDA regulatory, the safety evaluations for a biogenic substance for food use require four aspects, including the safety of the production strain, the substance component, the manufacturing process, and an evaluation of dietary exposure to the preparation. Based on scientific literature review, *Erwinia herbiola* is considered as a non-toxigenic and non-pathogenic organism under ordinary conditions of use. Besides, current scientific evidence regarding the safety of INPs suggests that no toxicity has been found. The safety evaluations of our study suggest that INPs can be produced in compliance with required standards and the suggested use level is considered to be safe under the intended use based on previous toxicity studies. Therefore, based on the literature review and results in our study, INPs we used meet all the requirements for GRAS notification and thus should be eligible to be approved by FDA as GRAS for food applications.

Introduction

According to the FDA regulatory, any addition of a new substance for food use has two options for achieving regulatory compliance. They can either submit GRAS (generally recognized as safe) notification or food additive petition. Both regulatory compliances require the data and information to establish that the substance is safe for

intended use. A wide variety of biogenic enzymes have been used in food processing as GRAS, such as glucoamylase from *Aspergillus niger* (GRAS Notice 657), mannoprotein from the cell wall of baker yeast (*Saccharomyces cerevisiae*) (GRAS Notice 000284). The safety evaluations of these materials majorly contain four aspects, including the safety of the production strain, the enzyme component, the manufacturing process, and an evaluation of dietary exposure to the preparation. Among these aspects, the safety of the production strain is the prime consideration.

Generally, current scientific evidence regarding the safety of ice-nucleation active bacteria suggests that no toxicity has been found. For instance, a subacute inhalation toxicity study of commercialized snow making samples containing ice nucleation active bacteria, suggested that there was no mortality, moribudity or any biologically significant differences in clinical signs, food consumption, body weight or clinical pathology observed (Goodnow, Katz, Haines, & Terril, 1990). During an in vitro human lymphocytes study, no mutagenic activity was induced by the whole cell of ice nucleation active bacteria, their metabolic product and intracellular compounds in sonicated bacteria (Lialiaris, Mourelatos, Stergiadou, & Constantinidou, 1990). The health risk assessment conducted by French health authorities also suggested that the ice nucleation active bacterium *Pseudomonas syringae* as snow making additives, did not show any pathogenic capacity to humans and its endotoxin level in artificial snow did not show a danger beyond that of exposure to *P. syringae* endotoxins naturally present in snow (Lagriffoul et al., 2010). The assessment was based on a review of

scientific literature supplemented by professional consultations, and potential human health hazards were considered from aspects of infectious, toxic and allergenic capacities regarding human populations liable to be exposed and the means of possible exposure.

Recent literature also suggests *Erwinia herbiola* as a non-toxigenic and non-pathogenic organism under ordinary conditions of use. An effective regulation regarding using *Erwinia herbicola* (*Pantoea Agglomerans*) as a biopesiticides on pears and apples, has showed human health assessment of the microorganism, including toxicology assessment, exposure and risk characterization (Ashby, Cole, & Sadowsky, 2006). The scientific results gathered by this regulation establishment conclude that the strain is not toxic under the intended use as biopesticide. Members of the group described as *E. herbicola* are found in soil, water, air, and associated with plants and animals, including humans as commensal microbes. The acute oral toxicity and pathogenicity testing of *Erwinia herbicola* in rats showed no deaths of animals occurred during the course of the study and no significant clinical findings were noted. Based on the data generated for acute oral toxicity, other safety studies (e.g. acute dermal irritation, intravenous injection, immune response, teratogenicity, virulence enhancement, mammalian mutagenicity, chronic testing, oncogenicity testing, etc.) were not required. Thus, the conclusion based on the submitted and cited data suggests that *Erwinia herbicola* (*Pantoea agglomerans*) strain do not pose an incremental dietary and non-dietary risk to the adult human, children and infants

under their intended use. *Erwinia herbicola* (fermentation) has also been commercially used for enzymatic production of a drug (i.e. L-DOPA) for Parkinson's disease in pharmaceutical industries in the last few decades (Min, Park, Park, & Yoo, 2015; Zaidi, Ali, Ali, & Naaz, 2014). However, strains within the *E. herbicola* complex have been implicated in plant disease situations and have been loosely implicated as clinical isolates in several disease situations in humans. But related evidence also suggests that the presences of these organisms in clinical pathology are considered as secondary colonizers, especially in cases where an underlying pathology has compromised the immune system. A non-toxigenic organism is defined as "one which does not produce injurious substances at levels that are detectable or demonstrably harmful under ordinary conditions of use or exposure". Therefore, based on the scientific evidence discussed above, ice-nucleation active bacteria, especially *Erwinia herbicola,* are very likely to be recognized as non-toxigenic. If the organism is non-toxigenic and non-pathogenic, then it is assumed that food or food ingredients produced from the organism, using current Good Manufacturing Practices, is safe to consume.

For the safety of INPs, there is currently no direct scientific evidence established. However, previous study showed negative results when the sonicated ice-nucleation active bacteria were tested for possible intracellular mutagenic components, which contained INPs in the sonicated suspension mixture (Lialiaris et al., 1990). Meanwhile, other ice-active proteins, such as ice structuring protein, have recently been approved

for food use (GRAS Notice No. GRN 000117, 2003). Previous studies suggested that both ice structuring protein and INPs might be consisted of very similar chemical moieties (i.e. β-helical fold, repetitive TXT motif) but differences in molecular size (Graether & Jia, 2001; Kajava, 1995; Kawahara et al., 2004). Thus, the digestion products from INPs are very likely to be same as ice structuring protein. The safety evaluation of ice-structuring protein produced by recombinant baker's yeast, showed no evidence of genotoxicity and subchronic toxicity (Hall-Manning, Spurgeon, Wolfreys, & Baldrick, 2004). The application of using ice-structuring protein as a new food additive in edible ices and frozen desserts has already been permitted by European Food Safety Authority, Food Standards Australia New Zealand, Health Canada and USFDA.

Therefore, the safety aspects of preparation process and dietary exposure level of INPs prepared for this study were evaluated in this work. The consistency of INP preparation process was evaluated by comparing the INA and yield of different batches prepared in our lab during the past five years. The accordance of our preparation steps with good manufacturing process was also evaluated based on established enzyme preparations from microorganisms. The freezing efficiency of INPs at the suggested use level was determined under different freezing conditions and in different food systems. The safety of dietary exposure of INPs in freezing technology applications was evaluated by comparing the use level in our study with the results from previous toxicity studies.

Materials and methods

Materials

E. herbicola subsp. Ananas, obtained from the American Type Culture Collection (ATCC; ATCC Cat. No.11530), was used as the source of microbial INPs in these studies. Yeast extract was obtained from BD Biosciences (Franklin Lakes, NJ, USA). Sucrose (>99.9%), tris (Hydroxymethyl) aminomethane, potassium sulfate (K_2SO_4), and magnesium sulfate ($MgSO_4$), were obtained from Fisher Scientific (Fair Lawn, NJ, USA). L-serine, L-alanine and magnesium chloride ($MgCl_2$) were purchased from Sigma-Aldrich (St. Louis, MO, USA). All reagents were of analytical grade, and deionized water from Milli-Q was used throughout the experiments.

Preparation and purification of ice nucleation proteins

Erwinia herbicola was stored frozen at -60 ℃ and grown in yeast extract (YE) media (20g/L), containing sucrose (10g/L), L-serine (2g/L), L-alanine (2g/L), K_2SO_4 (8.6g/L) and $MgSO_4$ (4g/L). Following culture expansion to a density of 10^8/L, the cells were collected by high-speed centrifugation (10,000×g 20 mins @ 4 ^oC), and the resulting pellet was re-suspended in 20mM Tris buffer containing 20mM $MgCl_2$. The suspension was then sonicated on ice, using three brief (10 sec) sonication bursts generated by a Brandson sonicator (Danbury, CT) set at the 4.5 power output setting. Following sonication, the suspension was centrifuged again as described above and the supernatant was isolated and ultra-centrifuged at 4 ^oC and 160,000×g for 2h. Finally, the resultant pellet was re-suspended in 20mM Tris buffer with 20mM $MgCl_2$, and

freeze-dried to obtain the INP powder. Lyophilized INPs isolated in this manner were stored at -18 ^{o}C prior to use (the procedure above was cited from Jin et al., 2017).

Drop-freezing method and specific ice nucleation activity

The ice nucleation activity (INA) was measured by the drop-freezing method. Protein solutions were serially diluted in DI water and 20 droplets with constant volume of 10uL were placed on the alumina plate incubated at -8 ^{o}C for 3mins. Total numbers of frozen droplets were counted after that and the value between 5 and 18 were considered to be statistically significant. The corresponding dilution factor was used for calculation through the below formula:

$$ina\,(T) = -\frac{\ln(1-f)}{V_d} \times D$$

T: incubation temperature

f: ratio of frozen droplets

V_d: droplet volume

D: dilution factor

The unit of INA based on the equation is units/uL.

Protein concentration of each solutions were measure by the Bio-Rad Protein Assay and interpreted using the standard curve that established by measuring absorbance of BSA at different concentrations. And specific ice nucleation activity (units/mg) was calculated by dividing ice nucleation activity with the protein concentration.

Determination of the supercooling point using DSC

The supercooling point of solutions containing different concentrations of INPs was measured by differential scanning calorimetry using a DSC 823E thermal analyzer (Mettler-Toledo Inc., Columbus, OH) charged with liquid nitrogen and compressed nitrogen gas as described in manufacturer's instructions. Briefly, 30µL of the seawater samples were transferred into 40-µL aluminum crucibles with lids and positioned in the unit. The temperature ramp of the DSC unit was set at different freezing rates of 0.2, 1 and 10 ^{o}C/min, from 4 ^{o}C to -25 ^{o}C. An empty crucible was used as the reference. The temperature point exhibiting the maximum observed heat flow was recorded as the supercooling point.

Results and discussions

Batch consistence of INPs and compliance to standard manufacturing practice

The specific INA and yield of INPs from different batches prepared in our lab over the past five years were compared, to evaluate the consistency of our preparation procedure. As shown in Table 10, the concentration of protein was steady in different batches. Since protein is considered as the major component of INPs, the result suggests the consistency of the preparation method. Also, there is no significant difference between specific INA and final yield of different batches, which indicates that the activity of cell culture as well as the prepared extracts are consistent during a long term period and suggests the practicality of producing INPs for commercial applications.

Based on the results above, using our current preparation process, INPs with consistent chemical property, INA and yield can be obtained. Since the function of INPs for food use is close to enzyme applications in food, the accordance of our INP preparation process with good manufacturing practice can be further evaluated based on established enzyme preparations obtained from microorganisms. As stated in Recommendations for Submission of Chemical and Technological Data for Food Additive Petitions and GRAS Notices, enzyme preparations obtained from microorganisms have specific manufacturing practice requirements regarding the fermentation process, isolation or purification process and materials used during the processes.

First, the fermentation process described should be able to maintain the proper growth conditions and purity and genetic stability of the culture. In our study, a naturally existed strain of *Erwinia herbicola* were fermented in controlled culture media, which is consisted of sufficient nutrients for stable cell growth and no nutrition limitation to ensure the absence of toxin production by the organism. The microorganism strain is preserved with glycerol and stored in freezer (i.e. -60 ^{o}C) to prevent changes in the characteristics of the strain, especially the introduction of microorganisms that could be the source of toxic materials and other undesirable substances. The stability of culture growth conditions is checked by determining the INA of culture at the end of each fermentation process. The results suggest that the INA of culture is stable and reproducible from batch to batch. Second, the description

of the enzyme isolation from the cellular material or from the fermentation broth should include all chemical and physical treatments and quality controls. In our study, INPs are extracted from the culture by sonication and differential centrifugation under standardized conditions. The sonication step is designed to inactivate all bacteria by breaking down the cells, so our INP preparation does not contain intact microorganisms which will not cause any increase in the total microbial count in the treated food. Third, all materials used in the fermentation and subsequent downstream processing should be identified and shown to be suitable for use in food processing. In our study, the culture media used for INP preparation contains no residues harmful to health in the finished food. The sonication and centrifugation steps do not bring any additional materials.

Therefore, INPs prepared and used in our study are produced in accordance with accepted principles of good manufacturing practices that established for existing enzyme preparation procedures for food applications. Thus, our INP preparation has the potential to be further developed into a standard manufacturing practice. However, our results only showed the protein content consistency. To further establish conformance of the enzyme preparation with the specifications, other chemical analysis might need to be performed, such as tests to confirm the absence of undesirable compounds at biologically significant levels.

Activity of INPs at suggested use level under different freezing conditions

The use level of INPs applied in freezing technologies is 10^{-2} mg/mL. Before the

safety evaluation, the effectiveness of INPs controlling the supercooling point at the use level of 10^{-2} mg/mL was measured by DSC under different cooling rates of 10 ^{o}C/min, 1 ^{o}C/min and 0.2 ^{o}C/min (Figure 29). Without the addition of INPs, the nucleation temperature of seawater decreased with the increase of cooling rate with a difference of 8.68 ^{o}C in supercooling point between the cooling rate of 10 ^{o}C/min and 0.2 ^{o}C/min . With the addition of INPs at the concentration of 10^{-2} mg/mL, the nucleation temperature only slightly decreased with the increase of cooling rate and the difference of nucleation temperatures between 10 ^{o}C/min and 0.2 ^{o}C/min became much smaller as 1.72 ^{o}C. This significant difference strongly suggests that the efficiency of INPs on reduction of supercooling degree under different cooling rates, especially fast freezing under which INPs can significantly elevated the nucleation temperature as compared to controls. Based on this result, consistent product quality can be obtained with the addition of INPs under freezing temperature fluctuations, especially in the cases of freezing biological materials in which the excessive supercooling during high cooling rate was considered as the major reason for poor quality with intracellular ice formation. Another interesting observation was that the standard error bars of samples with INPs is much smaller than the controls, which further suggested that the control of ice nucleation by INPs could remain consistent under different freezing conditions, and could be further utilized for various freezing applications.

The results indicate that INPs at the suggested use level of 10^{-2} mg/mL can

effectively control the supercooling point under different freezing rates, which strongly supports that INPs can function as effective ice nucleators for controlling nucleation temperatures under various freezing conditions. The elevated nucleation temperature also suggests significant energy savings for freezing equipment.

Activity of INPs at suggested use level in different food systems

The freezing efficiency of INPs at the use level of 10^{-2} mg/mL was also determined by measuring its effect on nucleation temperature of different food systems (Figure 30). At the suggested use level, INPs could significantly elevate the supercooling point of food systems including seawater, juice, milk, 10% sucrose and 5% BSA. Those food systems are typically study models for either freeze concentration or freeze drying. At the suggested use level, all the food materials could be freezable above the freezing temperature of -8 ^{o}C, which suggests the great savings of energy consumption related to cooling systems, as well as quality improvement related to freezing damage. Thus, this result suggests that at the suggested use level of 10^{-2} mg/mL, INPs can effectively control the nucleation temperature of typical food systems and improve the efficiency of both freeze concentration and freeze drying processes based on the results in Chapter IV and V.

Safe evaluation of INPs at suggested use level

The safety of adding INPs into food applications was evaluated by comparing the suggested use level in our study with the results from other toxicity studies. In our case, the prepared INPs will be used in a range of liquid and solid products, including

drinking water, juice, milk, freeze dried powders. They are applied to facilitate the freezing technologies with improved efficiency and reduced cost, not supposed to change other properties of the products. Take liquid products for example. The estimated daily intake for water or beverage consumption is 2 liters. If assuming all the water or beverage consumed contains INPs at the suggested level of 10^{-2} mg/mL, the estimated daily intake of INPs is 20 mg/day. This estimation is based on the maximum consumption of INPs at the suggested use level. The acute oral toxicity/pathogenicity results from established regulation exemption regarding the *Erwinia herbicola* strain suggest no deaths of animals occurred during the course of the study and no significant clinical findings were noted (EPA, 2006). This means that if our estimated daily intake of INPs is lower than the dose level of the acute oral toxicity/pathogenicity study, the suggested use level of INPs in our study should be considered as safe. As described in the test guidelines for the acute oral toxicity/pathogenicity study, the dose level of at least 10^8 units of the microorganisms per test animal should be used (Microbial Pesticide Test Guidelines, OPPTS 885.3050 Acute Oral Toxicity/Pathogenicity). Based on our INP preparation results of different batches, the average amount of INPs inside 10^8 units of bacterial cells is around 300-400 mg. Therefore, the estimated daily intake of INPs (i.e. 20 mg) from consumption of INP added products at our suggested use level (i.e. 10^{-2} mg/mL) is be well below the non-toxic dosage (i.e. 300-400 mg) of acute oral toxicity/pathogenicity study in rats.

Besides bacteria origin, ice nucleation proteins are also widely distributed in other natural sources, such as fungus, animals and plants (Pummer et al., 2015). This suggests the plenty of human exposure to these biogenic ice nucleators. Previous study also suggests that INPs are very sensitive to high temperature and chemicals (e.g. protease and lipase), so that they are very likely to be already degraded during the subsequent processes like thermal step. Furthermore, the previous study of immobilizing INPs on magnetic nanoparticles in our lab also suggested a promising potential of effectively removing the proteins from the final products (Zhou et al., 2014). A previous study also indicates that INPs might be the aggregation structure of ice structuring protein (ISP), and ISP is considered to be not toxic at the use level of 0.01% by weight (Hassas-Roudsari & Goff, 2012). Compared to that, our suggested use level of INPs is 0.001% by weight. Therefore, the application of INPs at our suggested use level is very likely to be generally safe based on the comparison with currently published toxicity studies.

In conclusion, the preparation process of INPs is consistent between each batch and adheres to good manufacturing practice described in other biogenic substance preparation from microorganisms. Significant enhancement of nucleation temperature is achieved at the suggested use level of INPs under different freezing conditions and in different food systems. The safety evaluation based on the results from previous toxicity studies, indicates that the suggested use level of INPs in our study is very likely to be generally safe under its intended use. Therefore, based on current

literature review and results in our study, the fundamental information regarding the safety of INPs can meet all the FDA requirements for GRAS notification. Other ice-active proteins like ice structuring protein (ISP), which has similar structure to INPs, has already been approved as GRAS (GRAS Notice No. GRN 000117) by FDA for commercial use as a texturizer in frozen novelty desserts. ISP was announced as GRAS in 2003, because the gathered literature review and scientific results demonstrate that the safety of ISP can meet all FDA requirements for GRAS notification as discussed above regarding the safety of INPs, which include the safety of production strain, the substance component, the manufacturing process and the dietary exposure. Currently, ISP has been commercially used by Unilever Company in their Good Humor-Breyers ice cream products. Based on the approval and commercial use of ISP in food products, INPs should be eligible to be approved by FDA as GRAS for food applications.

Table 10 Comparison of protein concentration, specific INA and yield from different batches

batch	pro conc (mg/uL)	specific INA(unit/mg)	yield (g)
080610	0.49	2.01E+06	0.39
071511	0.48	3.92E+06	0.32
122113	0.46	1.51E+06	0.32
041014	0.47	1.95E+06	0.34
042615	0.48	3.35E+06	0.31

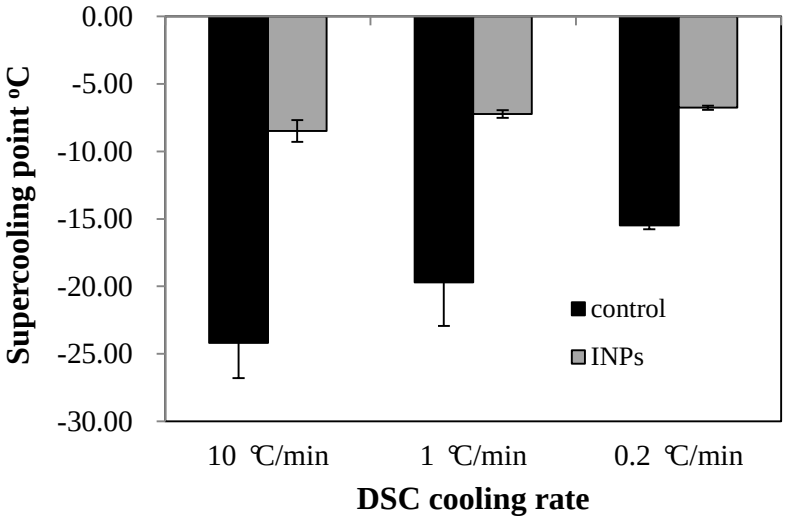

Figure 29 Effect of INPs on supercooling point under different DSC cooling rate. (INP conc: 10^{-2} mg/mL)

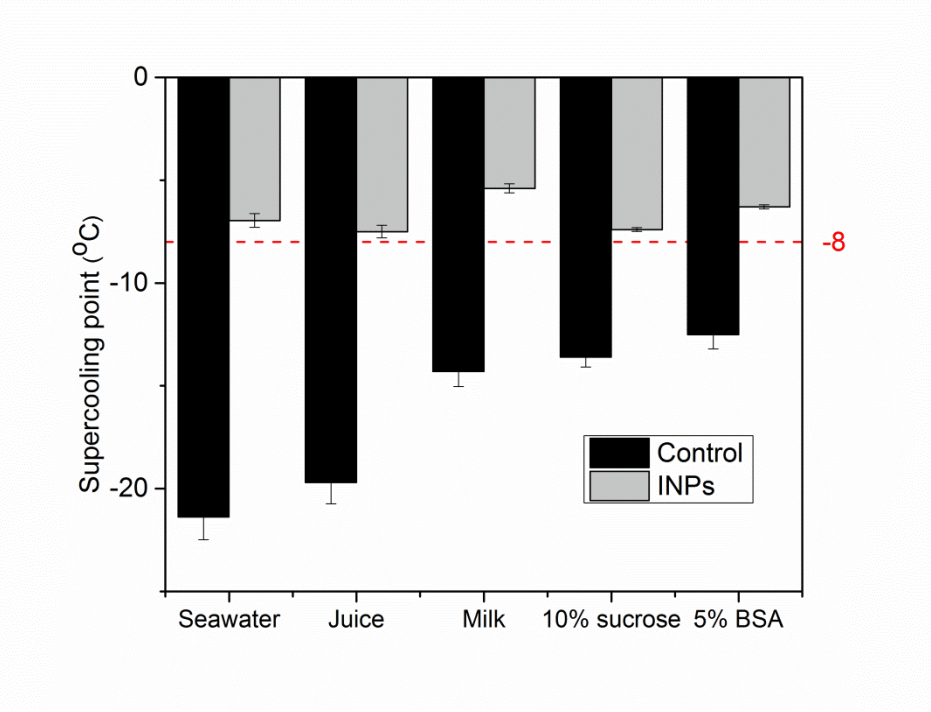

Figure 30 The effect of INPs on nucleation temperature of different food systems. (INP conc: 10^{-2} mg/mL)

Appendix C: Mechanisms of INPs altering ice morphology

This part of work is to update and summarize the useful information regarding the mechanism for the interaction between INPs and ice crystals to explain why INPs can alter ice morphology.

Our results suggested that ice nucleation proteins (INPs) were capable of altering ice morphology inside frozen matrix. It was the first time to discover that INPs could not only affect the nucleation rate but also influence subsequent macroscopic ice structure. This observation sheds light on the mechanism of freezing technology efficiency improvement and also suggests the potential of applying INPs as a promising additive for frozen product morphology alteration in food, pharmaceutical, and beverage applications. Before further application, it is crucial for us to understand the reason for such alteration made from INPs. Since INPs are a group of unique proteins that possess the ability of catalyzing a physical change, the investigation can be considered from physical and chemical perspectives.

From physical perspective, ice morphology is significantly influenced by freezing kinetic parameters, such as temperature gradient, freezing front velocity, solute characteristics and content. The characteristics feature of ice morphology observed in INP frozen samples is the lamellar ice structure, which have also been reported in other freezing morphology studies under different freezing parameters. By applying bidirectional freezing technique, ceramic particles successfully assembled into porous

scaffolds with large scale aligned, lamellar structure at the centimeter level, which is achieved by the control of ice crystal nucleation and growth under dual temperature gradients (Bai, Chen, Delattre, Tomsia, & Ritchie, 2015). The ice-templating study of alumina suspensions investigated the relationship between freezing front velocity and ice crystal morphology, which indicated that lamellar ice morphology formed at intermediate velocity and changed to cellular structure when the velocity increased (Lasalle et al., 2012). Besides, during unidirectional freezing of ceramic suspensions, the lamellar structure was lost when the solid content increased above a critical value, which indicated the importance of solute characteristics and amount (Delattre et al., 2013).

Under these freezing conditions, the lamellar ice structure can be explained through the nature of anisotropic growth of the ice crystals. The anisotropic growth of ice crystal is resulted from the different growth rates between three primary crystal faces of hexagonal ice (including the basal face, the prism face, and the secondary prism), which are depended on temperature, pressure and other related environmental conditions suggested by an extensive and systematic molecular dynamics study (Rozmanov & Kusalik, 2012). Under certain situation, it was demonstrated that the growth of the basal face is two orders of magnitude slower than the prism and the secondary prism faces, indicating lamellar ice morphology (Deville et al., 2009).

These observations of similar lamellar ice structure suggested that the ability of INPs altering ice morphology might be closely related to their influence on

controlling ice nucleation temperature and related freezing parameters like freezing rate, temperature gradient. However, although the morphology from these conditions shared some similarities, the physical parameters might not be the determinant reason. We are more interested in the chemical aspects of INP effect on ice morphology, since mechanisms based on chemical properties are usually more specific and precise.

A recent work regarding molecular dynamics simulation of heterogeneous ice nucleation using the clay mineral kaolinite as the model ice nucleating agent, suggested that ice nucleating materials not only affect nucleation rate but also could have an effect on macroscopic ice structure (Cox et al., 2013). Under ambient conditions, there are two crystal forms of ordinary ice, hexagonal ice (Ih) and cubic ice (Ic) (Raza et al., 2011). This study found that heterogeneous ice nucleation with kaolinite exclusively formed hexagonal ice while homogeneous ice nucleation contained a mixture of hexagonal and cubic ice crystals. Moreover, a variety of crystal orientation was observed in homogeneous ice nucleation whereas an ordered ice crystal growth along the prism face was observed in the ice formed on the kaolinite. These observations suggested that kaolinite as the ice nucleating agent could change the ice crystalline structure formed on its surface and promote the growth of the prism face over the based face, which might have consequences for the macroscopic ice structure.

Another interesting observation is the considerable rearrangement of water molecules in the second water layer without direct kaolinite surface contact. This

observation was confirmed by the measurement of second water layer density, indicating that such structural change is part of the nucleation mechanism. The mechanism for those observations was suggested as the arrangement of –OH group affected by the surface morphology of ice nucleating agent (Cox et al., 2013). By investigating the water molecule adsorption energy of both basal and prism faces during the heterogeneous ice nucleation with kaolinite, it indicated that prism face was more stable when increasing the number of ice layer. Further examination of ice layer structure showed that the bonding between basal face and kaolinite saturated all hydrogen bonds leaving no dangling hydrogen bonds that water molecules in above layers can attach to. On the other hand, prism face exhibited dangling hydrogen bonds by arranging water molecules in high-lying and low-lying pairs to donate and accept hydrogen bonds. Such growth of favored face might be closely related to the surface morphology of kaolinite, like the presence and arrangement of hydroxyl groups at its alumina sheet terminal. Other additives like PEG containing terminated hydroxyl groups were suggested to have the ability of inducing a transition from a disordered structure to a lamellar structure of ceramic scaffolds (Delattre et al., 2013).

However, this specific matching of hydrophilic residues like hydroxyl groups to the ice crystal lattice is still questionable, since there is increasing proof that hydrophobic interactions are also important, which could lead to significant entropic contributions by limiting the number of water molecules on protein/ice surfaces and can affect the ice morphology as well (Gibson, 2010). During the investigation of

material properties for ice nucleation characteristics, it pointed out the material surface morphology/property exhibited a significant role in initiating ice formation and at the meantime altering the resulting ice structure. It was suggested that the balance between the morphology of surface and its hydrophobicity can greatly affect the ice nucleation rate and lead to formation of different faces of ice on the same substrate (Fitzner et al., 2015). The study of synthetic macromolecules to mimic behavior of antifreeze proteins concluded that the presence of a hydrophobic face/pocket/region was essential for ice shaping activity, which could be the macroscopic effect as the result of the crystal habit changes of ice on the molecular level (Gibson, 2010). Further, the mutation of several polar residues to non-polar ones in AFP led to changes in morphology of seed ice crystals (Sönnichsen, DeLuca, Davies, & Sykes, 1996). It is known that hydrophobic groups on protein surface are important for high affinity between ice and protein, which were considered as the determinant factor for hydrogen bond lengths and angles and related ice structure with the influence on the orientation and accessibilities of the polar residues (Davies, 2014). Therefore, surface hydrophobicity might be an important indicator for determining the material surface characteristics related to ice morphology alteration, due to its role in steric position of OH group that restrict polar interactions or the hydrogen-bond formation between the protein and water (or ice).

Besides these observations and discussions from AFP and other ice nucleation materials, previous studies also suggest that INPs are very likely to share similar

mechanism by influencing the crystal face growth and hydrogen bond network. It was found that an INP from *Pseudomonas syringae* could bind to favor crystal face and exhibited an ability to shape an ice crystal (Kobashigawa et al., 2005). The results of ice growth experiments with INPs from *X. campestris* showed changed ice crystal growth rate in the *c*-axis with increased growth rates in directions perpendicular to the *c*-axis (Nada et al., 2010). Further, a recent study using Terahertz absorption spectroscopy found out that the lipoprotein ice nucleator produced from an ice nucleating insect could affect the H-bond network dynamics (Bäumer et al., 2016). These results suggest the ability of INPs to alter ice crystal face growth and hydrogen bond formation, which could further lead to the macroscopic change of ice structure.

Therefore, the mechanism for INPs altering ice morphology might be their control on nucleation temperature, or more likely might be their effect on molecular growth of ice crystals during freezing process. We have performed some studies regarding the surface hydrophobicity of INPs using fluorescent dyes, which indicated the presence of hydrophobic area on the INPs surface. The measurement of INP surface hydrophobicity could be the first step to understand the INPs surface property, and more research is suggested to further understand their interaction with ice, such as the effect of INPs on the growth and melting of single ice crystal by nanoliter osmometer, the influence of INPs on the crystal growth face and orientation by X-ray diffraction, the impact of INPs on hydrogen bond network and related OH arrangement by terahertz spectrometry.

Appendix D: Radiodensity distribution change of ice phase by INPs

This work is to provide supporting materials regarding the radiodensity change of ice phase by ice nucleation proteins.

Abstract

This study suggests the possibility of ice density change by INPs as indicated by the change of radiodensity distribution. The comparison of estimated density based on linear attenuation coefficients of X-ray CT images provides insight into the density variation between control and INP samples through the distribution of CT numbers. The results showed that radiodensity distribution was altered by INPs in both frozen DI water and seawater samples, indicating that INPs can change physical properties of ice crystals.

Introduction

X-ray Computed Tomography (CT) is a technique to examine samples using X-ray microscopy with tomographic algorithms and further analyze the spatial distribution of X-ray linear absorption coefficients of the samples based on reconstructed three dimensional CT images (Schoeman et al., 2016). During X-ray CT analysis, radiodensity refers to the property of being relatively resistant to the passage of electromagnetic radiation, especially X-rays. X-rays are part of the electromagnetic spectrum, having a wavelength range from 0.01 to 10 nm (Florez et al., 1998). Dense materials that inhibit the passage of X-rays show relatively opaque white appearance

in the radiographic images, while less dense materials that allow X-rays to pass exhibit darker appearance. Although radiodensity is commonly used for qualitative comparison in medical diagnosis, it can also be quantified based on the intensity of the transmitted X-ray beam expressed as CT value, or the Hounsfield unit (HU) (Kawamura, 1990). The CT value is defined as $HU = 1000(\mu - \mu_w)/\mu_w$, where μ and μ_w are the linear attenuation coefficients of a substance of interest and water (Tanaka et al., 2011). So the Hounsfield scale is a linearly transformed from the original attenuation coefficient, where water has a value of 0 HU and air has a value of -1000 HU. Since the coefficient of a material μ is proportional to its bulk density, the change in the Hounsfield unit represents the change in density. Besides the bulk density, the linear absorption coefficient also depends on chemical composition of the materials and the applied X-ray energy. Substances with higher bulk density and higher atomic numbers result in higher attenuation of X-rays. Since X-ray attenuation is sensitive to material density variations, X-ray CT analysis based on CT value can also offer quantitative density measurement. Its rapid and quantitative results can easily be used to map subtle detailed density variations of samples in three-dimensional analysis (Tanaka et al., 2011).

Method

The frozen samples were prepared in the cooling bath at temperature of -18^{o}C until completely frozen. For seawater samples, the brine was removed from frozen seawater samples by centrifuging under 2000 rpm for 10 mins. All the samples were

scanned using the Albira PET/CT Imaging System (Bruker, Billerica, MA) set at low voltage and low current (i.e., 35kV and 200μA, respectively). A set of 400 image projections was taken throughout a 360^{o} rotation of the sample. The reconstructed image of the sample showed as a three dimensional map of attenuation coefficient for a material of any desired section (slice). The histogram of each sample was determined and analyzed using VivoQuant image analysis software (version 1.23, inviCRO LLC, Boston MA). All the frozen samples were scanned using X-ray computed tomography at Molecular Imaging Center at Rutgers University.

Results and Discussions

Radiodensity of frozen DI water samples

Histogram of CT value (HU) illustrates the number of pixels distributed on image (y-axis) found for each CT value. The effect of INPs on radiodensity of frozen DI water samples indicated as CT value (HU) is shown in Figure 31. As shown in Figure 31A&B, the majority of pixels appears in control and INPs samples are within the CT value range of -30 to 0 under our current experiment settings, which indicates that radiodensity for ice is between -30 and 0 in this study. The histogram of control sample (Figure 31A) has the peak around the CT value of -8.76, when the histogram of INP sample (Figure 31B) has the peak around the CT value of -9.46. This comparison suggests that INP sample have more pixels with lower radiodensity as compared to control sample. The histogram shown in Figure 31C is the subtraction of CT value in control from that in INP sample. The subtraction of control from INP

samples confirms the left-shift radiodensity distribution in INP samples, indicating the change of attenuation coefficient and related ice density.

Radiodensity of centrifuged frozen seawater sample

The effect of INPs on radiodensity indicated as CT value (HU) of centrifuged frozen seawater samples is shown in Figure 32. The purpose of centrifugation is to remove the brine solution from the frozen matrix to leave only ice phase for further analysis. In Figure 32A&B, the majority of pixels appeared in control and INP samples are within the CT value range of -30 to 0, which is consistent with the radiodensity (CT value) distribution in the pure water sample shown above and suggests that almost only ice phase is left in the frozen seawater samples after centrifugation. The histogram of control sample (Figure 32A) has the peak around the CT value of -8.45, when the histogram of INP sample (Figure 32B) has the peak around the CT value of -11.76. This comparison also suggests that INP sample have more pixels with lower radiodensity as compared to control sample. The histogram shown in Figure 32C is the subtraction of CT value in control from that in INP sample. The subtraction of control from INP samples also confirms the left-shift radiodensity distribution in INP samples, indicating the change of attenuation coefficient and related ice density, which suggests that such change is independent of solute presence in the frozen solutions.

The results of this study suggest that INPs can change ice structure in frozen samples with lower radiodensity as compared to controls. As the radiodensity is

correlated to material density, this indicates that INPs are capable of influencing the physical properties of ice during its formation. This leads to the question what physical property is changed by INPs in these samples. In order to clarify this, the pixels of radiodensity in the histogram need to be defined first. The pixels stand for the frequency of the radiodensity under this CT value that appeared inside the scanned sample. And such value for the radiodensity is calculated based on the average X-ray absorption coefficient within the pixel size. The pixel size in this study is around $0.125mm^3$ which is larger than ice crystal diameter (around 0.03 to 0.05mm) observed in the optical microscope study. Based on this, the physical change of ice phase by INPs in this study includes the properties of ice crystals and the interphase between them. The shift of radiodensity distribution is also observed in the frozen DI water samples, which doesn't have any solute inclusion in the interphase of ice crystals. This might suggest that the major reason for the change of radiodensity distribution is the change of the molecular ice structure like ice crystalline pattern in INP samples.

A

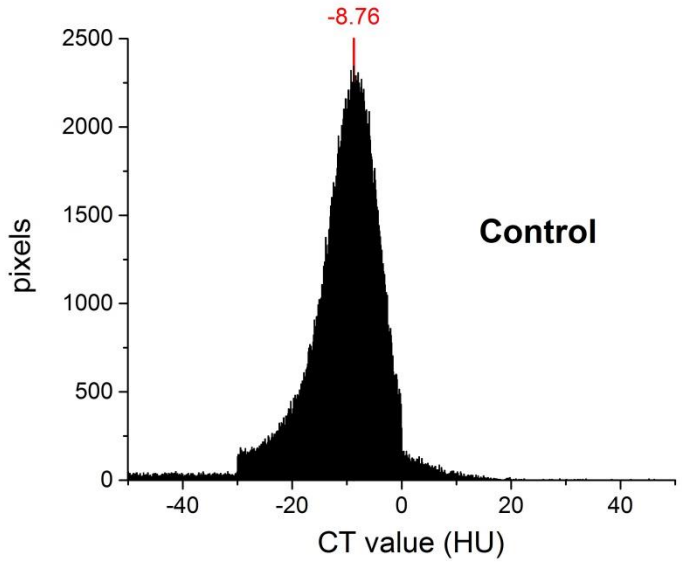
-8.76
2500
2000
1500
1000
500
0
pixels
Control
-40
-20
0
20
40
CT value (HU)

B

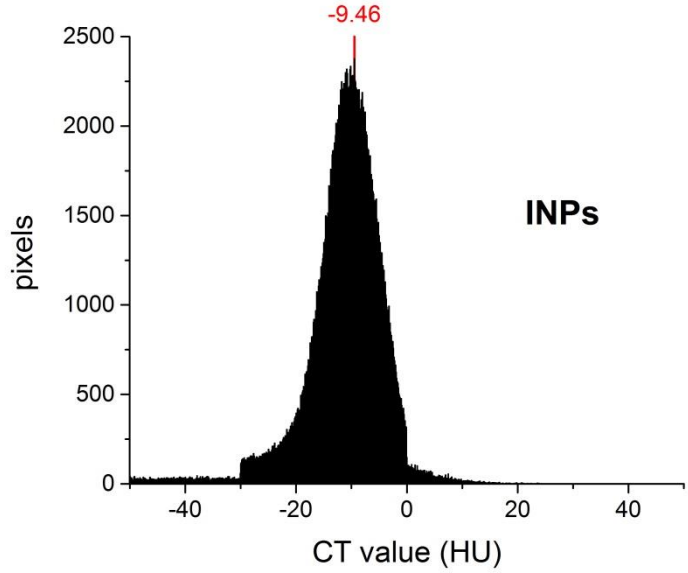
-9.46
2500
2000
1500
1000
500
0
pixels
INPs
-40
-20
0
20
40
CT value (HU)

C

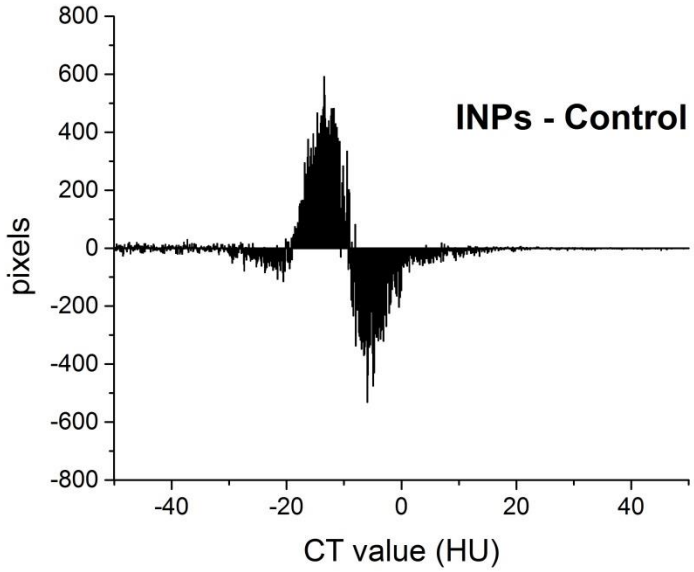

Figure 31 Effect of INPs on radiodensity of frozen DI water samples. (A) Histogram of Housfield unit for frozen DI water sample; (B) Histogram of Housfield unit for frozen DI water sample with INPs; (C) Histogram of Housfield unit for the difference of radiodensity distribution between control and INPs samples.

A

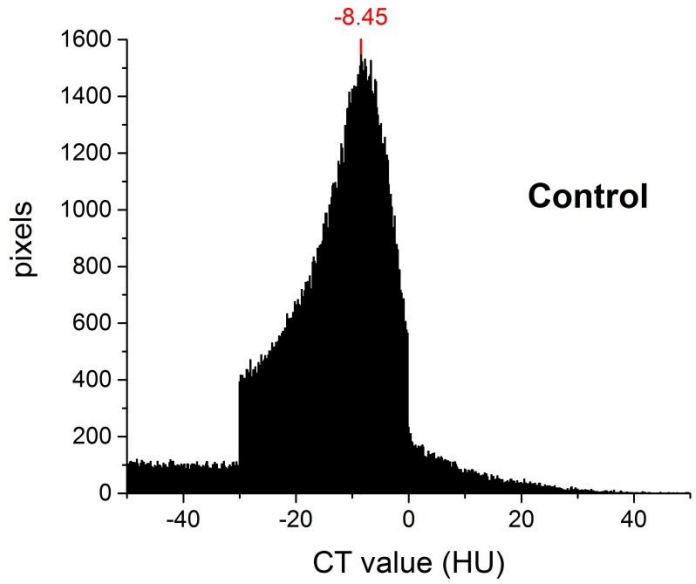
-8.45
1600
1400
1200
1000
800
600
400
200
0
pixels
Control
-40
-20
0
20
40
CT value (HU)

B

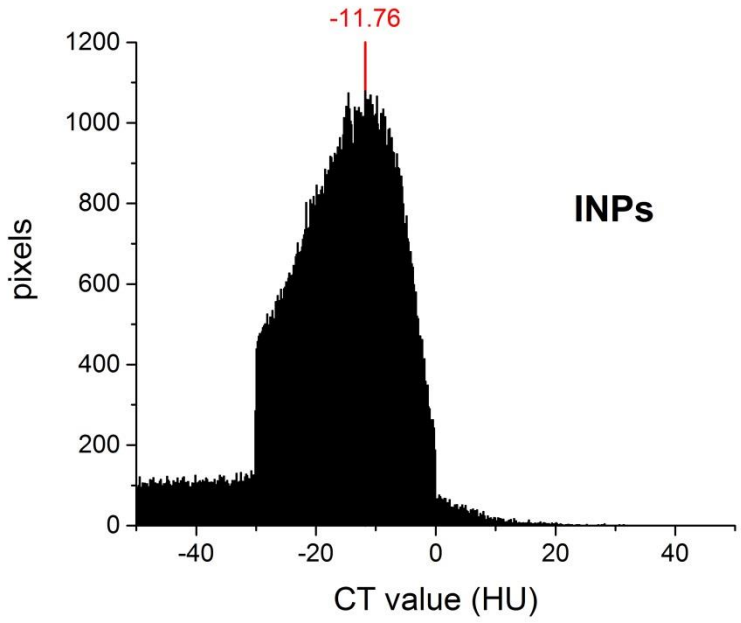
-11.76
1200
1000
800
600
400
200
0
pixels
INPs
-40
-20
0
20
40
CT value (HU)

C

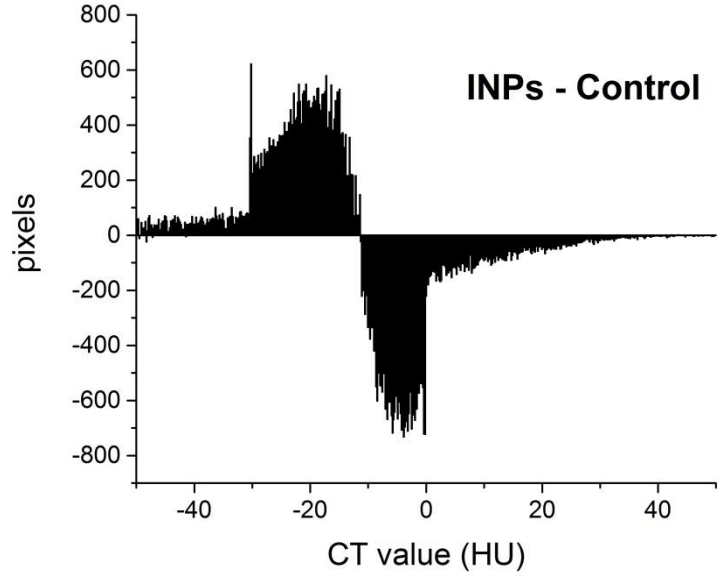

Figure 32 Effect of INPs on radiodensity (HU) of centrifuged frozen seawater samples. (A) Histogram of Housfield unit for centrifuged frozen seawater sample; (B) Histogram of Housfield unit for centrifuged frozen seawater sample with INPs; (C) Histogram of Housfield unit for the difference of radiodensity distribution between control and INPs samples.

References:

Abe, K., Watabe, S., Emori, Y., Watanabe, M., & Arai, S. (1989). An ice nucleation active gene of *Erwinia ananas* - Sequence similarity to those of *Pseudomonas* species and regions required for ice nucleation activity. *Febs Letters, 258*(2), 297-300.

Alizadeh-Pasdar, N., & Li-Chan, E. C. (2000). Comparison of protein surface hydrophobicity measured at various pH values using three different fluorescent probes. *Journal of Agricultural and Food Chemistry, 48*(2), 328-334.

Anuj, G. (2012). Short review on controlled nucleation. *International Journal of Drug Development and Research,* 4(3): 35-40.

Arai, S., & Watanabe, M. (1986). Freeze texturing of food materials by ice-nucleation with the bacterium *Erwinia ananas*. *Agricultural and Biological Chemistry, 50*(1), 169-175.

Ashby, D., Cole, L., & Sadowsky, D. (2006). *BIOPESTICIDES REGISTRATION ACTION DOCUMENT (Pantoea agglomerans strain C9-1) (Chemical PC Code 006470)*. U.S Environmental Protection Agency. Office of Pesticide Programs. Biopesticides and Pollution Prevention Division.

Atkinson, J. D., Murray, B. J., Woodhouse, M. T., Whale, T. F., Baustian, K. J., Carslaw, K. S., . . . Malkin, T. L. (2013). The importance of feldspar for ice nucleation by mineral dust in mixed-phase clouds. *Nature, 498*(7454), 355-358.

Bäumer, A., Duman, J. G., & Havenith, M. (2016). Ice nucleation of an insect lipoprotein ice nucleator (LPIN) correlates with retardation of the hydrogen bond dynamics at the myo-inositol ring. *Physical Chemistry Chemical Physics, 18*(28), 19318-19323.

Bai, H., Chen, Y., Delattre, B., Tomsia, A. P., & Ritchie, R. O. (2015). Bioinspired large-scale aligned porous materials assembled with dual temperature gradients. *Science advances, 1*(11), e1500849.

Bar-Dolev, M., Celik, Y., Wettlaufer, J. S., Davies, P. L., & Braslavsky, I. (2012). New insights into ice growth and melting modifications by antifreeze proteins. *Journal of the Royal Society Interface, 9*(77), 3249-3259.

Bareggi, A., Maire, E., Lasalle, A., & Deville, S. (2011). Dynamics of the Freezing Front During the Solidification of a Colloidal Alumina Aqueous Suspension: In Situ X‐Ray Radiography, Tomography, and Modeling. *Journal of the American Ceramic Society, 94*(10), 3570-3578.

Bleil, U., & Thiede, J. (2012). *Geological history of the polar oceans: Arctic versus Antarctic* (Vol. 308): Springer Science & Business Media.

Bruin, S., & Jongen, T. R. (2003). Food process engineering: the last 25 years and challenges ahead. *Comprehensive Reviews in Food Science and Food Safety, 2*(2), 42-81.

Burke, M. J., & Lindow, S. E. (1990). Surface properties and size of the ice nucleation site in ice nucleation active bacteria: theoretical considerations. *Cryobiology, 27*(1), 80-84.

Caretta, O., Courtot, F., & Davies, T. (2006). Measurement of salt entrapment during the directional solidification of brine under forced mass convection. *Journal of Crystal Growth, 294*(2), 151-155.

Chakravarty, P., Lee, R., DeMarco, F., & Renzi, E. (2012). Ice Fog as a Means to Induce Uniform Ice Nucleation During Lyophilization (Peer Reviewed). *BioPharm International, 25*(1), 33-38.

Christner, B. C. (2010). Bioprospecting for microbial products that affect ice crystal formation and growth. *Applied Microbiology and Biotechnology, 85*(3), 481-489.

Ciurzyńska, A., & Lenart, A. (2011). Freeze-drying-application in food processing and biotechnology-a review. *Polish Journal of Food and Nutrition Sciences, 61*(3), 165-171.

Cohen, J. S., & Yang, T. C. (1995). Progress in food dehydration. *Trends in Food Science & Technology, 6*(1), 20-25.

Coluzza, I., Creamean, J., Rossi, M. J., Wex, H., Alpert, P. A., Bianco, V., . . . Fröhlich-Nowoisky, J. (2017). Perspectives on the Future of Ice Nucleation Research: Research Needs and Unanswered Questions Identified from Two International Workshops. *Atmosphere, 8*(8), 138.

Cox, S. J., Raza, Z., Kathmann, S. M., Slater, B., & Michaelides, A. (2013). The microscopic features of heterogeneous ice nucleation may affect the macroscopic morphology of atmospheric ice crystals. *Faraday Discussions, 167*, 389-403.

Davies, P. L. (2014). Ice-binding proteins: a remarkable diversity of structures for stopping and starting ice growth. *Trends in Biochemical Sciences, 39*(11), 548-555.

De Duve, C., & Berthet, J. (1954). The use of differential centrifugation in the study of tissue enzymes. *International review of cytology, 3*, 225-275.

Delattre, B., Bai, H., Ritchie, R. O., De Coninck, J. l., & Tomsia, A. P. (2013). Unidirectional Freezing of Ceramic Suspensions: In Situ X-ray Investigation of the Effects of Additives. *ACS applied materials & interfaces, 6*(1), 159-166.

Deshpande, S. S., Cheryan, M., Sathe, S. K., & Salunkhe, D. K. (1984). Freeze concentration of fruit juices. *Crc Critical Reviews in Food Science and Nutrition, 20*(3), 173-248.

Deville, S., Maire, E., Lasalle, A., Bogner, A., Gauthier, C., Leloup, J., & Guizard, C. (2009). In Situ X‐Ray Radiography and Tomography Observations of the Solidification of Aqueous Alumina Particle Suspensions—Part I: Initial Instants. *Journal of the American Ceramic Society, 92*(11), 2489-2496.

Deville, S., Maire, E., Lasalle, A., Bogner, A., Gauthier, C., Leloup, J., & Guizard, C. (2010). Influence of Particle Size on Ice Nucleation and Growth During the Ice-Templating Process. *Journal of the American Ceramic Society, 93*(9), 2507-2510.

EPA. (2006). Pantoea Agglomerans Strain C9-1; Exemption from the Requirement of a Tolerance. *Federal Register, 71*(80), 24590-24596.

Fall, A. L., & Fall, R. (1998). High-level expression of ice nuclei in Erwinia herbicola is induced by phosphate starvation and low temperature. *Current Microbiology, 36*(6), 370-376.

Fall, R., & Wolber, P. (1995). Biochemistry of bacterial ice nuclei. *Biological ice nucleation and its applications*, 63-83.

Fitzner, M., Sosso, G. C., Cox, S. J., & Michaelides, A. (2015). The Many Faces of Heterogeneous Ice Nucleation: Interplay Between Surface Morphology and Hydrophobicity. *Journal of the American Chemical Society, 137*(42), 13658-13669.

Florez, M. V., Evans, J. M., & Daly, T. R. (1998). The radiodensity of medications seen on x-ray films. *Mayo Clinic Proceedings*, 73(6): 516-519.

Fujioka, R., Wang, L. P., Dodbiba, G., & Fujita, T. (2013). Application of progressive freeze-concentration for desalination. *Desalination, 319*, 33-37.

Gabellieri, E., & Strambini, G. B. (2003). Perturbation of protein tertiary structure in frozen solutions

revealed by 1-anilino-8-naphthalene sulfonate fluorescence. *Biophysical Journal, 85*(5), 3214-3220.

Garnham, C. P., Campbell, R. L., Walker, V. K., & Davies, P. L. (2011). Novel dimeric β-helical model of an ice nucleation protein with bridged active sites. *BMC structural biology, 11*(1), 36.

Geciova, J., Bury, D., & Jelen, P. (2002). Methods for disruption of microbial cells for potential use in the dairy industry—a review. *International Dairy Journal, 12*(6), 541-553.

Geidobler, R., & Winter, G. (2013). Controlled ice nucleation in the field of freeze-drying: fundamentals and technology review. *European Journal of Pharmaceutics and Biopharmaceutics, 85*(2), 214-222.

Gezgin, Z., Lee, Tung-Ching, & Huang, Q. (2013). Engineering Functional Nanothin Multilayers on Food Packaging: Ice-Nucleating Polyethylene Films. *Journal of Agricultural and Food Chemistry, 61*(21), 5130-5138.

Gibson, M. I. (2010). Slowing the growth of ice with synthetic macromolecules: Beyond antifreeze (glyco) proteins. *Polymer Chemistry, 1*(8), 1141-1152.

Goff, H., Dutcher, J., & Marangoni, A. (2005). Foods at subzero temperatures. *Soft materials: structure and dynamics*, 299-320.

Golden, K., Eicken, H., Heaton, A., Miner, J., Pringle, D., & Zhu, J. (2007). Thermal evolution of permeability and microstructure in sea ice. *Geophysical Research Letters, 34*(16).

Goodnow, R., Katz, G., Haines, D., & Terril, J. (1990). Subacute inhalation toxicity study of an ice-nucleation-active Pseudomonas syringae administered as a respirable aerosol to rats. *Toxicology letters, 54*(2), 157-167.

Graether, S. P., & Jia, Z. C. (2001). Modeling Pseudomonas syringae ice-nucleation protein as a beta-helical protein. *Biophysical Journal, 80*(3), 1169-1173.

Graether, S. P., Kuiper, M. J., Gagné, S. M., Walker, V. K., Jia, Z., Sykes, B. D., & Davies, P. L. (2000). β-Helix structure and ice-binding properties of a hyperactive antifreeze protein from an insect. *Nature, 406*(6793), 325-328.

Graether, S. P., & Sykes, B. D. (2004). Cold survival in freeze‐intolerant insects. *European Journal of Biochemistry, 271*(16), 3285-3296.

Guriansherman, D., & Lindow, S. E. (1993). Bacterial ice nucleation: significance and molecular basis. *Faseb Journal, 7*(14), 1338-1343.

Hall-Manning, T., Spurgeon, M., Wolfreys, A., & Baldrick, A. (2004). Safety evaluation of ice-structuring protein (ISP) type III HPLC 12 preparation. Lack of genotoxicity and subchronic toxicity. *Food and chemical toxicology, 42*(2), 321-333.

Hartel, R. W. (2013). Advances in Food Crystallization. In M. P. Doyle & T. R. Klaenhammer (Eds.), *Annual Review of Food Science and Technology, Vol 4* (Vol. 4, pp. 277-292).

Hasanuzzaman, M., Saidur, R., & Masjuki, H. (2008). Investigation of Energy Consumption and Energy Savings of Refrigerator-Freezer During Open and Closed Door Condition. *Journal of Applied Sciences, 8*(10).

Haskard, C. A., & Li-Chan, E. C. (1998). Hydrophobicity of bovine serum albumin and ovalbumin determined using uncharged (PRODAN) and anionic (ANS-) fluorescent probes. *Journal of Agricultural and Food Chemistry, 46*(7), 2671-2677.

Hassas-Roudsari, M., & Goff, H. D. (2012). Ice structuring proteins from plants: Mechanism of action

and food application. *Food Research International, 46*(1), 425-436.

Hawe, A., Sutter, M., & Jiskoot, W. (2008). Extrinsic fluorescent dyes as tools for protein characterization. *Pharmaceutical Research, 25*(7), 1487-1499.

Hottot, A., Nakagawa, K., & Andrieu, J. (2008). Effect of ultrasound-controlled nucleation on structural and morphological properties of freeze-dried mannitol solutions. *Chemical Engineering Research & Design, 86*(A2), 193-200.

Hottot, A., Vessot, S., & Andrieu, J. (2007). Freeze drying of pharmaceuticals in vials: Influence of freezing protocol and sample configuration on ice morphology and freeze-dried cake texture. *Chemical Engineering and Processing: Process Intensification, 46*(7), 666-674.

Iannone, R., Chernoff, D., Pringle, A., Martin, S., & Bertram, A. (2011). The ice nucleation ability of one of the most abundant types of fungal spores found in the atmosphere. *Atmospheric Chemistry and Physics, 11*(3), 1191-1201.

Jiang, X. B., Wang, J. K., & Hou, B. H. (2012). Coarse crystal layer growth and liquid entrapment study with gradient freeze technology. *Crystal Research and Technology, 47*(6), 649-657.

Jin, J., Yurkow, E. J., Adler, D., & Lee, Tung-Ching. (2017). A Novel Approach To Improve the Efficiency of Block Freeze Concentration Using Ice Nucleation Proteins with Altered Ice Morphology. *Journal of Agricultural and Food Chemistry,* 65(11), 2373-2382.

Jung, H.-C., Park, J.-H., Park, S.-H., Lebeault, J.-M., & Pan, J.-G. (1998). Expression of carboxymethylcellulase on the surface of Escherichia coli using Pseudomonas syringae ice nucleation protein. *Enzyme and microbial technology, 22*(5), 348-354.

Junge, K., Eicken, H., & Deming, J. W. (2004). Bacterial activity at− 2 to− 20 C in Arctic wintertime sea ice. *Applied and Environmental Microbiology, 70*(1), 550-557.

Junge, K., Krembs, C., Deming, J., Stierle, A., & Eicken, H. (2001). A microscopic approach to investigate bacteria under in situ conditions in sea-ice samples. *Annals of Glaciology, 33*(1), 304-310.

Jusoh, M., Yunus, R. M., & Abu Hassan, M. (2009). Performance investigation on a new design for progressive freeze concentration system. *J Appl Sci, 9*(17), 3171-3175.

Kajava, A. V. (1995). *Molecular modeling of the three-dimensional structure of bacterial Ina proteins*. American Phytopathological Society (APS) Press.

Kajava, A. V., & Lindow, S. E. (1993). A model of the three-dimensional structure of ice nucleation proteins. *Journal of Molecular Biology, 232*(3), 709-717.

Kasper, J. C., & Friess, W. (2011). The freezing step in lyophilization: Physico-chemical fundamentals, freezing methods and consequences on process performance and quality attributes of biopharmaceuticals. *European Journal of Pharmaceutics and Biopharmaceutics, 78*(2), 248-263.

Kasper, J. C., Winter, G., & Friess, W. (2013). Recent advances and further challenges in lyophilization. *European Journal of Pharmaceutics and Biopharmaceutics, 85*(2), 162-169.

Kawahara, H. (2002). The structures and functions of ice crystal-controlling proteins from bacteria. *Journal of Bioscience and Bioengineering, 94*(6), 492-496.

Kawahara, H., Nakano, Y., Omiya, K., Muryoi, N., Nishikawa, J., & Obata, H. (2004). Production of two types of ice crystal-controlling proteins in Antarctic bacterium. *Journal of Bioscience and Bioengineering, 98*(3), 220-223.

Kawamura, T. (1990). Nondestructive, three‐dimensional density measurements of ice core samples by X ray computed tomography. *Journal of Geophysical Research: Solid Earth (1978–2012), 95*(B8), 12407-12412.

Khalloufi, S., Kharaghani, A., Almeida-Rivera, C., Nijsse, J., van Dalen, G., & Tsotsas, E. (2015). Monitoring of initial porosity and new pores formation during drying: a scientific debate and a technical challenge. *Trends in Food Science & Technology, 45*(2), 179-186.

Kiani, H., & Sun, D.-W. (2011). Water crystallization and its importance to freezing of foods: A review. *Trends in Food Science & Technology, 22*(8), 407-426.

Kishimoto, T., Yamazaki, H., Saruwatari, A., Murakawa, H., Sekozawa, Y., Kuchitsu, K., . . . Ishikawa, M. (2014). High ice nucleation activity located in blueberry stem bark is linked to primary freeze initiation and adaptive freezing behaviour of the bark. *AoB Plants, 6*, plu044.

Kobashigawa, Y., Nishimiya, Y., Miura, K., Ohgiya, S., Miura, A., & Tsuda, S. (2005). A part of ice nucleation protein exhibits the ice-binding ability. *Febs Letters, 579*(6), 1493-1497.

Kobayashi, A., Shirai, Y., Nakanishi, K., & Matsuno, R. (1996). A method for making large agglomerated ice crystals for freeze concentration. *Journal of Food Engineering, 27*(1), 1-15.

Koga, T., Okahashi, N., Takahashi, I., Kanamoto, T., Asakawa, H., & Iwaki, M. (1990). Surface hydrophobicity, adherence, and aggregation of cell surface protein antigen mutants of Streptococcus mutans serotype c. *Infection and immunity, 58*(2), 289-296.

Kozloff, L., Turner, M., Arellano, F., & Lute, M. (1991). Phosphatidylinositol, a phospholipid of ice-nucleating bacteria. *Journal of Bacteriology, 173*(6), 2053-2060.

Kozloff, L. M., Lute, M., & Westaway, D. (1984). Phosphatidylinositol as a component of the ice nucleating site of Pseudomonas syringae and Erwinia herbicola. *Science, 226*, 845-847.

Kozloff, L. M., Schofield, M. A., & Lute, M. (1983). Ice nucleating activity of Pseudomonas syringae and Erwinia herbicola. *Journal of Bacteriology, 153*(1), 222-231.

Kozloff, L. M., Turner, M. A., & Arellano, F. (1991). Formation of bacterial membrane ice-nucleating lipoglycoprotein complexes. *Journal of Bacteriology, 173*(20), 6528-6536.

Lagriffoul, A., Boudenne, J.-L., Absi, R., Ballet, J.-J., Berjeaud, J.-M., Chevalier, S., . . . Gadonna-Widehem, P. (2010). Bacterial-based additives for the production of artificial snow: What are the risks to human health? *Science of the Total Environment, 408*(7), 1659-1666.

Lasalle, A., Guizard, C., Leloup, J., Deville, S., Maire, E., Bogner, A., . . . Courtois, L. (2012). Ice-Templating of Alumina Suspensions: Effect of Supercooling and Crystal Growth During the Initial Freezing Regime. *Journal of the American Ceramic Society, 95*(2), 799-804.

Li, J., Izquierdo, M. P., & Lee, Tung-Ching. (1997). Effects of ice‐nucleation active bacteria on the freezing of some model food systems. *International Journal of Food Science & Technology, 32*(1), 41-49.

Li, J., & Lee, Tung-Ching. (1998). Bacterial extracellular ice nucleator effects on freezing of foods. *Journal of Food Science, 63*(3), 375-381.

Li, J. K., Izquierdo, M. P., & Lee, Tung-Ching. (1997). Effects of ice-nucleation active bacteria on the freezing of some model food systems. *International Journal of Food Science and Technology, 32*(1), 41-49.

Li, J. K., & Lee, Tung-Ching. (1995). Bacterial ice nucleation and its potential application in the food industry. *Trends in Food Science & Technology, 6*(8), 259-265.

Li, J. K., & Lee, Tung-Ching. (1998). Enhanced production of extracellular ice nucleators from Erwinia herbicola. *Journal of General and Applied Microbiology, 44*(6), 405-413.

Lialiaris, T., Mourelatos, D., Stergiadou, H., & Constantinidou, H. (1990). Cytogenetic study for possible mutagenic activity induced by ice-nucleation bacteria or their metabolic products in human lymphocytes in vitro. *Mutation Research/Genetic Toxicology, 242*(2), 163-168.

Liou, Y.-C., Tocilj, A., Davies, P. L., & Jia, Z. (2000). Mimicry of ice structure by surface hydroxyls and water of a β-helix antifreeze protein. *Nature, 406*(6793), 322-324.

Lorv, J. S., Rose, D. R., & Glick, B. R. (2014). Bacterial Ice Crystal Controlling Proteins. *Scientifica, 2014*.

Lundheim, R. (2002). Physiological and ecological significance of biological ice nucleators. *Philosophical Transactions of the Royal Society B: Biological Sciences, 357*(1423), 937-943.

Luo, C. S., Chen, W. W., & Han, W. F. (2010). Experimental study on factors affecting the quality of ice crystal during the freezing concentration for the brackish water. *Desalination, 260*(1-3), 231-238.

Lupi, L., & Molinero, V. (2014). Does hydrophilicity of carbon particles improve their ice nucleation ability? *The Journal of Physical Chemistry A, 118*(35), 7330-7337.

Mahdavi, M., Mahvi, A. H., Nasseri, S., & Yunesian, M. (2011). Application of Freezing to the Desalination of Saline Water. *Arabian Journal for Science and Engineering, 36*(7), 1171-1177.

Mancosu, N., Snyder, R. L., Kyriakakis, G., & Spano, D. (2015). Water Scarcity and Future Challenges for Food Production. *Water, 7*(3), 975-992.

Marentes, E., Griffith, M., Mlynarz, A., & Brush, R. A. (1993). Proteins accumulate in the apoplast of winter rye leaves during cold acclimation. *Physiologia Plantarum, 87*(4), 499-507.

Matsumoto, K., Akimoto, T., & Teraoka, Y. (2010). Study of scraping force of ice growing on cooling solid surface. *international journal of refrigeration, 33*(2), 419-427.

Matsumoto, K., Inuzuka, M., Teraoka, Y., Hayashi, K., & Murahashi, K. (2012). Fundamental study on freezing characteristics of trehalose solution (investigation based on scraping characteristics). *International Journal of Refrigeration-Revue Internationale Du Froid, 35*(4), 897-906.

Min, K., Park, K., Park, D.-H., & Yoo, Y. J. (2015). Overview on the biotechnological production of L-DOPA. *Applied Microbiology and Biotechnology, 99*(2), 575-584.

Miyawaki, O., Liu, L., Shirai, Y., Sakashita, S., & Kagitani, K. (2005). Tubular ice system for scale-up of progressive freeze-concentration. *Journal of Food Engineering, 69*(1), 107-113.

Moejes, S., & van Boxtel, A. (2016). Energy saving potential of emerging technologies in milk powder production. *Trends in Food Science & Technology,* 60, 31-42.

Moreno, F., Robles, C., Sarmiento, Z., Ruiz, Y., & Pardo, J. (2013). Effect of separation and thawing mode on block freeze-concentration of coffee brews. *Food and Bioproducts Processing, 91*(4), 396-402.

Morris, C. E., Conen, F., Alex Huffman, J., Phillips, V., Pöschl, U., & Sands, D. C. (2014). Bioprecipitation: a feedback cycle linking Earth history, ecosystem dynamics and land use through biological ice nucleators in the atmosphere. *Global change biology, 20*(2), 341-351.

Mousavi, R., Miri, T., Cox, P. W., & Fryer, P. J. (2007). Imaging food freezing using X-ray microtomography. *International Journal of Food Science and Technology, 42*(6), 714-727.

Muryoi, N., Matsukawa, K., Yamade, K., Kawahara, H., & Obata, H. (2003). Purification and properties

of an ice-nucleating protein from an ice-nucleating bacterium, Pantoea ananatis KUIN-3. *Journal of Bioscience and Bioengineering, 95*(2), 157-163.

Nada, H., Zepeda, S., Miura, H., & Furukawa, Y. (2010). Significant alterations in anisotropic ice growth rate induced by the ice nucleation-active bacteria Xanthomonas campestris. *Chemical Physics Letters, 498*(1), 101-106.

Nagashima, K., & Furukawa, Y. (1997). Solute distribution in front of an ice/water interface during directional growth of ice crystals and its relationship to interfacial patterns. *Journal of Physical Chemistry B, 101*(32), 6174-6176.

Nakagawa, K., Hottot, A., Vessot, S., & Andrieu, J. (2006). Influence of controlled nucleation by ultrasounds on ice morphology of frozen formulations for pharmaceutical proteins freeze-drying. *Chemical Engineering and Processing, 45*(9), 783-791.

Nakagawa, K., Hottot, A., Vessot, S., & Andrieu, J. (2007). Modeling of freezing step during. freeze-drying of drugs in vials. *Aiche Journal, 53*(5), 1362-1372.

Nemecek-Marshall, M., Laduca, R., & Fall, R. (1993). High-level expression of ice nuclei in a Pseudomonas syringae strain is induced by nutrient limitation and low temperature. *Journal of Bacteriology, 175*(13), 4062-4070.

Nguyen, N.-T., & Wereley, S. T. (2002). *Fundamentals and applications of microfluidics*: Artech House.

O'sullivan, D., Murray, B., Malkin, T., Whale, T., Umo, N., Atkinson, J., . . . Webb, M. (2014). Ice nucleation by fertile soil dusts: relative importance of mineral and biogenic components. *Atmospheric Chemistry and Physics, 14*(4), 1853-1867.

Obbard, R. W., Troderman, G., & Baker, I. (2009). Imaging brine and air inclusions in sea ice using micro-X-ray computed tomography. [Letter]. *Journal of Glaciology, 55*(194), 1113-1115.

Okawa, S., Ito, T., & Saito, A. (2009). Effect of crystal orientation on freeze concentration of solutions. *international journal of refrigeration, 32*(2), 246-252.

Orlowska, M., Havet, M., & Le-Bail, A. (2009). Controlled ice nucleation under high voltage DC electrostatic field conditions. *Food Research International, 42*(7), 879-884.

Otero, L., Sanz, P., Guignon, B., & Sanz, P. (2012). Pressure-shift nucleation: A potential tool for freeze concentration of fluid foods. *Innovative Food Science & Emerging Technologies, 13*, 86-99.

Palaiomylitou, M., Kalimanis, A., Koukkou, A., Drainas, C., Anastassopoulos, E., Panopoulos, N., . . . Kyriakidis, D. (1998). Phospholipid Analysis and Fractional Reconstitution of the Ice Nucleation Protein Activity Purified from *Escherichia coli* Overexpressing the *inaZ* Gene of *Pseudomonas syringae*. *Cryobiology, 37*(1), 67-76.

Parker, A., Rigby‐Singleton, S., Perkins, M., Bates, D., Le Roux, D., Roberts, C. J., . . . Johnson, R. E. (2010). Determination of the influence of primary drying rates on the microscale structural attributes and physicochemical properties of protein containing lyophilized products. *Journal of Pharmaceutical Sciences, 99*(11), 4616-4629.

Passot, S., Trelea, I. C., Marin, M., Galan, M., Morris, G. J., & Fonseca, F. (2009a). Effect of Controlled Ice Nucleation on Primary Drying Stage and Protein Recovery in Vials Cooled in a Modified Freeze-Dryer. *Journal of Biomechanical Engineering-Transactions of the Asme, 131*(7).

Passot, S., Trelea, I. C., Marin, M., Galan, M., Morris, G. J., & Fonseca, F. (2009b). Effect of controlled ice nucleation on primary drying stage and protein recovery in vials cooled in a modified freeze-dryer. *Journal of biomechanical engineering, 131*(7), 074511.

Patapoff, T. W., & Overcashier, D. E. (2002). The importance of freezing on lyophilization cycle development. *BIOPHARM-EUGENE-*, *15*(3), 16-21.

Patel, S. M., Bhugra, C., & Pikal, M. J. (2009). Reduced pressure ice fog technique for controlled ice nucleation during freeze-drying. *Aaps Pharmscitech*, *10*(4), 1406.

Pawelec, K., Husmann, A., Best, S. M., & Cameron, R. E. (2014). Understanding anisotropy and architecture in ice-templated biopolymer scaffolds. *Materials Science and Engineering: C*, *37*, 141-147.

Peters, B.-H., Molnár, F., & Ketolainen, J. (2014). Structural attributes of model protein formulations prepared by rapid freeze-drying cycles in a microscale heating stage. *European Journal of Pharmaceutics and Biopharmaceutics*, *87*(2), 347-356.

Petzold, G., & Aguilera, J. (2013). Centrifugal freeze concentration. *Innovative Food Science & Emerging Technologies*, *20*, 253-258.

Petzold, G., & Aguilera, J. M. (2009). Ice Morphology: Fundamentals and Technological Applications in Foods. *Food Biophysics*, *4*(4), 378-396.

Petzold, G., Moreno, J., Lastra, P., Rojas, K., & Orellana, P. (2015). Block freeze concentration assisted by centrifugation applied to blueberry and pineapple juices. *Innovative Food Science & Emerging Technologies*, 30, 192-197.

Petzold, G., Niranjan, K., & Aguilera, J. (2013). Vacuum-assisted freeze concentration of sucrose solutions. *Journal of Food Engineering*, *115*(3), 357-361.

Phelps, P., Giddings, T. H., Prochoda, M., & Fall, R. (1986). Release of cell-free ice nuclei by Erwinia herbicola. *Journal of Bacteriology*, *167*(2), 496-502.

Pringle, D., Miner, J., Eicken, H., & Golden, K. (2009). Pore space percolation in sea ice single crystals. *Journal of Geophysical Research: Oceans (1978–2012)*, *114*(C12).

Pummer, B., Budke, C., Augustin-Bauditz, S., Niedermeier, D., Felgitsch, L., Kampf, C., . . . Moschen, T. (2015). Ice nucleation by water-soluble macromolecules. *Atmospheric Chemistry and Physics*, *15*(8), 4077-4091.

Raymond, J. A., Janech, M. G., & Fritsen, C. H. (2009). Novel ice-binding proteins from a psychrophilic Antarctic alga (Chlamydomonadaceae, Chlorophyceae). *Journal of Phycology*, *45*(1), 130-136.

Raza, Z., Alfe, D., Salzmann, C. G., Klimeš, J., Michaelides, A., & Slater, B. (2011). Proton ordering in cubic ice and hexagonal ice; a potential new ice phase—XIc. *Physical Chemistry Chemical Physics*, *13*(44), 19788-19795.

Rezanezhad, F., Quinton, W. L., Price, J. S., Elrick, D., Elliot, T., & Heck, R. J. (2009). Examining the effect of pore size distribution and shape on flow through unsaturated peat using computer tomography. *Hydrol. Earth Syst. Sci.*, 13, 1993-2002.

Rosenberg, M. (1984). Bacterial adherence to hydrocarbons: a useful technique for studying cell surface hydrophobicity. *FEMS Microbiology Letters*, *22*(3), 289-295.

Rozmanov, D., & Kusalik, P. G. (2012). Anisotropy in the crystal growth of hexagonal ice, Ih. *The Journal of chemical physics*, *137*(9), 094702.

Rudy, S. (2009). Energy consumption in the freeze-and convection-drying of garlic. *TEKA Kom. Mot. Energ. Roln.-OL PAN*, *9*, 259-266.

Ruggles, J. A., Nemecek-Marshall, M., & Fall, R. (1993). Kinetics of appearance and disappearance of classes of bacterial ice nuclei support an aggregation model for ice nucleus assembly. *Journal of*

Bacteriology, 175(22), 7216-7221.

Sánchez, J., Ruiz, Y., Raventos, M., Auleda, J., & Hernandez, E. (2010). Progressive freeze concentration of orange juice in a pilot plant falling film. *Innovative Food Science & Emerging Technologies, 11*(4), 644-651.

Sönnichsen, F. D., DeLuca, C. I., Davies, P. L., & Sykes, B. D. (1996). Refined solution structure of type III antifreeze protein: hydrophobic groups may be involved in the energetics of the protein–ice interaction. *Structure, 4*(11), 1325-1337.

Saidur, R., Masjuki, H., & Choudhury, I. (2002). Role of ambient temperature, door opening, thermostat setting position and their combined effect on refrigerator-freezer energy consumption. *Energy Conversion and Management, 43*(6), 845-854.

Saidur, R., Masjuki, H., Mahlia, T., & Nasrudin, A. (2002). Factors affecting refrigerator-freezers energy consumption. *ASEAN Journal on Science and Technology for Development, 19*(2), 57-68.

Sanchez, J., Hernandez, E., Auleda, J. M., & Raventos, M. (2011). Review: Freeze Concentration Technology Applied to Dairy Products. *Food Science and Technology International, 17*(1), 5-13.

Sanchez, J., Ruiz, Y., Auleda, J. M., Hernandez, E., & Raventos, M. (2009). Review. Freeze Concentration in the Fruit Juices Industry. *Food Science and Technology International, 15*(4), 303-315.

Scheel, J. F., Kunert, A. T., Kampf, C. J., Mauri, S., Weidner, T., Pöschl, U., & Fröhlich-Nowoisky, J. (2016). *Identification & Characterization of Fungal Ice Nucleation Proteins.* Paper presented at the EGU General Assembly Conference Abstracts.

Schmid, D., Pridmore, D., Capitani, G., Battistutta, R., Neeser, J.-R., & Jann, A. (1997). Molecular organisation of the ice nucleation protein InaV from Pseudomonas syringae. *Febs Letters, 414*(3), 590-594.

Schoeman, L., Williams, P., du Plessis, A., & Manley, M. (2016). X-ray micro-computed tomography (μCT) for non-destructive characterisation of food microstructure. *Trends in Food Science & Technology, 47*, 10-24.

Schoof, H., Bruns, L., Fischer, A., Heschel, I., & Rau, G. (2000). Dendritic ice morphology in unidirectionally solidified collagen suspensions. *Journal of Crystal Growth, 209*(1), 122-129.

Searles, J. A., Carpenter, J. F., & Randolph, T. W. (2001). Annealing to optimize the primary drying rate, reduce freezing‐induced drying rate heterogeneity, and determine Tg′ in pharmaceutical lyophilization. *Journal of Pharmaceutical Sciences, 90*(7), 872-887.

Searles, J. A., Carpenter, J. F., & Randolph, T. W. (2001). The ice nucleation temperature determines the primary drying rate of lyophilization for samples frozen on a temperature-controlled shelf. *Journal of Pharmaceutical Sciences, 90*(7), 860-871.

Shi, K., Yu, H., & Lee, Tung-Ching. (2013). A novel approach for improving yeast viability and baking quality of frozen dough by adding biogenic ice nucleators from Erwinia herbicola. *Journal of Cereal Science, 57*(2), 237-243.

Shi, K., Yu, H. L., Jin, J., & Lee, Tung-Ching. (2013). Improvement to baking quality of frozen bread dough by novel zein-based ice nucleation films. *Journal of Cereal Science, 57*(3), 430-436.

Shibkov, A. A., Golovin, Y. I., Zheltov, M. A., Korolev, A. A., & Leonov, A. A. (2003). Morphology diagram of nonequilibrium patterns of ice crystals growing in supercooled water. *Physica*

a-Statistical Mechanics and Its Applications, 319, 65-79.

Shibkov, A. A., Zheltov, M. A., Korolev, A. A., & Leonov, A. A. (2003). Kinetic phase diagram of fractal and euclidean nonequilibrium growth patterns of ice I-h in supercooled water. *Doklady Physical Chemistry, 389*(4-6), 94-97.

Shirai, Y., Wakisaka, M., Miyawaki, O., & Sakashita, S. (1999). Effect of seed ice on formation of tube ice with high purity for a freeze wastewater treatment system with a bubble-flow circulator. *Water Research, 33*(5), 1325-1329.

Smith, C. E., & Schwartzberg, H. G. (1985). Ice crystal size changes during ripening in freeze concentration. *Biotechnology Progress, 1*(2), 111-120.

Southworth, M. W., Wolber, P. K., & Warren, G. J. (1988). Nonlinear relationship between concentration and activity of a bacterial ice nucleation protein. *Journal of Biological Chemistry, 263*(29), 15211-15216.

Spicer, A. (1974). *Advances in preconcentration and dehydration of foods*: Applied Science Publishers Ltd.

Stand, E. (1989). The development of aligned columnar sea ice: a field investigation. *Journal of Glaciology, 35*(120), 217-223.

Tanaka, A., Nakano, T., & Ikehara, K. (2011). X-ray computerized tomography analysis and density estimation using a sediment core from the challenger mound area in the porcupine seabight, off western Ireland. *Earth, planets and space, 63*(2), 103-110.

Tang, X. L., & Pikal, M. J. (2004). Design of freeze-drying processes for pharmaceuticals: Practical advice. *Pharmaceutical Research, 21*(2), 191-200.

Turner, M. A., Arellano, F., & Kozloff, L. M. (1991). Components of ice nucleation structures of bacteria. *Journal of Bacteriology, 173*(20), 6515-6527.

Vanhaecke, E., Remon, J., Moors, M., Raes, F., De Rudder, D., & Van Peteghem, A. (1990). Kinetics of Pseudomonas aeruginosa adhesion to 304 and 316-L stainless steel: role of cell surface hydrophobicity. *Applied and Environmental Microbiology, 56*(3), 788-795.

Wang, S., Agyare, K., & Damodaran, S. (2009). Optimisation of hydrolysis conditions and fractionation of peptide cryoprotectants from gelatin hydrolysate. *Food Chemistry, 115*(2), 620-630.

Wang, S. Y., & Damodaran, S. (2009). Ice-Structuring Peptides Derived from Bovine Collagen. *Journal of Agricultural and Food Chemistry, 57*(12), 5501-5509.

Warren, G., & Wolber, P. (1991). Molecular aspects of microbial ice nucleation. *Molecular Microbiology, 5*(2), 239-243.

Waschkies, T., Oberacker, R., & Hoffmann, M. (2011). Investigation of structure formation during freeze-casting from very slow to very fast solidification velocities. *Acta Materialia, 59*(13), 5135-5145.

Watanabe, M., & Arai, S. (1987). Freezing of Water in the Presence of the Ice Nucleation Active Bacterium, *Erwinia ananas*, and Its Application for Efficient Freeze-drying of Foods. *Agricultural and Biological Chemistry, 51*(2), 557-563.

Watanabe, M., & Arai, S. (1994). Bacterial Ice-Nucleation Activity and its Application to Freeze Concentration of Fresh Foods for Modification of their Properties. *Journal of Food Engineering, 22*(1-4), 453-473.

Watanabe, M., & Arai, S. (1995). *Applications of bacterial ice nucleation activity in food processing*.

APS, St. Paul, MN.

Watanabe, M., & Watanabe, J. (1994). Screening, Isolation, and Identification of Food-originated Compounds Enhancing the Ice-nucleation Activity of *Xanthomonas campestris*. *Bioscience Biotechnology and Biochemistry, 58*(1), 64-66.

Watanabe, M., Watanabe, J., Kumeno, K., Nakahama, N., & Arai, S. (1989). Freeze concentration of some foodstuffs using ice nucleation-active bacterial cells entrapped in calcium alginate gel. *Agricultural and Biological Chemistry, 53*(10), 2731-2735.

Wathen, B., Kuiper, M., Walker, V., & Jia, Z. C. (2004). New simulation model of multicomponent crystal growth and inhibition. *Chemistry-a European Journal, 10*(7), 1598-1605.

Whale, T. F., Rosillo-Lopez, M., Murray, B. J., & Salzmann, C. G. (2015). Ice Nucleation Properties of Oxidized Carbon Nanomaterials. *The journal of physical chemistry letters, 6*(15), 3012-3016.

Williams, P. M., Ahmad, M., Connolly, B. S., & Oatley-Radcliffe, D. L. (2015). Technology for freeze concentration in the desalination industry. *Desalination, 356*, 314-327.

Wilson, S. L., & Walker, V. K. (2010). Selection of low-temperature resistance in bacteria and potential applications. *Environmental Technology, 31*(8-9), 943-956.

Wolber, P. K. (1993). Bacterial ice nucleation. *Advances in microbial physiology, 34*, 203-203.

Xanthakis, E., Havet, M., Chevallier, S., Abadie, J., & Le-Bail, A. (2013). Effect of static electric field on ice crystal size reduction during freezing of pork meat. *Innovative Food Science & Emerging Technologies, 20*, 115-120.

Yamaguchi, H. (2008). *Engineering fluid mechanics* (Vol. 85): Springer Science & Business Media.

Yamanaka, K. (1999). Cold shock response in Escherichia coli. *Journal of molecular microbiology and biotechnology, 1*(2), 193-202.

Yu, F., Liu, X., Tao, Y., & Zhu, K. (2013). High saturated fatty acids proportion in Escherichia coli enhances the activity of ice-nucleation protein from Pantoea ananatis. *FEMS Microbiology Letters, 345*(2), 141-146.

Zaidi, K. U., Ali, A. S., Ali, S. A., & Naaz, I. (2014). Microbial tyrosinases: promising enzymes for pharmaceutical, food bioprocessing, and environmental industry. *Biochemistry research international, 2014*.

Zhang, Z. L., & Hartel, R. W. (1996). A multilayer Freezer for freeze concentration of liquid milk. *Journal of Food Engineering, 29*(1), 23-38.

Zhou, Z., Jin, J., Yue, T., & Lee, Tung-Ching. (2014). Optimization of covalent immobilization of extracellular ice nucleators from erwinia herbicola on magnetic Fe3O4/chitosan nanoparticles for potential application in freeze concentration. *Food and bioprocess technology, 7*(11), 3259-3268.

Zhu, X., & Lee, Tung-Ching. (2007). Application of a biogenic extra cellular ice nucleator for food processing: effects on the freeze-thaw stability of fish actomyosin from tilapia. *International Journal of Food Science and Technology, 42*(6), 768-772.